HUMAN GUT BACTERIA AND FOOD PRODUCTION CHEMICALS

IMPACT OF FOOD PRODUCTION AND FOOD PROCESSING CHEMICALS ON THE GROWTH AND TRANSCRIPTION OF HUMAN GASTROINTESTINAL BACTERIA

By

SAAD A. SYED, B. Arts Sc.

A Thesis Submitted to the School of Graduate Studies in Partial Fulfillment of the Requirements for the Degree

Doctor of Philosophy

McMaster University DOCTOR OF PHILOSOPHY (2023)
Hamilton, Ontario (Biochemistry and Biomedical Sciences)

TITLE: Impact of food production and food processing chemicals on the growth and transcription of human gastrointestinal bacteria

AUTHOR: Saad A. Syed, B. Arts Sc. (McMaster University)

SUPERVISOR: Dr. Michael G. Surette

NUMBER OF PAGES: i-xv, 1-175

Lay Abstract

Humans use chemicals to grow, process, and package food. With every meal, humans consume small amounts of these chemicals. How these chemicals impact gut bacteria is not understood. Bacteria that live in the human gut are important for many normal functions, including nutrition, bowel function, and infection prevention. Here, I describe how I tested many gut bacteria with common food production, processing, and packaging chemicals. I show that there are a few bacteria affected in their growth by some chemicals, including some thought to be harmless to bacteria and humans. This growth inhibition can be specific to only some or very similar subsets of species of bacteria, such as with bisphenol S. I also show that even if they are not growing any different, food dyes can change how bacteria behave. This work helps us better understand how food chemicals impact our gut bacteria. What these findings mean for human health will require further studies.

Abstract

Recent studies have associated several pesticides, food packaging chemicals, and food processing chemicals with changes in microbiome composition and function. These agri-food chemicals are pervasive in modern food consumption, but no systematic approach has been taken to understand the extent of their direct impact at concentrations relevant to dietary exposure in the general population. I asked: what is the impact of agri-food chemicals on the growth and function of gastrointestinal microbiota? I screened 58 representative gastrointestinal bacteria species in the presence of 30 widely used agri-food chemicals at 1μM. I further characterized one observed growth interaction between Bisphenol S (BPS) and *Bifidobacterium adolescentis* by screening 31 *B. adolescentis* strains. Comparative genomics analysis of these strains was performed to identify enriched functions. A subset of seven chemicals and eight bacteria from our growth screen were also selected for RNA-seq to assess sub-inhibitory transcriptional response in the absence of growth inhibition. A *Salmonella* Typhimurium promoter library was screened to better characterized findings from the RNA-seq experiment. I observed 15% of bacteria were impacted by at least one agrochemical and 41% of agri-food chemicals impacted the growth of at least one bacteria. Azo food dyes and bisphenols were overrepresented in growth impacts among all compounds screened. Further screening with BPS and *Bifidobacterium* found that 52% of screened *B. adolescentis* were impacted. Comparative genomics analysis correlated the growth impact with functions relating to phage-associated and cell wall proteins. Transcriptomics of 56 different agrochemical-bacterial pairs found notable

impacts of azo dyes, even in the absence of growth impacts. These impacts were found to relate to invasion and metabolic functions in random promoter library assays. These results characterize direct agri-food chemicals impacts on microbial growth and function, broaden our understanding of xenobiotic-microbiome interactions, and raise key questions regarding the widespread use of agri-food chemicals.

Acknowledgements

The nature of science required the involvement of several people in all aspects of this work and without whom none of this would be possible.

I am thankful to Dr. Michael Surette, who has been a truly remarkable scientific mentor and created a research environment where I was free to learn and test new tools and hypotheses. It has been almost a decade since we first met in the Farncombe Atrium and still in every encounter we have, you embody every value that guides me as a scientist and a clinician: deep curiosity, tremendous work ethic, and soft-spoken kindness. I attribute any of my success to your unwavering support and mentorship.

Thank you to my committee members, Dr. Eric Brown, and Dr. Jonathan Schertzer. Your guidance as my project evolved has been invaluable and your support of my project – including to go as far as to lend equipment from your labs that was pivotal to the data that started it all in Chapter 2 – has been incomparable. It has been a privilege to have been advised by such accomplished scientists.

I am thankful to all the members of the Surette laboratory – present and past. I am lucky to count so many of you as friends and some as mentors.

I am also indebted to my collaborators from the GETBAT team, who have been involved in this project and allowed me to be a part of several other studies.

Finally, thank you to my family and friends, who have supported me in my pursuit of becoming a clinician-scientist in innumerable ways and to whom I am constantly grateful.

This work was done while I was in receipt of a Canada Graduate Scholarship – Master's award and later a Vanier Canada Graduate Scholarship. The studies detailed herein were funded by the Canadian Institutes of Health Research.

Table of Contents

List of Figures

List of Tables

List of Abbreviations

5-ASA	5-aminosalicylic acid (or mesalazine)
ASV	amplicon sequence variants
AUC	Area under the curve
BHI	Brain heart infusion
BPAF	Bisphenol AF
BPA	Bisphenol A
BPB	Bisphenol B
BPF	Bisphenol F
BPS	Bisphenol S
BWA	Burrows-Wheeler Aligner
cDNA	Complementary DNA
CMC	carboxymethylcellulose
COGs	Clusters of Orthologous Groups of proteins
DMSO	Dimethyl sulfoxide
DNA	Deoxyribonucleic acid
EPSPS	5-enolpyruvylshikimate-3-phosphate synthase
FDA	Food and Drug Administration
$FMNH_2$	flavin mononucleotide (reduced)
FMT	Fecal microbial transplant
HMP	Human Microbiome Project
IBD	Inflammatory bowel disease
iTOL	Interactive Tree of Life

LB	Luria broth
MetaHIT	Metagenomics of the Human Intestinal Tract
mGAM	modified Gifu Anaerobic Media
MOPS	3-(N-morpholino)propanesulfonic acid
mRNA	Messenger RNA
NCBI	National Center for Biotechnology Information
NSAID	Non-steroidal anti-inflammatory drug
OATP2B1	Organic anion transporting polypeptide 2B1
OD	Optical density
OTU	Operational taxonomic units
PCA	Principal Component Analysis
PCR	Polymerase chain reaction
PD-1	Programmed cell death protein 1
PPR	Pattern-recognition receptors
RegIIIγ	Regenerating islet-derived protein 3 gamma
RNA	Ribonucleic acid
RNA-seq	RNA sequencing
rRNA	Ribosomal RNA
SCFA	Short chain fatty acid
SFB	Segmented filamentous bacteria
sRNA	Short RNA
T_H17	T helper 17

Declaration of Academic Achievement

The work presented within this thesis is my own except where noted within each chapter and below where some aspects were done in collaboration. Experimental designs were developed by me with input from Dr. Michael Surette and members of the Surette laboratory and members of the Genes/Environment Team on Brown Adipose Tissue.

Throughout the dissertation, Dr. Hooman Derakshani, Victoria Marko, and Steve Bernier cultured and sequenced the gastrointestinal microbiota strains used in my studies. Laura Rossi performed library preparation for all RNA-seq samples.

In Chapter 2, Dr. Sharok Shekkariz assisted in visualization of the initial screening data.

In Chapter 3, Jake Sczamosi and Dr. Allison Holloway provided key input into the development of the experimental design and Jake Sczamosi also provided key guidance with the statistical analysis plan.

In Chapter 4, Carolyn Southward provided key advice into the re-creation of the promoter library. Dr. Hooman Derakshani provided key input into the sequencing strategy and Dr. Sharok Shekkariz assisted in processing sequencing data for sample identification.

The dissertation was completely written by me, with editing notes from Abraham Redda, Dr. Sharok Shekarriz, Dominique Tertigas, and Dr. Michael Surette.

Chapter 1. Introduction

1.1. The Human Gastrointestinal Microbiome

Humans, on average, have as many bacterial cells in their gastrointestinal tract as they do somatic and germ cells in their entire body (Sender et al., 2016). Despite the sheer number of cells and genes in the gastrointestinal microbiome, it is a community largely consisting of only five phyla: Bacillota (formerly Firmicutes), Bacteroidota (formerly Bacteroidetes), Actinomycetota (formerly Actinobacteria), Pseudomonadota (formerly Proteobacteria), and Verrucomicrobiota (formerly Verrucomicrobia) (Eckburg et al., 2005). The term *microbiota* refers to not only this large collection of bacteria, but also to archaea, viruses, and fungi that live in the human gastrointestinal tract. Although the gastrointestinal tract spans from the mouth to the anus, most of this multi-kingdom collection of organisms live in the largely anaerobic environment of the human colon (Sender et al., 2016).

The term *microbiome* refers to the genetic collective of multi-kingdom collection of organisms (Marchesi & Ravel, 2015). The human microbiome is substantially larger than the human genome: there are estimated to be 100 times as many microbial genes in the human microbiome than genes in the human genome (Turnbaugh et al., 2007). Further, while the human genome is greater than 99% identical across the human species, individual microbiomes can vary by greater than 50% (Gilbert et al., 2018). Together, the expansive and variable microbial genes in the gastrointestinal tract illustrate the genetic flexibility housed within this 'pseudo-organ'. This extensive microbial genetic catalogue has evolved over millions of years in symbiosis with humans and expands the functional capabilities of the human body.

1.2. Key Functions of the Gastrointestinal Microbiome

Studies ranging from *in vitro* systems and mouse models to clinical trials have highlighted important, interconnected, functions of the gastrointestinal microbiome to immunity, nutrient acquisition, and infection.

For example, axenic mouse models have provided a tool for the empirical probing of fundamental questions surrounding host-microbiome symbiosis in a variety of health and disease (reviewed in: Round and Mazmanian 2009; Atkinson and Chervonsky 2012; Maruvada et al. 2017). Axenic mouse models are *Mus musculus* which have been raised in the absence of microorganisms. These models provide direct comparisons to typical specific-pathogen-free laboratory mouse models for determining the role of the microbiome, albeit with notable physiological and immunological derangements due to breeding without any microbial exposures (Bäckhed et al., 2004; Bauer et al., 1963; Gordon, 1960; Savage et al., 1981). Colonization of axenic mice with bacterial monoculture, defined bacterial communities, or xenografted fecal samples has also been used to link the microbiota with host phenotype (reviewed in: Ericsson and Franklin 2015).

Other research has leveraged human samples and experiments to compare between those with disease with those without the pathology to determine differences between the two groups. A notable example is the case of peptic ulcer disease and Barry Marshall's discovery of culturable *Helicobacter pylori* capable of causing gastritis (Marshall & Warren, 1984; Robin Warren & Marshall, 1983). Determination that these microbes resided in the stomachs of those with peptic ulcer disease required biopsy sampling and culture. Another, more recent, but ongoing and complex,

example is inflammatory bowel diseases where differences observed in the microbiome between patients and healthy volunteers is challenging due to differences in study methodologies (reviewed in: Huttenhower et al. 2014). Nevertheless, these studies note consistent reductions in *Eubacterium* and *Akkermansia* in disease populations are observed.

1.2.1. Regulation of immunity

Broadly, immunity can be divided into innate and adaptive immunity.

Innate immunity, broadly, consists of first line defense against infections. Examples of innate immunity include physical barriers such as skin or the gut epithelial barrier and general host receptors on cell surfaces and in host cells, called pattern-recognition receptors (PRRs), which survey for the presence of pathogenic factors.

Notably, many mechanistic insights in the relationship between innate immunity and the microbiome have been derived from mice models. However, human studies have linked altered intestinal mucosal barrier histopathology with gastrointestinal diseases ranging from celiac disease to inflammatory bowel diseases (IBD) (Alipour et al., 2016; Sapone et al., 2011). Whether these are cause, consequence, or some mix of both regarding the diseases' etiology, is poorly understood.

With respect to adaptive immunity, segmented filamentous bacteria (SFB) were one of the first microbes identified to have immunomodulatory relationships with their host, *Mus musculus* (Umesaki et al., 1995). These microbes were first found by microscopy due to their notable adherence to intestinal walls in the terminal small

intestine (Davis & Savage, 1974; Koopman et al., 1987). This biogeographical location of colonization proximal to the host where many immune cells are located led to research highlighting their key role in chemokine, antimicrobial production stimulation, and T helper 17 (T_H17) cell differentiation by the host (Schnupf et al., 2017; D. Zheng et al., 2020).

Despite its initial promise, SFB research has been limited by an inability to culture the organism in isolation as well as its small genome size and limited biosynthetic capability (Jonsson et al., 2020). All of these qualities are likely closely linked and result in highly specific host-SFB relationships where SFB from *Mus musculus* cannot colonize *Rattus norvegicus*, and vice versa (Tannock et al., 1984).

The existence of SFB in healthy humans also remains controversial. The only known whole genome sequence data supporting SFB colonization of a human arises from an ileostomy sample (Jonsson et al., 2020). At the same time, the ability of SFB to potently stimulate host immunity is not unique – one study cultured axenic mice with individual isolates of human gastrointestinal bacteria and found that *Bifidobacterium adolescentis* induced T_H17 cells in mice at levels similar to SFB (Tan et al., 2016). While SFB may be best described in mice, *B. adolescentis* is well described in the core human microbiome and, therefore, it is possible that prevalent, and known members of the human microbiome have immunomodulatory properties.

Adaptive immune functions of the human microbiota have been shown to have significant clinical implications, as evidenced by their intersection with anti-neoplastic therapy. For example, species of *Bifidobacterium* have been shown to enhance the T-cell dependent effects of checkpoint inhibitor immunotherapy (Sivan et al.,

2015). Fecal microbial transplant (FMT) has been shown to be effective in melanoma patients with resistance to anti- programmed cell death protein-1 (PD-1) checkpoint inhibitor immunotherapy (Baruch et al., 2021; Davar et al., 2021). Notably, microbiome analysis of fecal samples from patients after FMT notes members of the family *Bifidobacteriaceae*, which *B. adolescentis* is part of, are enriched after transplantation and with improved immunotherapy efficacy. Whether any species of *Bifidobacteriaceae* is sufficient, rather than necessary, is more difficult to disentangle because the degree of functional redundancy in the gut microbiome is poorly understood.

1.2.2. Fermentation to produce key metabolites

Outside of immune function, host-microbe symbiosis is tied with metabolism to produce nutritional benefits for both the human host and the microbiota. For example, bacteria, such as *Bacteroides*, can express glycoside hydrolases that digest dietary complex polysaccharides (such as xylan-, pectin-, and arabinose-containing polysaccharides) and endogenous intestinal mucus into simple sugars, which humans lack the genetic machinery to degrade (Lapébie et al., 2019). Products of the fermentation process not only produce sugars that the host can utilize but also produce the precursors necessary for other gastrointestinal bacteria to generate short chain fatty acids (SCFAs).

The majority of SCFAs produced are butyrate, propionate, and acetate (Cummings et al., 1987). Butyrate is not only the primary carbon source for human colonocytes but also has been shown to induce apoptosis of colon cancer cells, and beneficially influence energy homeostasis via activation of intestinal gluconeogenesis (De Vadder et al., 2014). Butyrate is also essential for the consumption of oxygen by

epithelial cells via β- oxidation and thus contributes to the generation of a hypoxic colonic environment (Byndloss et al., 2017). Similarly, propionate has been implicated in colonization resistance against an array of pathogens from the *Enterobacteriaceae* family and regulates hepatic gluconeogenesis (De Vadder et al., 2014). Acetate is an essential metabolite for the growth of certain gastrointestinal bacteria and can reach peripheral tissues where it is involved in cholesterol metabolism and lipogenesis (Frost et al., 2014). In a recent open-label, parallel group, randomised control trial comparing treatment as usual versus treatment as usual with a high-fiber diet in type 2 diabetes patients, higher SCFA production by the gastrointestinal microbiome correlated with lower diet-induced obesity and reduced insulin resistance (Zhao et al., 2018). Together, bacterial fermentation and SCFA production serve as just one example of host-microbiome mutualism where microbes benefit from access to dietary and endogenous polysaccharides as food and, in turn, the host benefits from the production of various key metabolites.

Host-microbiome metabolic symbiosis reflects three distinct but interrelated levels of the microbiome, the host, and the environment (Bäckhed et al., 2005). At the microbiome level, there are individual microbial growth rates, adaptation capabilities and rates, substrate utilization patterns and chemical interactions between microbes. At the host level, there are heritable components to gut microbiota composition and host cell function, mucosal immunity, colonic motility, and biogeographical niches/gradients of nutritional components and host secretions. At the environment level, there are fluctuations in fluids, macronutrients, and xenobiotics. Disturbances at

any of the three levels of host-microbiome symbiosis impacts the other levels and can impact human health.

1.2.3. Resistance to pathogen colonization

On such example of deleterious consequences of disurbances in the host-microbiome symbiosis is in patients with short bowel syndrome. In these patients, small intestinal bacterial overgrowth is a common and recurring complication where normally commensal bacteria cause severe adverse clinical outcomes almost entirely attributable to the altered host anatomy of decreased bowel length.

Specific food components also correlate with different microbiota in mice and rat studies. For example, sugar alternatives such as sucralose fed to mice for 6 months increased the expression of bacterial pro-inflammatory genes and altered faecal metabolites (Bian et al., 2017).

Gastrointestinal infection secondary to oral antibiotics is one prominent example of a single chemical, in the form of an antibiotic, altering the gastrointestinal microbiota. Such a chemical that is not naturally produced or expected in the host is more broadly called a xenobiotic. In the case of antibiotics, their broad-spectrum activity results in concomitant depletion of commensal microbiota along with the target pathogen. A known consequence of this depletion is reduced host resistance to infection by pathogens such as *Salmonella enterica,* or *Clostridioides* (formerly *Clostridium*) *difficile*. The commensal microbiota mediate this host resistance either indirectly, via host immunomodulation, or directly, by producing antimicrobial products or occupying necessary nutritional niches. Studies in mice models have illustrated the ability of certain strains of *Bacteroides* and *Bifidobacterium* to stimulate host innate

immunity in the production of regenerating islet-derived protein 3 gamma (RegIIIγ), a C-type lectin with antimicrobial properties against Gram-positive bacteria like *Enterococcus* species (Cash et al., 2006; S. G. Kim et al., 2019; Natividad et al., 2013; Vaishnava et al., 2011). Similarly, *Bacillus thuringiensis* isolated from human fecal samples has been shown to produce antimicrobials that kill *C. difficile* (Rea et al., 2010). In arguably the least combative but still effective of mechanisms, other commensal microbiota leverage nutrient availability to prevent infection mechanisms from being initiated by pathogenic bacteria, as with commensal *Escherichia coli* directly competing with *Citrobacter rodentium* for carbohydrates to prevent *C. rodentium* infection (Kamada et al., 2012).

Nonetheless, pathogens may also be able to utilize nutrients for overcoming commensal microbiota resistance mechanisms. For example, recent evidence in mice suggests that, in the presence of nitrate, the pathogen *Salmonella* Typhimurium can use propionate as an energy source in anaerobic respiration to overcome colonization resistance from gastrointestinal microbiota and increase its growth rate (Shelton et al., 2022).

Clinically, improved understandings of colonization resistance has led to arguably the most successful microbiota-based therapy to date: FMT. FMT has now become the standard of care for patients with *C. difficile* diarrhea and recently also led to the Food and Drug Administration (FDA) approval of the first fecal microbiota product (McDonald et al., 2018; Walter & Shanahan, 2023). While complex, due to the evolving nature of the sample being administered, significant, positive results have been achieved clinically, with outcomes illustrating effectiveness on par with antibiotic

therapy (Juul et al., 2018). However, understanding of the underlying mechanism remains modest at best and probably relating to complexities of the host-microbe symbiosis relationship.

1.3. Human Therapeutic Drugs and the Human Gastrointestinal Microbiome

1.3.1. Modern human therapeutic drugs

Drug therapy in medicine dates to prehistoric times when xenobiotics in crude plant extracts were used to treat diseases with poor purity, dosing, efficacy, and, therefore, significant adverse effects. In the late 19th century and early 20th century, a massive expansion in chemical development occurred with the discovery of the first non-steroidal anti-inflammatory drug (NSAID), acetylsalicylic acid (aspirin), for pain, digoxin and nitroglycerin, for cardiac disease, insulin, for diabetes mellitus, and sulfa drug antibiotics, for bacterial infections. These medications were subsequently mass produced and are still mainstays in health care. Further development since their arrival has greatly expanded the medical repertoire to thousands of chemicals and drug therapy remains at the center of the medical management of disease.

While many of these medications greatly improved mortality and morbidity, side effects, toxicity, and varying efficacy across patient populations persisted and remained puzzling. For example, at the time of their initial development and research, NSAIDs and antibiotics were noted to have accompanying gastrointestinal side effects (Binns, 1956; Douthwaite & Lintott, 1938). In addition, digoxin toxicity varied

between patients and the drug was shown to be less toxic to some patients (Luchi & Gruber, 1968).

These outstanding concerns have persisted for decades since, despite ongoing efforts to improve drug efficacy and safety.

1.3.2. Modulation of drug toxicity by the gastrointestinal microbiome

Recent investigations have linked these medications with the gastrointestinal microbiota highlighting a substantial role of the microbiome in pharmacotherapy.

Next-generation sequencing studies have illustrated interactions between a wide range of drugs - from NSAIDs, to antibiotics, to proton-pump inhibitors, to anti-psychotics – and the gut microbiome (Flowers et al., 2017; Forslund et al., 2013; Imhann et al., 2016; Jackson et al., 2016; Rogers & Aronoff, 2016). These studies were unable to ascertain direct versus indirect (i.e. host-mediated, diet-mediated) relationships between the gut microbiota and therapeutic drugs.

The ability of the microbiota to impact drug toxicity was noted as early as 1982, when the key role of a common gut microbe, *Eggerthella lenta* (formerly *Eubacterium lentum*), in digoxin inactivation and reduced toxicity was observed (Dobkin et al., 1983). Recent work by Haiser, Seim, Balskus, and Turnbaugh have identified specific genes in *Eggerthella lenta* responsible for this inactivation (Haiser et al., 2014).

Inversely, the microbiome produces β-glucuronidases, which convert irinotecan, an anti-cancer agent, into SN-38, the molecule responsible for clinically significant side-effects such as severe diarrhea requiring hospitalization or cessation of chemotherapy (Bhatt et al., 2020; Wallace et al., 2010). Beyond irinotecan, recent studies have systematically mapped *in vitro* human microbiome drug metabolism with

microbiome gene content, finding 176/271 (67%) of screened drugs were metabolized by at least one bacterial strain (Zimmermann et al. 2019).

1.3.3. Modulation of drug efficacy by human microbiota

In addition to the previously discussed examples of cancer therapies, the gastrointestinal microbiome can also mediate the efficacy of medications used for a range of diseases, from IBD to Parkinson's disease. Notably, Zimmermann et al. (2019) suggested that food components serve as key substrates in microbiota metabolism of human drugs.

Sulfasalazine is a commonly used anti-inflammatory prodrug used in the management of IBD with a noted azo linkage that is metabolized by the gut microbiota into the active molecule, mesalazine (5-ASA). 5-ASA is metabolized further into inactive N-acetyl 5-ASA, a chemical transformation that 44% of culturable anaerobic bacteria were found capable of performing (Maier et al., 2018; van Hogezand et al., 1992). Individual microbiota positioning on the fulcrum of azo linkage cleavage and acetylation has been hypothesized to explain differences in sulfasalazine efficacy between patients (Koppel et al., 2017). Recent studies have linked the presence of certain bacterial enzymes in the gastrointestinal microbiota with efficacy of 5-ASA (Mehta et al., 2023).

Levodopa is the mainstay medication in the management of Parkinson's disease, with increasing dosing necessitated by disease worsening, but the medication is also associated with severe adverse effects. The efficacy of levodopa is variable between individuals and dependent on non-metabolized molecule reaching the central nervous system after oral consumption and blood stream passage. Recent studies have

highlighted not only the activity of a conserved bacterial tyrosine decarboxylase in metabolizing levodopa in the gastrointestinal tract but also identified small molecule inhibitors that dampening this microbial metabolism in mice models (Rekdal et al., 2019; van Kessel et al., 2019, 2021).

These findings highlight the key role of the microbiota in explaining variations in drug efficacy between patients and potential avenues for personalized medical interventions dependent on individual microbiota functionality.

1.3.4. Assessing direct growth impacts on gastrointestinal microbiota

In addition to metabolizing drugs, the gastrointestinal microbiota is also impacted in its growth by medications.

One of the earliest examples of the utility of *in vitro* characterization was by Kwok, Tally, Sutter, and Finegold in 1975, who demonstrated the testing of routinely used antibiotics on 55 different human microbiota isolates, thus providing the foundation for routine clinical laboratory susceptibility testing in anaerobic infections (Kwok et al., 1975). This work also quantified the substantive impact of antibiotics on growth of non-target microorganisms.

Since these initial experiments with antibiotics, the repertoire of chemicals available to clinicians has expanded significantly, particularly non-antibiotic drugs targeting host pathways. A systematic screen of 40 human gut microbiota species clarified that many of these drugs caused direct impacts on microbial growth (Maier et al., 2018). Such experiments, provide entire subfields of research for improving understanding of xenobiotic mechanism, drug response, and adverse effects.

1.4. Agri-food chemicals and the Human Gastrointestinal Microbiota

1.4.1. Expansion of agrochemical use and associated health effects

Like pharmacotherapy for human diseases, for centuries, humans have utilized pesticides for crop diseases, packaging for food safety, and colouring for food aesthetics. These agri-food chemicals vastly improved global food security over the past century and facilitated significant progress in human development but have also raised contentious concerns about their effects on human and environmental health.

The earliest examples of pesticides were chemicals extracted from the environment, such as in the case of elemental sulfur dusting, or pyrethrum, extracted from chrysanthemums. With the expansion of chemicals for human therapeutics in the early 1900s also came the expansion of chemicals for agricultural use as insecticides, herbicides, and fungicides. This was marked by Paul Müller's discovery of the pesticidal activity of dichlorodiphenyltrichloroethane (or DDT) (Müller, 1946). DDT proved to not only be highly effective in curbing vector-borne diseases such as malaria and typhus, but it also quickly became a popular agent in households and commercial crops for pest control. Evidence decades later highlighted separate functions of DDT in endocrine disruption in wildlife and humans, and likely carcinogenicity, at exposure doses relevant to malaria control (Cohn et al., 2015; Matthiessen et al., 2017).

While DDT was banned in many countries starting in the 1970s, newer pesticides, such as organophosphates, have undergone similar courses, from initial discovery to widespread use, to concerns about environmental health, and finally

either decline or restrictions of use (reviewed in: Hertz-Picciotto et al. 2018). Global usage data for pesticide use remains of poor quality or scant; however, the trend of pesticide usage, as estimated by various sources, has persistently increased, with the global north using the highest quantity of pesticides, but with significant growth in usage in developing countries in recent years (reviewed in: Landrigan et al. 2018; Swagata Sarkar et al. 2021). This is despite the well-established negative impact of many these chemicals on human and environmental health.

Advances in food packaging have also revolutionized modern food security, preventing spoilage, lengthening shelf life, and enabling efficient transportation. Over the past two centuries, materials and techniques such as tin canning, and later, plastics were invented and deployed in food production. Little testing was conducted to assess the safety of many of these compounds for human consumption despite evidence that they do leach into food and liquids (Brotons et al., 1995; M. He et al., 1993; Paseiro Losada et al., 1993; Rufus et al., 1994). Most famously, bisphenol A (BPA) is used in the lining of canned foods and for the synthesis of polymers to construct plastic containers. BPA has been linked with a range of endocrinologic issues and had widespread replacement by other bisphenols, such as bisphenol S (BPS) and bisphenol F (BPF). The health implications of the bisphenols in humans, from reproductive implications to metabolic disease, is likely, but highly controversial, and of ongoing inquiry (reviewed in: Vandenberg et al. 2009).

In addition to food production and packaging xenobiotics that unintentionally are ingested, food additives are intentionally added to foods. Food additives have been a part of human diets beginning with the addition of preserving agents and food

colours. Due to public concern regarding unknown colourants and several noteworthy mortalities caused by dangerous food colouring, food dyes were some of the first agri-food chemicals to be regulated (Burrows, 2009). Most countries now limit acceptable synthetic food dyes to a small list of, typically, less than 10 compounds (Lehto et al., 2017).

But early and strict regulation has not limited the controversy regarding the role of food colouring in human disease and evidence supporting the link between food colouring and neuropsychiatric conditions, such as attention-deficit hyperactivity disorder in children, continues to be contentious (McCann et al., 2007). Other possible health concerns linked to food dyes include a possible role in colitis, hypersensitivity reactions, and carcinogenicity (Hashem et al., 2010; Z. He et al., 2021; Kobylewski & Jacobson, 2013).

Research to understand risks associated with agrochemical exposure is complicated by several factors, including: the ethical considerations of running any potential randomized control trials with toxin exposure; the inadequacy of national and international systems in quantifying the route and amount of exposure between people in the general people across various regions; and misaligned incentives between stakeholders (Allen et al., 2015; Pingali, 2012). Even a systematic understanding of global pesticide exposure mapping and risk to human health is lacking, with one for environmental impacts to soil, water, and atmosphere only recently completed (Maggi et al., 2019). Similarly, little is known about plastics in human biology and a disconnect was noted, in one recent scoping review, between public interest in safety

for human health and research foci on improved production and processing techniques (Yates et al., 2021).

Despite these challenges, various forms of study designs have allowed for consistent evidence linking various agrochemical exposures with chronic increased risks for neoplasias, reproductive abnormalities, immunological dysfunction, and metabolic derangement (Roingeard et al., 2021; Rubio-Rivas et al., 2017; Sharma et al., 2021). The power of these studies to elucidate mechanism or risk models has been limited as most are retrospective and observational epidemiologic studies.

To address the lack of mechanism, others have focused on laboratory testing in animal models with the goal of elucidating any such mechanism of action (Z. He et al., 2021; Polic, 2018; Wang et al., 2021). However, it is unclear whether the health effects of individual chemicals is more likely to be a stochastic risk with increasing exposure or deterministic risk where one exposure may be sufficient to cause harm. Such risks may not be captured well in typical laboratory experiments.

Many of the human diseases linked with agrochemical exposure have notably also been correlated with gut microbiota and therefore have led to hypotheses and emerging evidence that the gut microbiota may be the mediating element in agrochemical-related health effects (Z. He et al., 2021; Liang et al., 2019; Velmurugan et al., 2017).

1.4.2. Pesticides and the gastrointestinal microbiota

With increased attention to the microbiome in the past decade, research has expanded significantly assessing the impact of pesticides on the gastrointestinal microbiota. The majority of this research has focused on evaluating the microbiome

with sequencing. This experimental design typically involves the application of a herbicide, insecticide or fungicide to an animal model. Exposure windows on the model organism are either focused on either developmental or adult exposure and a wide range of exposure concentrations (reviewed in: Chiu et al. 2020). These studies have highlighted a wide range of pesticide chemicals that correlate with microbiome changes and commonly described host impacts, such as metabolic derangements. Notably, a couple of studies, using chlorpyrifos and permethrin, have also noted changes in SCFA levels (Guardia-Escote et al., 2020; Nasuti et al., 2016).

One recent study in honeybees (*Apis mellifera*), which highlighted microbiome changes with glyphosate exposure (Motta et al., 2018). These changes are likely a result of a homologous gene in the honeybee gut microbiota to 5-enolpyruvylshikimate-3-phosphate synthase (EPSPS), the target of glyphosate in plants for weed control (Mesnage & Antoniou, 2020). This impact in turn results in decreased levels of key microbes necessary for colonization resistance to the bee pathogen *Serratia marcescens*. This effect was not observed with metabolites of glyphosate and also was noted to be ablated with certain variants of EPSPS.

EPSPS is not present in vertebrates, but is present in plants, archaea, and bacteria. With both the increased prevalence of glyphosate resistance in weeds and an increased understanding of the role of the human microbiota in human health, efforts to better characterize EPSPS have led to bioinformatic analysis to classify variants of EPSPS and predict glyphosate-resistant and -sensitive protein sequences. In an *in silico* screen of over 250 gut microbiota genomes, one tool conservatively predicted that

over 50% of common gut microbiota strains are sensitive to glyphosate (Mesnage & Antoniou, 2020).

Considering the evidence of impacts of these chemicals directly on host physiology in animal studies, it is uncertain whether the observed changes in microbiome composition and metabolite profile is mediated via the host environment or is a result of direct impacts on the microbiota. Few studies have extended their research to directly test the impact of pesticides on gut microbiota.

1.4.3. Food additives and the gastrointestinal microbiota

Food additives, from emulsifiers to azo food dyes, are known to interact with a wide range of gastrointestinal microbiota. Although almost all of these chemicals have been generally regarded as safe, research completed at the time of their regulation was focused on direct impacts on host physiology, such as assessments pertaining to neoplasia risk.

Work by Chassaing and colleagues, first in mice in 2015 and, more recently, in a randomized control trial in humans, highlighted the impact of commonly used emulsifiers on gastrointestinal microbiota (Chassaing et al., 2015, 2022). In mice, these changes were found to result in colitis. Similarly, in humans, subtle pathological changes of intestinal inflammation secondary to microbiota encroachment into the intestinal epithelial layer were noted in 2 participants exposed to the synthetic emulsifier carboxymethylcellulose (CMC). While neither of these studies definitely link emulsifiers with the onset of inflammatory bowel diseases or other inflammatory conditions in humans, they provide further support that this link may be mediated by the gut microbiota- agrochemical interaction.

Similarly, synthetic food dyes are ubiquitous in modern food consumption and azo food dyes, characterized by the azo bond chemical motif within their structure, are the most common synthetic food dyes in the world. Azo dyes have been shown to interfere with gastrointestinal drug absorption in axenic mice by inhibition of the Organic anion transporting polypeptide 2B1 (OATP2B1) intestinal transporter with reintroduction of microbiota restoring this function (Zou et al., 2020). The microbiota is known to cleave azo bonds via reductive metabolism under anaerobic conditions, although this functionality varies across different species and is not well characterized with respect to the sequence of chemical reactions, *in vivo* dynamics, and possible metabolites produced. Considering nitrogen may be the limiting metabolite in the mammalian intestine and azo dyes have recently been linked with colitis in mice, the role of azo dyes and their metabolites as potential nitrogen sources may relate to eutrophication and degradation of the intestinal environment (Reese et al., 2018). As well, typical dietary concentrations of azo dyes in diets rich in processed foods may saturate the enzymatic capabilities of the gut microbiota to reduce azo dyes, resulting in clinically meaningful alterations in drug efficacy and toxicity (Zou et al., 2020).

1.4.4. Food-packaging chemicals and the gastrointestinal microbiota

Public interest in the effects of plastic compounds on human health is substantial although little is known regarding exposure levels in diets and what breakdown products may be liberated and physiologically meaningful. Notably, public concern regarding BPA has led to the increased usage of several different derivatives, such as BPS. BPS is generally regarded as safe by regulators such as the FDA, although emerging evidence in animal models suggests they may impact host

physiology and reproduction adversely through independent pathways from BPA (Chen, Shu, et al., 2016).

The focus of the current literature on bisphenols and the gut microbiota has consisted almost entirely on BPA, which has been shown to alter microbiota composition in various animal models (Linares et al., 2021; McDonough et al., 2021; Ni et al., 2021). One recent report did note that zebrafish exposed to BPA, BPS, and BPF had altered microbiome composition with sequence-based analysis, compared to fish treated with BPB or BPAF (Catron et al., 2019). Surprisingly, microbiome alterations were inversely related to host physiological dysfunction in this study, leaving questions regarding the nature of the host-microbiota-bisphenol relationship. Further, this study was conducted during the developmental stage in zebrafish, highlighting the potential role of early life exposure to these chemicals in shaping the gastrointestinal microbiota as it changes through development. Notably, recent epidemiological studies have linked certain plastic-related compounds with immunologic disease risk in children years after their exposure, highlighting the importance of early life immunologic development, which the gastrointestinal microbiota is involved in (Navaranjan et al., 2021).

1.5. Studying the Human Gastrointestinal Microbiome and Microbiota

As mentioned in the previous section, the methodology selected limits the type and amount of data collected, which, in turn, offers only one particular point of view from which we can draw conclusions about the microbiome.

Available methodologies for the study of human gastrointestinal microbiome and microbiota began with culture-dependent methods from Antonie van Leeuwehoek in the 1600s and Louis Pasteur in the 1800s to culture-independent molecular approaches in the 2000s. These techniques also leveraged taxonomic classification systems that began with Carl Linnaeus in the 1700s to classify distinct organisms. Although the past two decades have seen a rapid increase in appreciation for and excitement about the human gastrointestinal microbiome, much of this has focused on leveraging culture-independent methods. However, there is now growing appreciation that the gastrointestinal microbiota is largely culturable and that culturing enables mechanistic understanding of microbiota of interest not achievable from culture-independent approaches alone (Browne et al., 2016; Lagier et al., 2016; Lau et al., 2016).

1.5.1. Culture-independent approaches

Advances in high-throughput sequencing technologies over the past two decades have enabled extensive, high-resolution surveys such as The Human Microbiome Project (HMP) in the United States and Metagenomics of the Human Intestinal Tract (MetaHIT) in Europe (J. Li et al., 2014; Turnbaugh et al., 2007). These initiatives leveraged techniques such as 16S ribosomal ribonucleic acid (rRNA) gene sequencing to characterize complex microbial communities.

16S rRNA gene sequencing first came to prominence in 1977 with Woese and Fox's discovery of the three domains of life (Bacteria, Archeae, and Eukarya) (Woese & Fox, 1977). This gene contains areas of high conservation and high variability across the bacterial and archaeal kingdoms, enabling the distinction of distantly and

closely related organisms for taxonomic assignment. Ten years after this initial application, the first technique for efficient 16S gene sequencing was developed (Lane et al., 1985). The 1990s saw the general acceptance of the universal Tree of Life by the scientific community and by 1994, more than 1,500 Bacteria and Archaea 16S rRNA genes had been sequenced (Pace et al., 2012; Woese et al., 1990; Zhulin, 2016). Today, the current release of the SILVA rRNA database project (August 2020) contains over 9 million rRNA sequences (Glöckner et al., 2017; Pruesse et al., 2007).

High-throughput sequencing techniques, such as with Illumina platforms, allow for sequencing regions of the 16S rRNA gene at relatively high volume and low cost compared to previous techniques. Universal primers that complement conserved regions of the 16S rRNA gene enable amplification reactions for 16S rRNA variable regions from samples with mixed bacterial communities (Bartram et al., 2011; Caporaso et al., 2011). Barcoded regions in these primers enabled indexing and pooling of many samples into a single Illumina sequencing reaction.

But with substantially increased sequencing throughput comes significant computational bottlenecks. Gigabytes of sequences produced from a single sequencing reaction must undergo demultiplexing by sample barcodes, removal of sequencing-associated adapters, and be binned into operational taxonomic units (OTUs) or amplicon sequence variants (ASVs) (Callahan et al., 2016; Konstantinidis & Tiedje, 2005). These OTUs, or ASVs, are then assigned taxonomy using databases such as the SILVA database. Outputs can then be parsed further and analyzed using any number of tools and statistical methods to answer research questions about taxonomic differences between groups, and so on.

Several other culture-independent techniques have become increasingly common in the analysis of polymicrobial samples.

Shotgun metagenomic sequencing surveys the genetics of an entire community and includes not only bacterial sequencing data, but also viral, fungal and archaeal sequencing data (reviewed in: Gilbert and Dupont 2010). Deoxyribonucleic acid (DNA) from a sample is tagmented for sequencing and ligated with adapters that enable binding Illumina sequencing. Data from metagenomics can provide insight beyond just community composition and extends into gene and pathway enrichment analysis, assembly of metagenomes, and calculation of single nucleotide variant frequencies.

Metatranscriptomic sequencing identifies the genes that are actively expressed in a community at the given time the sample was extracted (reviewed in: Bashiardes et al. 2016). This allows for further resolution beyond the genetics of the community to what the community is actively expressing. RNA from a sample is depleted of rRNA, the most highly expressed RNA sequence in a sample and a common obfuscator of changes in messenger RNA (mRNA) or small RNA levels (sRNA). This depleted sample is converted to complementary DNA (cDNA) and the cDNA undergoes adapter ligation/amplification for high-throughput sequencing.

Metabolomics and metaproteomics is the characterization of metabolites and proteins produced by a microbial community, respectively (Stamboulian et al., 2022). While several methods exist, typically for metabolomics samples are pre-treated to extract molecules which are then separated by liquid or gas chromatography and analyzed by mass-spectrometry. Results from mass-spectrometry provide quantities of

molecules and databases can be used for identification of each signature from the spectrometer.

Each shotgun-based approach has shared known obstacles, including insufficient taxonomic resolution, particularly of less abundance organisms, to a reliance on reference databases in their relative infancy to only providing a snapshot from when the sample was extracted. Genomic-based approaches also suffer from an inability to distinguish between live and dead bacteria. To tackle these challenges, microbiota studies in the laboratory on cultured bacteria have gained traction because they permit more mechanistic probing of the function of microbiota members to address these limitations.

1.5.2. Culture-dependent approaches

Culture-dependent methods enable microbiota studies in the laboratory. While culture-based approaches are commonly criticized in many culture-independent publications over the past two decades for only capturing a small portion of the gastrointestinal microbiota, this criticism has been shown to be inaccurate. As early as 1974, Sydney Finegold demonstrated the cultivability of hundreds of species from gastrointestinal samples by using a broad panel of agar plates (Finegold et al., 1974). Specific growth conditions can also be included to enrich for certain microbiota species, particularly those in low abundance or those that are fastidious growers (Derrien et al., 2004; Sibley et al., 2011). Recently, by using a range of agar plates with various growth conditions, almost all of the human gastrointestinal microbiome, as measured by metagenomics, is culturable (Browne et al., 2016; Lagier et al., 2016; Lau et al., 2016).

Further, unlike metagenomic studies, where distinguishing between live and dead bacteria in a community is not possible, culture-dependent approaches are able to characterize the live members of the microbiota. By culturing and isolating gastrointestinal microbiota species, experiments involving *in vitro* characterization of function are made possible.

While shotgun metagenomic sequencing can provide metagenomically assembled genomes, well-assembled genomes are often limited to the most abundant bacteria in a population. By leveraging culture-based methods, isolated bacterial colonies can be used for whole-genome sequencing and provide high-quality draft genomes for less abundant species.

An extension from genomic characterization of bacteria is gene expression characterization to determine what genes of a given bacterial genome are actively expressed in a given environment. Several approaches exist to capture a global image of gene expression from *in vitro* bacterial cultures, from random promoter libraries to RNA sequencing (RNA-seq; Bjarnason et al., 2003; Kuchina et al., 2021).

Random promoter libraries are a high-throughput approach enabling non-invasive, non-terminal, monitoring of gene expression. The cloning vector used for library construction contains the entire *luxCDABE* operon from *Photorhabdus luminescens* (reviewed in: Meighen 1991; Meighen 1993). *luxA* and *luxB* encode the two subunits of the luciferase responsible for catalyzing the critical reaction. *luxC*, *luxD*, and *luxE* express the fatty acid reductase complex responsible for synthesis of the luciferase substrate, a fatty acid aldehyde, from a fatty acid. The luciferase LuxAB oxidizes the aldehyde with reduced flavin mononucleotide ($FMNH_2$) to produce FMN, water, the

fatty acid, and light emission at 495nm. This bioluminescence operon is placed downstream of a promoter cloning site. Fusion of a transcribed gene promoter into the cloning site results in transcription of the *luxCDABE* operon and spontaneous production of bioluminescence. Bioluminescence can therefore be monitored as a marker for transcription of the gene promoter in a sensitive, rapid, accurate manner.

Random promoter library construction involves ligation of randomly fragmented genomic DNA from an organism, such as *Salmonella enterica* serovar Typhimurium, into this plasmid vector (Bjarnason et al., 2003). Clones are picked and screened for bioluminescence across several growth conditions which enable identification of the vast majority (>99%) of gene promoters in the genome. Identified clones are re-arrayed and constitute the final random promoter library.

This library can then be screened against several different growth conditions at numerous time points to determine the physiological state of the bacterium in different environments. Transcription can be measured using a microplate reader capable of counting chemiluminescence and varying levels of transcription can be quantified based on the intensity of light emission counted. Measurements can be taken as often as desired and standardization is readily possible between experiments to support reproducibility and comparability. Screening inputs are low because assaying can be performed manually with pin replicators and only requires access to a plate reader, incubator, and microplates.

While random promoter libraries are highly advantageous in regard to sensitivity, cost, reproducibility and ease of use, they rely on genetically tractable model organisms. For non-model organisms, high-throughput sequencing, is the

preferred method to detect temporal or environmental differences in gene expression. Even so, molecular and computational tools applicable to many non-model species are lacking.

RNAtag-seq involves the extraction of whole RNA from bacterial cultures followed by tagging of each sample and pooling of the tagged samples to enable multiplexing so fewer samples are prepared and therefore lower sequencing library preparation costs are incurred (Shishkin et al., 2015). rRNA is depleted from pooled samples to remove non-informative sequence data and cDNA is synthesized by reverse transcription (Huang et al., 2020). This single stranded cDNA is used as the template to ligate on adapters that include barcodes for further sample pooling and sequences to enable annealing onto high-throughput sequencing flow cells (like Illumina). Bioinformatic tools are then used to demultiplex samples, trim unwanted sequence data, and conduct statistical testing to answer the differential gene expression hypothesis being tested with the given experimental design.

1.6. Central Paradigm

The gastrointestinal microbiota has been increasingly studied as a mediator of human health, in the onset of disease, in disease progression, and as a key treatment target. While non-dietary components of human diets such as pharmacotherapy have been systematically characterized to better understand the relationship between the microbiota and xenobiotics, little research exists assessing the direct impact of agri-food chemicals on the human gastrointestinal microbiota, particularly at doses relevant to exposure for the general population. However, greater appreciation and

attention has been given to both the impact of agri-food chemicals on environmental health and the role of the human microbiome. In order to better understand the relationship between agri-food chemicals and the human gastrointestinal microbiota, the direct impact of agri-food chemicals on gastrointestinal microbiota needs to be better understood.

I hypothesize that, using anaerobic screening of a representative panel of gastrointestinal microbiota species, I will identify direct and novel toxicity and transcriptional modulation of gut bacteria by an array of agri-food chemicals pervasive in modern diets. This approach will also allow for probing of key findings using highly sensitive real-time changes with *in vitro* screening in a random promoter library. Finally, to assess for rapid and cost-effective differences in metabolite production, biosensors will be developed to facilitate future studies to assess metabolomic impacts of agri-food chemicals.

1.6.1. Specific Hypotheses

1. I hypothesize that a subset of microbiota strains will be impacted in their growth and transcription upon exposure to physiologically relevant concentrations of individual common agri-food chemicals.
2. I hypothesize that at concentrations sub-inhibitory to growth impacts, I will observe changes in transcriptional profiles.

Aims

To address my hypotheses, my research aims to:

1) Characterize gut microbiota growth in the presence of an annotated agricultural chemical library (**Chapter 2**).

2) Characterize gut microbiota transcription in the presence of select agri-food chemicals of interest (**Chapter 3**).
3) Construct and screen a random promoter library in the gut-adapted microbe *Salmonella* Typhimurium to confirm and expand on transcriptional impacts of a particular agrochemical. Apply the same methodology to develop SCFA biosensors that enable profiling of microbial fermentation products from bacterial cultures (**Chapter 4**).

Chapter 2. Impact of agri-food chemicals on human gastrointestinal microbiota

Preface

Research presented as part of this chapter has been prepared for publication as:

Syed SA, Rossi L, Shekkariz S, Derakshani H, Marko VA, Bernier SP, Barra NG, Holloway AC, Schertzer JD, Khan WI, Steinberg GR, Morrison KM, & Surette MG. Bisphenol S, a BPA-substitute, impacts growth of commensal gastrointestinal *Bifidobacterium adolescentis*. *In preparation*.

Author contributions: SAS, LR, SS, HD, NBG, ACH, JDS, WIK, GRS, KMM, and MGS contributed to the intellectual design of the study. SAS, performed all experiments. LR assisted with library preparation of RNA samples. Isolate collection and sequencing was performed by HD, VAM, and SPB. Data analysis was performed by SAS, SS, and MGS. SAS wrote the manuscript.

This publication is in preparation for publication and up to date as March 19, 2023.

Title page and author list

Bisphenol S, a BPA-substitute, impacts growth of commensal gastrointestinal *Bifidobacterium adolescentis*

Saad A. Syed[1], Laura Rossi[2], Shahrokh Shekkariz[1], Hooman Derakshani[1], Nicole G. Barra[1], Alison C. Holloway[1,3], Jonathan D. Schertzer[1], Waliul I. Khan[1], Gregory R. Steinberg[1,2], Morrison KM[1] & Michael G. Surette[1,2,*]

[1]Department of Biochemistry and Biomedical Sciences, McMaster University, Hamilton, Canada

[2]Department of Medicine, McMaster University, Hamilton, Canada

[3]Department of Obstetrics and Gynecology, McMaster University, Hamilton, Canada

* To whom correspondence should be addressed:

surette@mcmaster.ca

2.1. Abstract

BACKGROUND: Recent studies have associated several pesticides, food packaging chemicals, and food processing chemicals with changes in microbiome composition and chronic diseases. No systematic approach has been taken to understand the extent of the direct impact of these agri-food chemicals on the gastrointestinal microbiota, at concentrations relevant to human dietary exposure.

METHODS: We screened 57 representative gastrointestinal bacteria species in the presence of 30 widely used agri-food chemicals at 1μM. We further characterized a growth interaction between Bisphenol S (BPS) and *Bifidobacterium* by screening 31 *B. adolescentis* strains and 20 strains of other *Bifidobacterium* species. Whole genome and RNA-seq was conducted to characterize the relationship of *B. adolescentis* exposed to BPS.

RESULTS: We observed 41% of agri-food chemicals impacted the growth of at least one bacterial species. A diverse structural range of screened molecules impacted gastrointestinal microbiota growth, although notably, bisphenols and azo food dyes were overrepresented. To better characterize the overrepresentation of bisphenols, further screening with BPS and *Bifidobacterium* found that 51% of screened *B. adolescentis* and 20% of other *Bifidobacterium* species were impacted. Comparative genomics analysis correlated the observed phenotype with both ancestral and mobilome components. Transcriptomics of *B. adolescentis* exposed to BPA and BPS identified BPS specific transcriptional changes to metabolism and stress response distinct from that of BPA.

DISCUSSION: Our results characterize direct agri-food chemicals impacts on microbial growth and function, broaden our understanding of xenobiotic-microbiome

interactions, and raise critical regulatory considerations for the usage of these chemicals in modern food production.

2.2. Introduction

Agri-food chemicals have been vital in improving global food security but also have known adverse effects on metabolic, immune, and reproductive health (Chen, Shu, et al., 2016; Kwon et al., 2022; Wang et al., 2021). Studies assessing the 'off-target' impacts of these drugs and their mechanisms of action on human health provide key areas for regulatory intervention and inform efforts to use safer alternatives in agriculture(Hertz-Picciotto et al., 2018).

Although persistent amounts of agri-food chemicals have been noted in human food consumption and the gut microbiome itself is both sensitive to xenobiotics and pivotal to human health, the impact on the gastrointestinal microbiota is poorly characterized (K. H. Kim et al., 2017; Maier et al., 2018; Maurice et al., 2013; Zimmermann et al., 2019). Recent studies in animals and humans have correlated exposure to certain agri-food chemicals with changes in microbiome composition and, in turn, host health (Chassaing et al., 2022; Chiu et al., 2020; Liang et al., 2019; Velmurugan et al., 2017). Another recent study on a handful of persistent organic pollutants described direct effects on certain gastrointestinal microbiota strains (Tian et al., 2020). Despite this emerging evidence connecting agri-food chemicals to the human microbiome, it remains unclear whether such effects are direct impacts on gastrointestinal microbiota. A major past obstacle to performing studies on direct impacts was the belief that many members of the gastrointestinal microbiota are unculturable (Eckburg et al., 2005; Hayashi et al., 2002). Our group showed that a combination of culture and molecular techniques enabled isolation of much of the

human gastrointestinal microbiota (Browne et al., 2016; Lagier et al., 2016; Lau et al., 2016).

Here, we systematically screen and characterize the interaction between individual cultured gut microbiota species and agri-food chemicals at physiologically relevant concentrations to the general human population. Our results provide novel insights into the direct impact of a poorly studied but ubiquitous type of xenobiotic, agri-food chemicals, on the human gastrointestinal microbiota. We also highlight and detail one such interaction between one species, *Bifidobacterium adolescentis* and bisphenol S.

2.3. Methods

2.3.1. Chemical selection

Screening chemicals (**Supplementary Table 1**), were selected based on their common usage in agriculture, food processing or food packaging, as previously described (Wang et al., 2021). All chemicals were purchased from Toronto Research Chemicals Inc. (Toronto, CA) and suspended in dimethyl sulfoxide (DMSO).

2.3.2. Bacterial strains and growth conditions

All strains, except for *Akkermansia muciniphila* ATCC-BAA835, were isolated as previously described (Lau et al., 2016). All strains were grown from frozen on on brain heart infusion (BHI) agar with 0.5g/L L-cysteine, 10mg/L hemin, 1mg/L vitamin K and then transferred to BHI broth (with the same supplements as above) or modified Gifu Anaerobic Media (mGAM) Broth for 48 hour incubations (see **Supplementary Table 2** for individual strain details). All bacteria were grown in anoxic conditions

within a Coy Laboratory (Grass Lake, United States) Vinyl Anaerobic Chamber (5 % CO_2, 2 % H_2, 93 % N_2) and incubations were done at 37°C. Media were pre-reduced in the anoxic environment for at least 4 hours before use. All strain taxonomies were identified using GTDB(Parks et al., 2022).

2.3.3. Species selection

Species were selected based on inclusion in previous systematic screens of gastrointestinal microbiota and other xenobiotics (Maier et al., 2018; Zimmermann et al., 2019). This yielded a dereplicated list of 58 unique species, of which 56 were selected from the Surette laboratory culture selection for screening.

2.3.4. Kinetic primary screen

Chemicals were purchased and dissolved in dimethyl sulfoxide at a concentration of 100mM. Chemicals were further diluted to 100µM to facilitate aliquoting. For experiments, chemicals were arrayed in the respective growth medium at 2X concentrations and stored at -20°C until use. Before inoculation, plates were pre-reduced in the anaerobic environment overnight.

Liquid cultures were standardized to an OD_{600} of approximately 0.02 (2X the desired starting optical density) and transferred to 96-well plates containing sterile broth and the chemical library at a final concentration of 1µM and 1% DMSO. After inoculation, plates were either sealed with breathable membranes (Breathe-Easy) or a mineral oil overlay was applied to prevent evaporation based on optimal growth conditions for each screen strained. Plates were incubated with shaking and measured manually in the anaerobic chamber using a Tecan (Männedorf, Switzerland) Sunrise plate reader. Reads were taken every 1-3 hours until stationary phase was reached.

Measurements were taken for approximately 16-24 hours. The experiment was performed with three replicates per agrochemical-bacterial pairing.

Blank reductions were performed automatically and data from each plate were inspected to discard only time points with sudden spikes in OD measurements characteristic of condensation or air bubbles in individual wells. Data was truncated at the transition from exponential to stationary phase. Area under the curve (AUC) was calculated using the trapezoidal rule with growthcurver (Version 0.3.1). The calculated AUC for each bacterial-chemical pair was normalized relative to the AUC vehicle control wells and a cutoff of an AUC equal to or less than 0.5 relative to vehicle control was used to identify agri-food chemicals with putative antimicrobial activity for further characterization.

2.3.5. Minimum inhibitory concentration and closely related organism screening

To validate results from the initial screen and further characterize them, minimum inhibitory concentration assays were conducted. Chemicals were arrayed in growth media at a starting concentration of 8µM and serially diluted two-fold to approximately 0.016µM. DMSO was at a final concentration of 1% in all wells. Inoculation occurred as described above and OD was measured at the approximate time when each assayed species reached stationary phase. A minimum of two replicates for each agrochemical-bacteria pair were conducted.

To better characterize the interaction between *B. adolescentis* and BPS, we screened 31 different *B. adolescentis* strains. As well, to expand screening to other members of the *Bifidobacterium* genera, 20 strains from other genera were screened. All strains were

screened at 1μM, and OD was measured at 24 hours after inoculation. A minimum of 3 replicates for each isolate were performed. Statistical difference between control and BPS were assessed using a paired t-test after ensuring normality by performing a Shapiro-Wilks test for normality (Shapiro & Wilk, 1965).

2.3.6. Library preparation and sequencing

After extraction of genomic DNA using the Wizard Genomic DNA Purification Kit (Promega, Madison, USA), library preparation for Illumina sequencing was performed under miniaturized conditions, as described previously (Derakhshani et al., 2020). Illumina sequencing of final libraries was performed on an Illumina HiSeq2500 platform with paired-end 2x250nt, at the McMaster Metagenomic Facility (Hamilton, CA).

2.3.7. Genome assembly and annotation

Our approach to genome assembly was described previously (Derakhshani et al., 2020). Briefly: Trimmomatic was performed for quality trimming and adapter removal with subsequent FastQC to assess sequence quality (Andrews, 2010; Bolger et al., 2014). Unicycler was used for de novo assembly (Wick et al., 2017). Pilon was used to polish assembly errors (Walker et al., 2014). Quast and anvi'o were used to assess quality of assemblies (Eren et al., 2015; Gurevich et al., 2013). Information on genome quality is available in **Supplementary Table 3**. Annotation was performed using bakta (Schwengers et al., 2021).

2.3.8. Sequence search

Publicly available non-fecal human-associated *B. adolescentis* genomes from National Center for Biotechnology Information's (NCBI) genome search were located by

excluding all isolates of human fecal origin. This yielded one isolate, from human milk and two rumen-associated isolates (Duranti et al., 2014, 2016; Seshadri et al., 2018).

2.3.9. Genomic analysis

Taxonomic analysis

16S ribosomal RNA (RNA) phylogenetic trees were generated by extracting the longest predicted 16S rRNA gene from genome assemblies of all organisms from the initial screen using barrnap (Seemann, n.d.). Sequences were aligned using SINA, and a tree was computed using FastTree before visualizing using Interactive Tree of Life (iTOL; Letunic & Bork, 2021; Price et al., 2010; Pruesse et al., 2012). Average nucleotide identity was determined using Pyani (Pritchard et al., 2015).

Phylogenomics of B. adolescentis

The anvi'o phylogenomics snakemake workflow was used with the default 71 curated single-copy core genes ("Bacteria_71") (Lee, 2019). Briefly, the workflow runs "anvi-get-sequences-for-hmm-hits," which uses FAMSA for protein sequence alignment (Deorowicz et al., 2016). TrimAI was used to remove gaps, and maximum likelihood phylogenetic trees were generated using IQ-TREE (Capella-Gutiérrez et al., 2009; Nguyen et al., 2015). *Eubacterium callanderi* and *Enterococcus faecalis* from this study were included as outlier genomes in the analysis for rooting.

Pangenomics and functional enrichment analysis

Pangenomic analysis was conducted using anvi'o, with the following modifications: a) NCBI's blastp was used to perform an amino acid sequence similarity search with all 31 *B. adolescentis* genomes, b) The minbit heuristic from ITEP was used to eliminate weak matches, and, c) MCL was used to identify clusters in the amino acid sequence

similarity search results, with an MCL inflation parameter of 10 (Altschul et al., 1997; Benedict et al., 2014; van Dongen, 2008). Visualization was also performed with anvi'o, clustering genomes by gene cluster presence absence.

Functional enrichment analysis was performed in anvi'o to identify Clusters of Orthologous Groups of proteins (COG) functions within phylogenomic clades that were enriched in sensitive strains, as described previously (Shaiber et al., 2020). Briefly, a binomial general linear model was fitted to each gene function using its clade affiliation as the explanatory variable. A Rao score test is used to test for equality of proportions by clade affiliation. Multiple testing was accounted for by computing q-values, using the package "qvalue" (Storey & Tibshirani, 2003). Enrichment was classified by a q-value below 0.05.

2.3.10. RNA sequencing

Bacterial growth and chemical exposure

B. adolescentis was grown for 48 hours and then sub-cultured to an OD_{600} of 0.01. These cultures were then grown to mid-exponential phase with an OD_{600} of 0.1-0.3 and then exposed to the chemicals and vehicle control for 2 hours. Agrochemical exposures were all performed at a final concentration of 1uM and to BPA and BPS, in triplicate.

Total RNA isolation

RNA isolation was based on the RNAsnap method, with modifications as previously described, and detailed in **Appendix File 1** (Stead et al., 2012). Briefly, 1ml of culture was centrifuged at 4,000 x *g* at room temperature for 2 minutes. Cell pellets were rapidly resuspended in the extraction solution (95% formamide, 18 mM ethylenediaminetetraacetic acid, 0.025% sodium dodecyl sulphate and 1% B-

mercaptoethanol) and incubated at 95°C for 7 minutes to lyse cells. The samples were then centrifuged at 16,000 x *g* for 5 minutes at room temperature and 200ul of the supernatant was transferred to a fresh tube for RNA clean up with the Zymo clean and concentrator kit (USA; #R1017 and #E1010) per manufacturer's instructions. Total RNA concentrations were measured using the Qubit RNA HS Assay Kit (ThermoFisher Scientific, USA; Q32855). RNA integrity was confirmed for all samples on a 0.8% agarose gel in TBE buffer and a random subset of 15 samples were also assessed using the Tapestation (Agilent Technologies, USA).

RNA-seq library preparation with RNAtag-Seq

The RNA-seq libraries were prepared using RNAtag-Seq, with minor modifications, as detailed in **Appendix File 2** (Shishkin et al., 2015). Briefly, we combined the library preparation of three replicates from chemical exposure samples and vehicle control samples. Unique barcoded adaptors (**Supplementary Table 5**) were used to tag each sample.

rRNA depletion was performed utilizing a previously described RNase H-based depletion protocol, with minor modifications, detailed in **Appendix File 3** (Huang et al., 2020). Probes were generated with 16S and 23S rRNA sequences extracted using barrnap from the sequenced genomes and are available in **Appendix File 4**. Probe pools were ordered as DNA oPools (Integrated DNA Technologies Inc.; Coralville, USA) at 50pmol per oligo and dissolved in DNase/RNase-free distilled water to achieve a final concentration of 1000ng/ul. Briefly, 500ng of whole RNA underwent annealing to ssDNA probes at a 1:10 ratio, followed by incubation with RNase H at 45°C for 30 minutes. Probes were removed using a 2X ratio of RNAClean XP beads

to sample volume and output was utilized for first strand synthesis and subsequent RNAtag-seq library preparation.

RNA-seq data analysis

The RNAtag-seq library was sequenced by single-end (1x100) Illumina sequencing at McMaster Genomics Facility (Hamilton, Canada) on the NextSeq platform. The pool was demultiplexed according to the unique 8nt ligated barcode adaptor for each sample using cutadapt (v3.4), retaining reads with a quality score > 20 and post-trimming lengths >25nt (Martin, 2011). Post-demultiplexing reads were assessed using multiQC (v1.14): The median sample read depth was 6,570,854 reads (range: 4,179,057 – 10,642,395) and no obvious bias in the number of final reads counted per sample was noted, with median assigned reads of 4.2M reads (range: 2.7-6.2M; **Supplementary Table 6**) (Ewels et al., 2016).

The sequenced bacterial genome was annotated with bakta. Reads were mapped after demultiplexing to this reference genome using Burrows-Wheeler Aligner (BWA), and indexed and sorted with SAMtools (H. Li et al., 2009; H. Li & Durbin, 2009). Read counts per gene were generated using HTSeq (Anders et al., 2015). Successful rRNA depletion was confirmed by quantifying reads mapped to rRNAs, noting <0.5% rRNA reads in all samples (**Supplementary Table 6**). Statistical analysis was performed with DESeq2 with an alpha of 0.05 and including sample replicate as a fixed effect as samples were noted to cluster by replicate number (data not shown). Visualization was performed with DESeq2 and ggplot2 (Love et al., 2014; Wickham et al., 2019).

All figures were finalized for publication using Inkscape (v1.2.1).

2.4. Results

In this study, we first monitored the growth of 57 taxonomically diverse gastrointestinal bacteria treated with 30 agri-food chemicals over time until stationary phase was reached (Figure 1a). Our chemical library was selected based on the use of included compounds in North America and/or pre-existing evidence in the literature connecting exposure to impacts on bacteria (Supplementary Table 1) (Wang et al., 2021). All screening was done under anaerobic conditions at 37°C with chemicals at 1μM concentrations.

To select a representative set of gastrointestinal bacteria species, we first reviewed bacterial species utilized in two systematic screens of gastrointestinal bacteria that selected their bacteria based on prevalence and abundance of organisms in the human gastrointestinal tract (Maier et al., 2018; Zimmermann et al., 2019). We then cross-referenced this strain list with our paired culture collection and screened all available strains for growth in rich media (brain heart infusion (BHI) broth with 0.5g/L L-cysteine, 10mg/L hemin, 1mg/L vitamin K or modified Gifu anaerobic media (mGAM) broth. While some species were unavailable in our culture collection or unable to grow in rich media, we selected 58 bacterial species from 16 families amenable for screening (**Supplementary Figure 1; Supplementary Table 2**). Two different strains of *Enterococcus faecium* and three different strains of *Phocaeicola vulgatus* were included, totalling 60 total strains. The vast majority (58/60) of strains were commensal organisms isolated from healthy adult volunteers in Hamilton, Canada. A laboratory strain of *Salmonella enterica* serovar Typhimurium (strain 14028), and a purchased ATCC BAA-835 strain of *Akkermansia muciniphila* were also included.

2.4.1. Agrochemical screen on gastrointestinal bacteria identifies growth-impacted strains

For our initial screen, chemicals were considered to impact growth of any bacteria if the area under the curve was reduced by >50% compared to vehicle control (Maier et al., 2018). We observed at least one compound within the bisphenols, food dyes, herbicides, and insecticides impacted the growth of gastrointestinal bacteria, demonstrating broad impacts across the chemical classes screened. All of the food dyes impacted growth of at least one screened bacterial strain. Growth impacts were also observed in 3 of the 9 bacterial strain to the insecticide Deltamethrin. Notably, growth impacts appear to be highly variable and compound and bacterial strain specific as we observed a lack of taxonomic conservation in our initial screen.

Of the 58 bacteria screened, nine were impacted in their growth (**Figure 1b**). These nine bacteria belonged to the families *Bacteroidaceae, Bifidobacteriaceae, Butyricoccaceae, Eubacteriaceae, Lachnospiraceae, and Rikenellaceae*. Certain bacteria appeared to be particularly susceptible to agrochemical impacts on growth, such as *Eubacterium callanderi.* None of the screened Proteobacteria or Verrucomicrobiota species were impacted in growth although only 3 and 1 species, respectively, were screened.

2.4.2. Minimum inhibitory concentrations suggest dose relevance of hits

To characterize the impact of different concentrations of chemicals, we performed minimum inhibitory concentration assays with our hits. Several of our hits were confirmed to have growth impacts in a concentration dependent manner. *Bifidobacterium adolescentis* was specifically noted to be impacted when exposed to less than 0.02uM of bisphenol S (BPS; **Figure 2a**). Notably, several strains were noted to

not illustrate a reproducible impact that was concentration-dependent (**Supplementary Figure 2**).

2.4.3. Screening of closely related bacteria highlight strain specific agrochemical relationships

From our in-house strain collection, we then identified 31 additional *B. adolescentis* strains, originally isolated from healthy adult human donors. 20 other *Bifidobacterium* strains, representing *B. breve, B. catenulatum, B. dentium, B. longum, and B. scardovii* were also utilized. These 51 strains were screened against BPS to assess for species and strain level variability. Notably, growth impact was noted in *B. adolescentis* strains when exposed to BPS (paired t-test, $p = 0.000004$) although this seemed to be driven by a subset of 16 of the 31 screened strains (**Figure 2b**). Almost all strains from other species were spared any impact ($p = 0.99$; **Supplementary Figure 3; Supplementary Table 3**).

2.4.4. Phylogenomic analysis of *Bifidobacterium adolescentis* reveals evolutionary relationship with bisphenol S susceptibility

To assess for explanations of this strain-specific response, we performed high-throughput genomic sequencing of all screened *B. adolescentis* strains. The sequenced genomes are high-quality, with low total contigs (median: 23 [range: 16-46]) and high N50 (median: 467,062 [range: 222,992-1,759,187]) (**Supplementary Table 4**). Phylogenomic analysis was performed to assess whether susceptibility to BPS may relate to an ancestral genomic trait. A clade of the tree contained most susceptibility-associated genomes, suggesting an evolutionary aspect to susceptibility (**Figure 3a**). Notably, however, our original strain from our screen did not fall within this branch,

leading us to question whether there may be accessory genetic components in the species that contribute to susceptibility to BPS.

To investigate the specificity of our strains to the human gastrointestinal tract and whether our findings may be relevant to non-human and non-gastrointestinal niches, we searched NCBI for whole genome sequencing of *B. adolescentis*. We found 1 sample isolated from human breast milk, as well as one sample from bovine rumen. Another sample from bovine rumen was found in the HUNGATE1000 database. Isolates from rumen clustered together and not in the clade with growth-impacted strains. Similarly, the isolate from breast milk did not cluster with growth-impacted strains, suggesting some aspect of ecologic niche-genomic relationship.

2.4.5. Pan-genomic analysis highlights relationship between several metabolic, mobilome, and cell wall synthesis functions and growth impact

Comparative pan-genome analysis of *B. adolescentis* strains was performed to identify shared and unique accessory genes and functions between the growth-impacted and non-impacted strains (**Figure 3b**). We noted 1131 unique COGs in the pangenome, across our 31 genomes by conducting an amino acid similarity search on all genomes and clustering results based on clusters in the similary search. We identified 964 (85.2%) of those COGs as present in all *B. adolescentis* genomes, representing the functional core. We applied functional enrichment analyses by conducting a binomial general linear model which was fitted to each gene function using its clade affiliation as the explanatory variable to the pangenomes. This revealed 16 unique enriched COGs (q-value <0.05; 1.4% of total COGs) that were depleted in the growth-

impacted strains (**Figure 3c**; **Table 1**). The most common functional category in enrichment analysis was carbohydrate metabolism, with four COGs. Three enriched functions related to prophage function. As well, nearly all non-impacted strains were noted to be enriched in cell wall biogenesis functions, including outer membrane protein, OmpA, and related peptidoglycan associated lipoproteins. Notably, a substantial portion of the accessory genome, over 1000 gene clusters, lacked COG function assignment, and were included in functional enrichment testing as such. Two enriched COGs were of unknown function.

Transcriptional impact of bisphenol S on *B. adolescentis*

We then performed RNA-seq to assess the impact on the transcriptome of the originally screened *B. adolescentis* (strain GC641) when exposed to BPS. Compared to control, BPS-exposed samples had a distinct transcriptional profile in principle component analysis plots (**Figure 4a**). Among 59 differentially expressed genes, metabolism-associated genes were the most common, including *nrdD*, which is essential in anaerobic metabolism (**Figure 4b-c**; **Table 2**). *merR*, a master regulator commonly seen in oxidative stress, and *recA*, involved in bacterial SOS response, were increased in expression. Notably, the profile for BPS was distinct from that of BPA, which more closely resembled the vehicle control condition and had only one differentially expressed gene (*upp*). Like our genomic analysis, a substantial portion (44/59) of differentially expressed genes in *B. adolescentis* were noted to lack high quality annotation.

2.5. Discussion

The industrial revolution and associated expansion of chemistry fundamentally altered human food production by discovering and applying pesticides, food additives and food packaging. Shortly thereafter, evidence of harms to human and environmental health became evident. While the gut microbiome was ill-studied at that time, it has now become an intense area of research due to connections with a wide range of clinical pathology, including inflammatory bowel diseases and metabolic diseases (Huttenhower et al., 2014; Maruvada et al., 2017). Some recent animal studies have linked agri-food chemicals with altered microbiome and host biology (Chiu et al., 2020). In this study, to better characterize the direct relationship between microbiome and human gastrointestinal microbiota, we leveraged advances in culturing the bacterial strains of the microbiome for *in vitro* experimentation to assess growth impact by agri-food chemicals.

We utilized relevant concentrations of compounds for our screening although ascertaining a true exposure is a known challenge. For example, human exposure to azo food dyes or plastic compounds can vary but can be much higher than 1μM (Xu et al., 2023; Zou et al., 2020). In addition, the fate of a chemical in the body also varies drastically and understanding of reduction mechanisms and products is incomplete. For example, in addition to non-enzymatic reduction, azo dyes are enzymatically reduced by gastrointestinal bacteria and this enzymatic activity could also become saturated at high doses (Zou et al., 2020).

In our initial screen, most bacterial-agrochemical pairs did not note any growth effect. Observed effects were limited to certain bacterial strains and did not align with a taxonomic clade.

We wondered if this may relate to the whether those organisms contained strain-specific accessory genome components responsible for this phenotype rather than the effect relating to a universally shared core genetic component. We applied strain-level genomics to further assess one interaction from our screening between *B. adolescentis* and BPS. BPS is an increasingly common building block for plastic polymers due to its use as a replacement for BPA (C. Liao et al., 2012). Notably, BPS has also been implicated in directly impact host biology, in a manner distinct from BPA (Chen, Shu, et al., 2016). In our experiments on *B. adolescentis*, we observed a strain-specific impact on certain strains which were depleted in various prophage and cell wall synthesis gene clusters. This also suggested the need for strain-level screening in future experiments, as supported both by results shown here on *B. adolescentis* but also work by others highlighting strain diversity in other bacteria, such as *Eggerthella lenta*, *Bacteroides* species, and *Lachnospiraceae* species (Bisanz et al., 2020; Shoemaker et al., 2001; Sorbara et al., 2020).

Strain specific dynamics may relate to mobile genetic elements, such as bacteriophage, or subtle differences in cell wall function. Bacteriophage, while canonically described as parasitic, also are known to provide several defense mechanisms and can modulate their host's metabolism (Carey et al., 2019; Schroven et al., 2021). Cell wall synthesis may relate to an ancestral aspect of how certain *B. adolesentis* strains defend against toxins as OmpA is a frequent marker gene in phylogenetic studies. *B. adolescentis* is a

gram-positive organism and therefore does not have an outer-membrane; regardless, such genes have been previously reported in gram-positive organisms as key component of cell wall genesis and function although much less is known about them (Park et al., 2012).

Similarly, although previous studies have suggested that human feces-associated *B. adolescentis* are monophyletic (Duranti et al., 2016), we did note isolates from human breast milk or bovine rumen are phylogenetically distinct from our impacted strains. We also found that BPS caused distinct alterations in bacterial gene transcription with notable changes in metabolism and stress response. This does lead us to speculate whether activation of stress response by BPS may lead to bacteriophage activation only in strains with phage present.

Notably, these expression differences were noted to be distinct from BPA, which had only one differentially expressed gene compared to control. BPS differs from BPA by the presence of a sulfone group as the central moiety in the chemical, compared to a carbon-based central moiety in BPA. Future experiments assessing how this sulfone group may relate to either differing interaction of the molecule with *B. adolescentis* or degradation of BPS into different metabolites may further elucidate these growth impacts.

Notably, a substantial part of the accessory genome and transcriptome lacked annotations and COG/KEGG functional assignments. This is substantial yet unavoidable limitation of this study as fewer genetic tools exist for non-laboratory strains or are applied to improve understanding of *Bifidobacterium* species biology.

Observed growth impacts of agri-food chemicals on gastrointestinal bacterial strains largely did not follow the expected bacteriostatic or bactericidal pattern of growth. Notably, this aberrant growth was similar to what was observed in a previous screen of drug impacts on gastrointestinal microbiota (Maier et al., 2018). These atypical growth curves may relate to rapidly emerging resistance, impact on growth only within a subpopulation of the total culture, or metabolic shifts in the function activity of the bacteria slowing growth. This merits further investigation. Nonetheless these species/strain specific impacts on growth would be expected to affect the bacteria's competitiveness within microbial communities in the human gut.

2.6. Acknowledgements

We thank the staff of the Farncombe Metagenomic Facility (Hamilton, CA) and all members of the Surette laboratory for constructive discussions and support in screening, sample preparations and library sequencing. We thank Eric Brown for providing the plate reader used for anaerobic screening. This work was supported by funding from Canadian Institutes for Health Research.

2.7. Figures

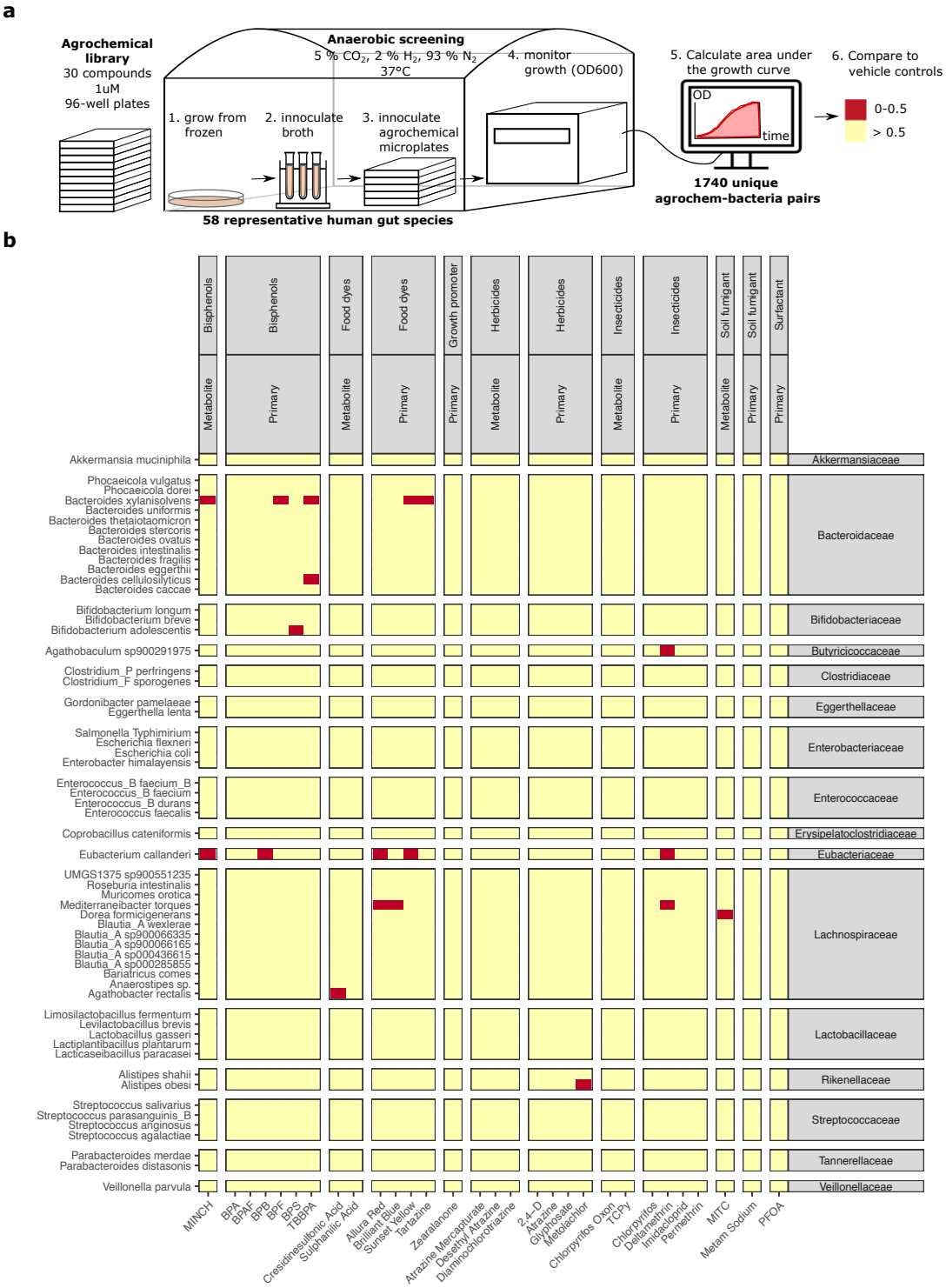

Figure 2. 1. Anaerobic kinetic screening of 60 strains grown with 30 diverse agri-food chemicals.

a) Graphical representation of methodology and legend for heatmap where red indicates greater than 50% reduced area under the growth curve compared to vehicle control. **b**) Heatmap output of screening. Bacterial strain IDs are shown. Primary indicates a native agrochemical and metabolite indicates the breakdown product of primary compounds. Average relative area under the curve is shown (n = 3) for each bacterial strain – agri-food chemical pair.

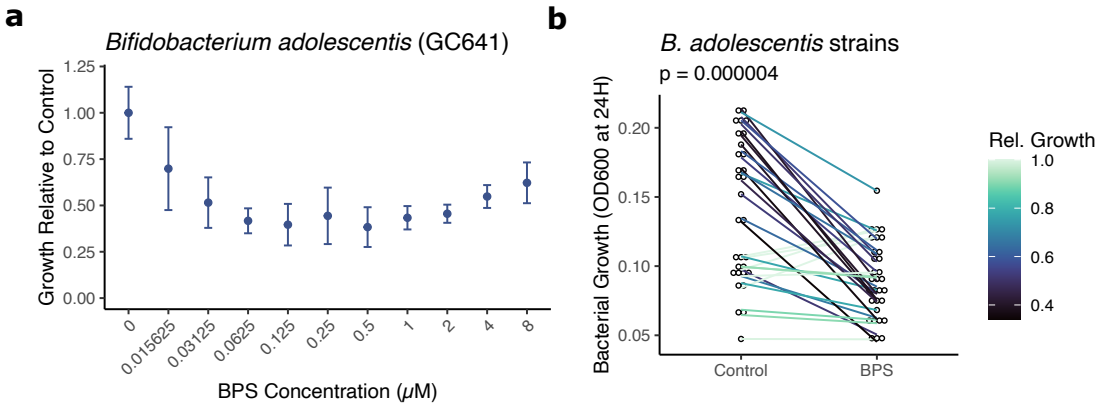

***Figure 2. 2. Concentration-dependent and strain-specific impact of bisphenol S on* Bifidobacterium adolescentis.**

a) Relative growth compared to vehicle control of *B. adolescentis* where each dot represents the average of replicates (n=2) and error bars represent standard deviation. b) OD_{600} measurements after subtraction of blank well reads are shown where each dot represents the average of replicates (n=3) of each strain grown in a condition. Lines connecting the same strains between both conditions are coloured by the relative decrease in growth when grown in BPS, compared to control. P-value for a paired t-test of strains in control versus BPS exposure is shown above the plot.

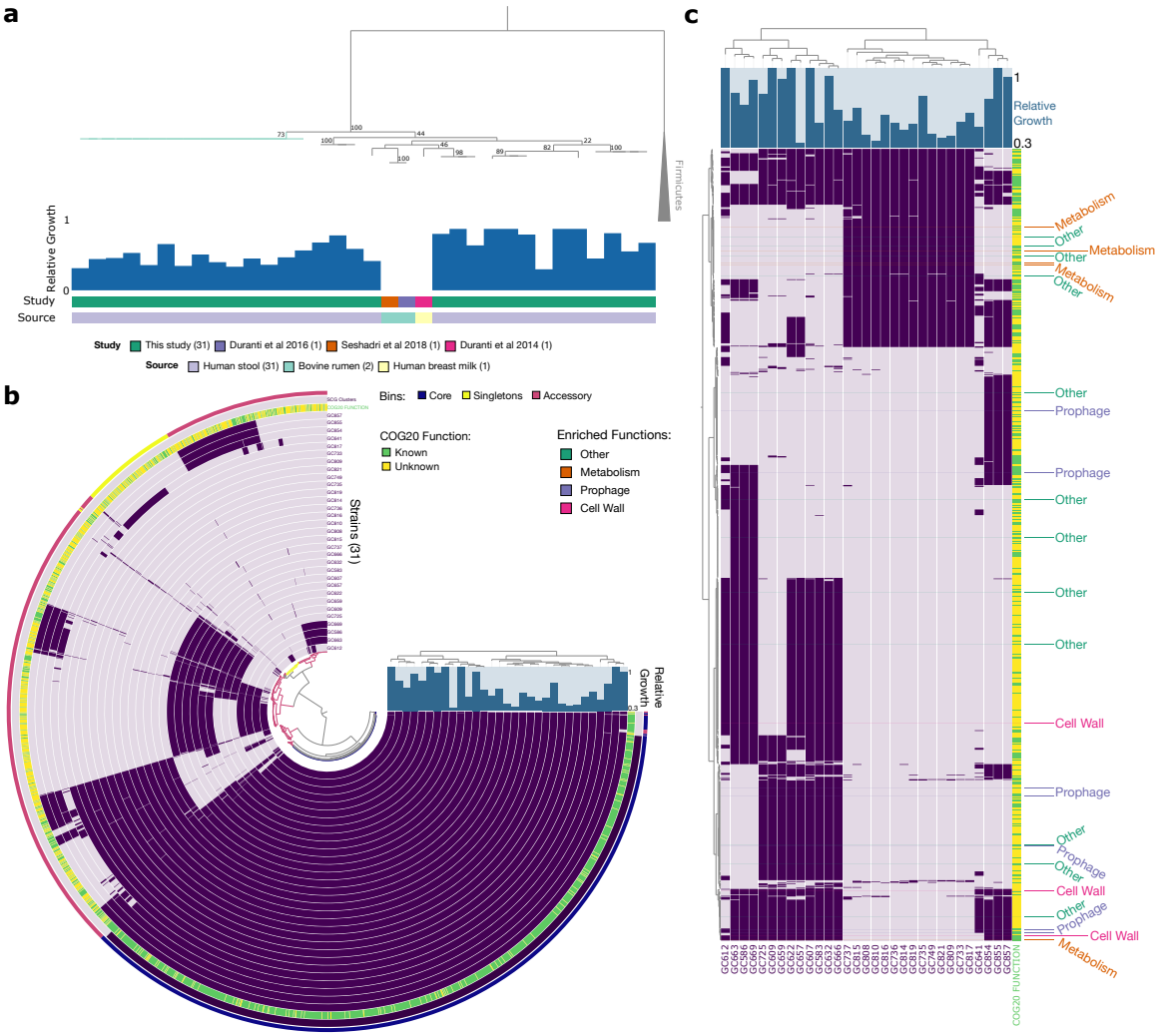

***Figure 2. 3. Phylogenomic, pangenomic, and functional enrichment analysis of* Bifidobacterium adolescentis.**

a) Phylogenomic analysis of strains from this study (31) and non-human feces-isolated strains (3; 2 from bovine rumen, 1 from human breast milk) from NCBI. Branch of the tree associated with growth impact is highlighted in cyan. Bootstrap support values are shown next to branches. b) Pangenomic analysis gene clusters from strains in this study. The inner dendrogram is constructed by the presence of gene clusters. The 31 inner layers signify each strain with dark purple representing presence and light purple representing absence. The next layer demonstrates whether a COG20 function is

associated with the associated gene cluster. The outermost layer denotes whether the gene cluster is core (in all genomes), a singleton (in only 1 genome), or accessory (all other genes). c) All functionally enriched gene clusters in the accessory genome. GO functional categories are noted on the right and colour-coded.

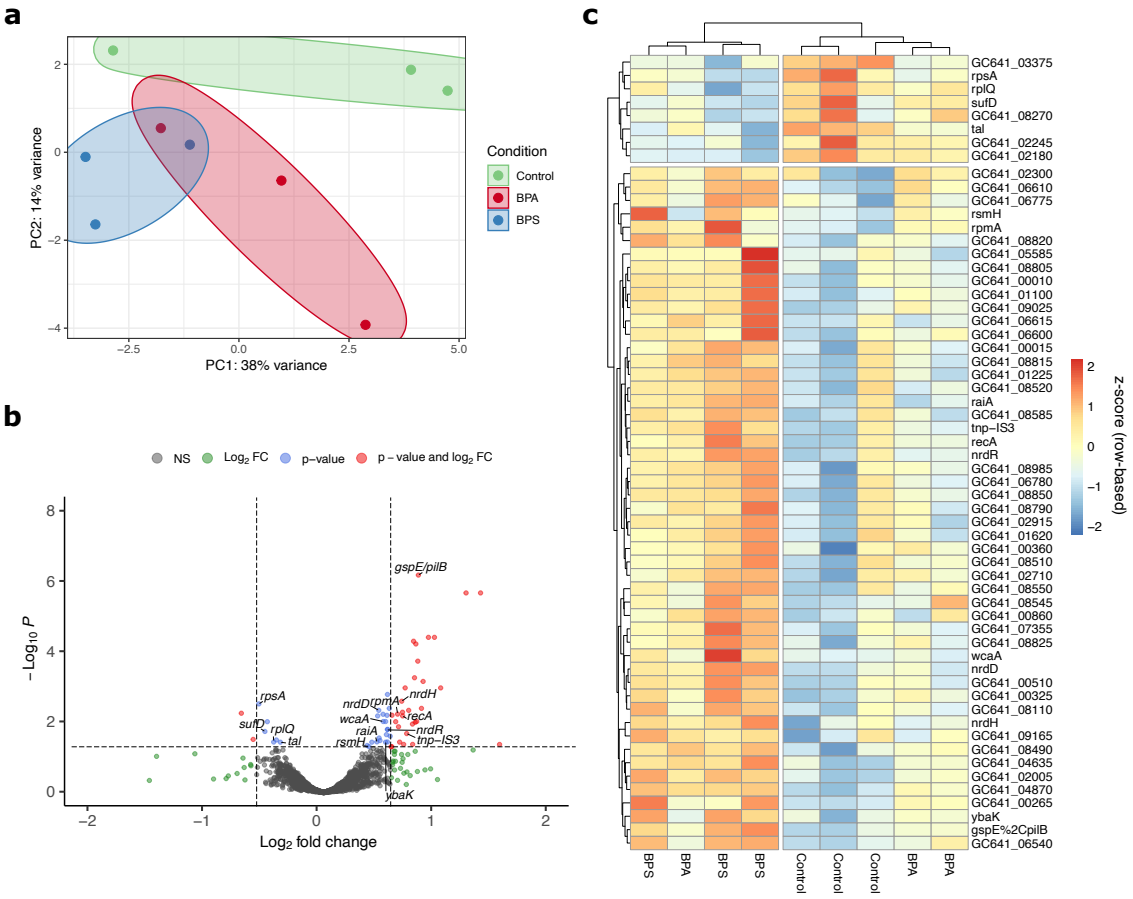

Figure 2. 4. Impact of bisphenol S on the* Bifidobacterium adolescentis *transcriptional program.

a) RNA-seq principal component analysis plot of 9 samples, 3 each exposed to BPS, BPA, or vehicle control during growth. b) Volcano plot of genes for vehicle control versus BPS samples. Significantly different genes are noted in red. Vertical lines indicate the level of adjusted p-value for significance. Horizontal lines indicate the minimum Log_2 fold change. c) Heatmap of all significant differentially expressed genes between Control and BPS. Strain shown is *B. adolescentis* strain GC641.

2.8. Tables

***Table 2. 1. Pan-genome functional enrichment analysis of growth-impacted* Bifidobacterium adolescentis *strains*.**

COG Function	Accession	COG Cat.	Enrich. Score	q Value	Presence/ Absence
ABC-type polysaccharide transport system, permease component (LplB)	COG4209	G	14.848	0.028	-
Beta-mannanase (ManB2)	COG4124	G	12.692	0.028	+
Glycosidase/amylase (phosphorylase) (AmyA)	COG0366	G	12.692	0.028	+
Glycogen debranching enzyme (alpha-1,6-glucosidase) (GDB1)	COG3408	G	12.692	0.028	+
tRNA1(Val) A37 N6-methylase TrmN6 (TrmN6)	COG4123	J	12.692	0.028	+
DNA-binding transcriptional regulator, XRE-family HTH domain (XRE)	COG1476	K	11.769	0.043	-
DNA topoisomerase IA (TopA)	COG0550	L	12.692	0.028	-
Integrase/recombinase, includes phage integrase (FimB)	COG0582	L/X	12.692	0.028	-
dTDP-glucose pyrophosphorylase (RmlA1)	COG1209	M	14.848	0.028	-
Outer membrane protein OmpA and related peptidoglycan-associated (lipo)proteins (OmpA)	COG2885	M	12.692	0.028	-
Serine protease inhibitor (SERPIN)	COG4826	O	12.692	0.028	+
Uncharacterized conserved protein YjbI, contains pentapeptide repeats (YjbI)	COG1357	S	14.848	0.028	+
Uncharacterized protein RhuM, Salmonella virulence factor (RhuM)	COG3943	S	12.692	0.028	+
Type IV secretory pathway, VirD4 component, TraG/TraD family ATPase (VirD4)	COG3505	U	12.692	0.028	-
Uncharacterized phage-associated protein, contains DUF4065 domain (GepA)	COG3600	X	14.848	0.028	-
Phage-encoded DNA-binding protein, contains HTH and DnaT DNA-binding domains (ECs1768)	COG5529	X	12.692	0.028	-

Table 2. 2. Differential gene-expression results of bisphenol S-exposed* Bifidobacterium adolescentis *versus control.

Gene ID	Mean Reads (control)	log2FoldChange	p_{adj}
gspE/pilB	1307.78	0.83	0.000000645
nrdD	4202.99	0.48	0.0046
nrdH	515.38	0.68	0.0025
nrdR	778.15	0.56	0.016
raiA	31826.42	0.47	0.036
recA	3101.62	0.69	0.0066
rplQ	13158.20	-0.44	0.037
rpmA	14256.48	0.65	0.0059
rpsA	22664.37	-0.56	0.0030
rsmH	2861.21	0.40	0.050
sufD	4011.05	-0.51	0.018
tal	21119.98	-0.38	0.037
tnp-IS3	322.57	0.72	0.021
wcaA	1666.59	0.52	0.0095
ybaK	354.39	0.54	0.037

*44/59 differentially expressed genes lacked a gene identification.

2.9. Supplementary Materials

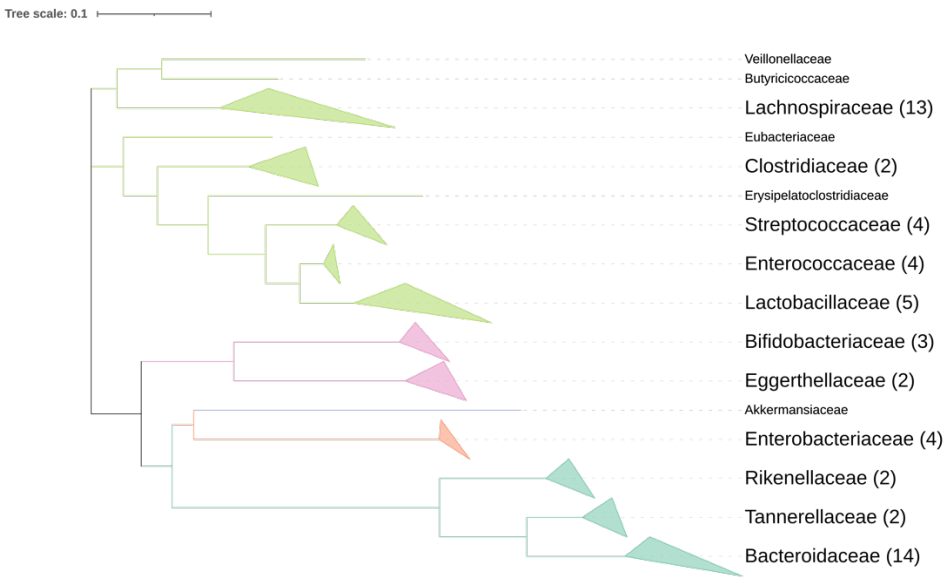

Supplementary Figure 2. 1. Phylogenetic tree of 16S nucleotide sequences from all 60 screened bacteria, representing 58 species.

Tree annotated to the family level with number of strains of each family noted in brackets, if more than one strain. Phyla noted by colour (Firmicutes - green, Bacteroidota - blue, Actinobacteriota - pink, Proteobacteria - orange, and Verrucomicrobiota - purple).

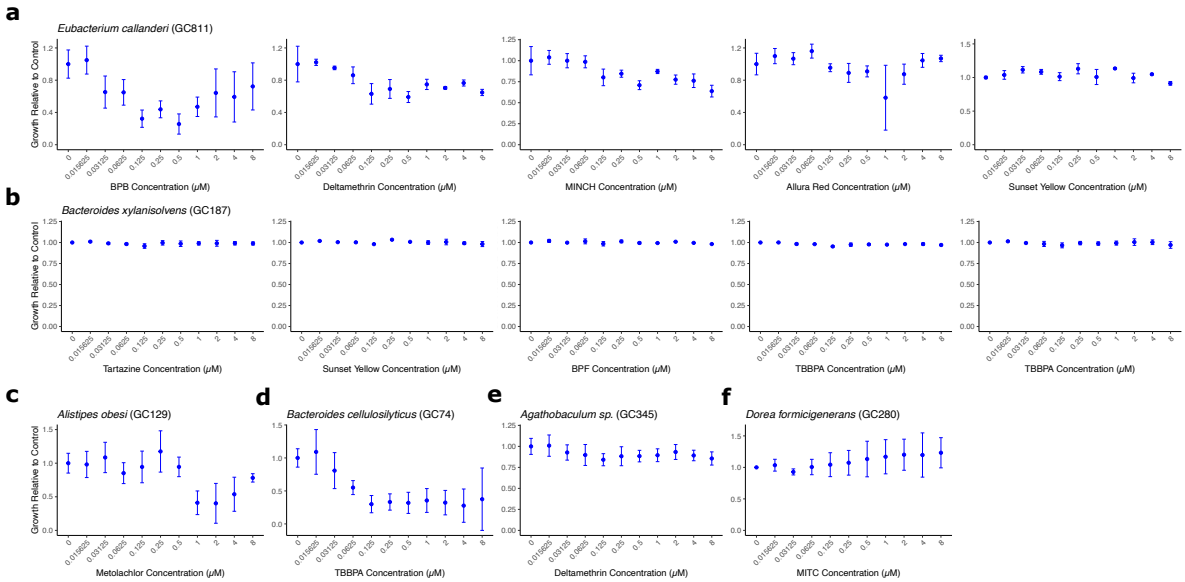

Supplementary Figure 2. 2. Concentration screening across all impacted species from primary screen.

Each dot represents average across replicates and error bars indicate standard deviation. If more than one chemical was noted per strain, each chemical is noted by its own plot. *Agathobacter rectalis* and *Blautia wexlerae* were excluded due to inability to achieve reproductible growth across concentrations.

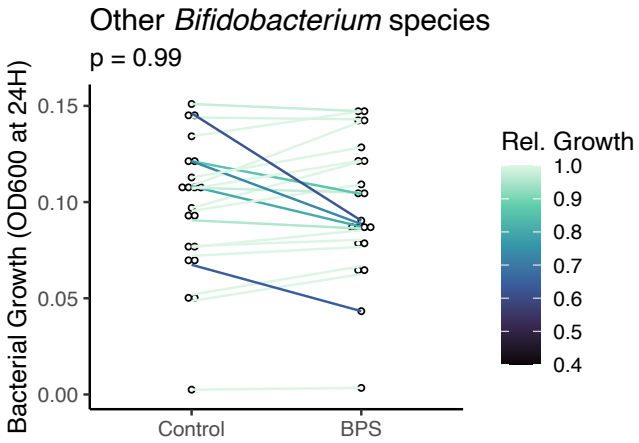

***Supplementary Figure 2. 3. Growth impact of BPS on all other* Bifidobacterium *strains*.**

OD_{600} measurements after subtraction of blank well reads are shown where each dot represents a strain grown in a condition. Lines connecting the same strains between both conditions are coloured by the relative decrease in growth when grown in BPS, compared to control with colors as noted in the legend to the right of the plot. P-value for a paired t-test of strains in control versus BPS exposure is shown above the plot.

Supplementary Table 2. 1. Agri-food chemicals used for screening.

Compounds	**Compound Type**
Chlorpyrifos	Insecticide
Deltametrin	Insecticide
Imidacloprid	Insecticide
Metam Sodium	Fungicide
Permetrin	Insecticide
Chlorpyrifos Oxon	Insecticide Metabolite
3,5,6-trichloro-2-pyridinol (TCPy)	Insecticide Metabolite
Methyl isothiocyanate (MITC)	Fungicide Metabolite
2,4-Dichlorophenoxyacetic acid (2,4-D)	Herbicide
Atrazine	Herbicide
Glyphosate	Herbicide
Metolachlor	Herbicide
Diaminochlorotriazine (DCA)	Herbicide Metabolite
Desethylatrazine (DEA)	Herbicide Metabolite
Atrazine mercapturate (Atr M)	Herbicide Metabolite
Aminomethylphosphonic acid (AMPA)	Herbicide Metabolite
Bisphenol A (BPA)	Food Packaging
Bisphenol AF (BPAF)	Food Packaging
Bisphenol B (BPB)	Food Packaging
Bisphenol F (BPF)	Food Packaging
Bisphenol S (BPS)	Food Packaging
Perfluorooctanoic acid (PFOA)	Food Packaging
Tetrabromobisphenol A (TBBPA)	Food Packaging
Cyclohexane-1,2-dicarboxylic acid-mono isononyl ester (MINCH)	Packaging Metabolite
Allura Red	Food Colouring
Brilliant Blue	Food Colouring
Sunset Yellow	Food Colouring
Tartazine	Food Colouring
Cresidinesulfonic acid (CSA)	Colouring Metabolite
Sulphanillic Acid (SA)	Colouring Metabolite

Supplementary Table 2. 2. Representative gut bacteria with growth conditions.

Strain ID	Phylum	Family	Genus and Species	Growth Media
GC133	Actinobacteriota	*Bifidobacteriaceae*	*Bifidobacterium longum*	0.5 BHI3 + 5% FBS
GC641	Actinobacteriota	*Bifidobacteriaceae*	*Bifidobacterium adolescentis*	0.5 BHI3 + 5% FBS
GC96	Actinobacteriota	*Bifidobacteriaceae*	*Bifidobacterium breve*	0.5 BHI3 + 5% FBS
GC495	Actinobacteriota	*Eggerthellaceae*	*Gordonibacter pamelaeae*	0.5 BHI3 + 5% FBS
GC684	Actinobacteriota	*Eggerthellaceae*	*Eggerthella lenta*	0.5 BHI3 + 5% FBS
GC101	Bacteroidota	*Bacteroidaceae*	*Bacteroides stercoris*	0.5 BHI3 + 5% FBS
GC137	Bacteroidota	*Bacteroidaceae*	*Bacteroides ovatus*	0.5 BHI3 + 5% FBS
GC186	Bacteroidota	*Bacteroidaceae*	*Phocaeicola vulgatus*	0.5 BHI3 + 5% FBS
GC187	Bacteroidota	*Bacteroidaceae*	*Bacteroides xylanisolvens*	0.5 BHI3 + 5% FBS
GC192	Bacteroidota	*Bacteroidaceae*	*Phocaeicola vulgatus*	0.5 BHI3 + 5% FBS
GC201	Bacteroidota	*Bacteroidaceae*	*Phocaeicola dorei*	0.5 BHI3 + 5% FBS
GC203	Bacteroidota	*Bacteroidaceae*	*Bacteroides caccae*	0.5 BHI3 + 5% FBS
GC211	Bacteroidota	*Bacteroidaceae*	*Phocaeicola vulgatus*	0.5 BHI3 + 5% FBS
GC239	Bacteroidota	*Bacteroidaceae*	*Bacteroides uniformis*	0.5 BHI3 + 5% FBS
GC404	Bacteroidota	*Bacteroidaceae*	*Bacteroides eggerthii*	0.5 BHI3 + 5% FBS
GC432	Bacteroidota	*Bacteroidaceae*	*Bacteroides intestinalis*	0.5 BHI3 + 5% FBS
GC465	Bacteroidota	*Bacteroidaceae*	*Bacteroides thetaiotaomicron*	0.5 BHI3 + 5% FBS
GC73	Bacteroidota	*Bacteroidaceae*	*Bacteroides fragilis*	0.5 BHI3 + 5% FBS
GC74	Bacteroidota	*Bacteroidaceae*	*Bacteroides cellulosilyticus*	0.5 BHI3 + 5% FBS
GC123	Bacteroidota	*Rikenellaceae*	*Alistipes shahii*	0.5 BHI3 + 5% FBS
GC129	Bacteroidota	*Rikenellaceae*	*Alistipes obesi*	0.5 BHI3 + 5% FBS
GC267	Bacteroidota	*Tannerellaceae*	*Parabacteroides distasonis*	0.5 BHI3 + 5% FBS
GC422	Bacteroidota	*Tannerellaceae*	*Parabacteroides merdae*	mGAM
GC210	Firmicutes	*Enterococcaceae*	*Enterococcus_B faecium_B*	0.5 BHI3 + 5% FBS
GC23	Firmicutes	*Enterococcaceae*	*Enterococcus_B faecium*	0.5 BHI3 + 5% FBS
GC27	Firmicutes	*Enterococcaceae*	*Enterococcus_B durans*	0.5 BHI3 + 5% FBS
GC28	Firmicutes	*Enterococcaceae*	*Enterococcus faecalis*	0.5 BHI3 + 5% FBS
GC273	Firmicutes	*Erysipelatoclostridiaceae*	*Coprobacillus cateniformis*	mGAM
GC1	Firmicutes	*Lactobacillaceae*	*Levilactobacillus brevis*	0.5 BHI3 + 5% FBS

GC2	Firmicutes	*Lactobacillaceae*	*Limosilactobacillus fermentum*	0.5 BHI3 + 5% FBS
GC37	Firmicutes	*Lactobacillaceae*	*Lactobacillus gasseri*	0.5 BHI3 + 5% FBS
GC4	Firmicutes	*Lactobacillaceae*	*Lactiplantibacillus plantarum*	0.5 BHI3 + 5% FBS
GC8	Firmicutes	*Lactobacillaceae*	*Lacticaseibacillus paracasei*	0.5 BHI3 + 5% FBS
GC104	Firmicutes	*Streptococcaceae*	*Streptococcus parasanguinis_B*	0.5 BHI3 + 5% FBS
GC79	Firmicutes	*Streptococcaceae*	*Streptococcus agalactiae*	0.5 BHI3 + 5% FBS
GC81	Firmicutes	*Streptococcaceae*	*Streptococcus salivarius*	0.5 BHI3 + 5% FBS
GC82	Firmicutes	*Streptococcaceae*	*Streptococcus anginosus*	0.5 BHI3 + 5% FBS
GC345	Firmicutes_A	*Butyricicoccaceae*	*Agathobaculum sp900291975*	0.5 BHI3 + 5% FBS
GC1500	Firmicutes_A	*Clostridiaceae*	*Clostridium_F sporogenes*	0.5 BHI3 + 5% FBS
GC1584	Firmicutes_A	*Clostridiaceae*	*Clostridium_P perfringens*	0.5 BHI3 + 5% FBS
GC811	Firmicutes_A	*Eubacteriaceae*	*Eubacterium callanderi*	0.5 BHI3 + 5% FBS
GC218	Firmicutes_A	*Lachnospiraceae*	*Bariatricus comes*	mGAM
GC223	Firmicutes_A	*Lachnospiraceae*	*Blautia_A sp900066165*	0.5 BHI3 + 5% FBS
GC279	Firmicutes_A	*Lachnospiraceae*	*Blautia_A sp000436615*	mGAM
GC280	Firmicutes_A	*Lachnospiraceae*	*Dorea formicigenerans*	mGAM
GC312	Firmicutes_A	*Lachnospiraceae*	*UMGS1375 sp900551235*	0.5 BHI3 + 5% FBS
GC327	Firmicutes_A	*Lachnospiraceae*	*Blautia_A sp900066335*	0.5 BHI3 + 5% FBS
GC447b	Firmicutes_A	*Lachnospiraceae*	*Roseburia intestinalis*	0.5 BHI3 + 5% FBS
GC450	Firmicutes_A	*Lachnospiraceae*	*Mediterraneibacter torques*	0.5 BHI3 + 5% FBS
GC458	Firmicutes_A	*Lachnospiraceae*	*Muricomes orotica*	mGAM
GC501	Firmicutes_A	*Lachnospiraceae*	*Blautia_A wexlerae*	mGAM
GC503	Firmicutes_A	*Lachnospiraceae*	*Anaerostipes sp.*	mGAM
GC544	Firmicutes_A	*Lachnospiraceae*	*Blautia_A sp000285855*	0.5 BHI3 + 5% FBS
GC839	Firmicutes_A	*Lachnospiraceae*	*Agathobacter rectalis*	mGAM
GC635	Firmicutes_C	*Veillonellaceae*	*Veillonella parvula*	0.5 BHI3 + 5% FBS
GC185	Proteobacteria	*Enterobacteriaceae*	*Escherichia flexneri*	0.5 BHI3 + 5% FBS
GC253	Proteobacteria	*Enterobacteriaceae*	*Escherichia coli*	0.5 BHI3 + 5% FBS
GC61	Proteobacteria	*Enterobacteriaceae*	*Enterobacter himalayensis*	0.5 BHI3 + 5% FBS
S14028	Proteobacteria	*Enterobacteriaceae*	*Salmonella enterica* serovar Typhimurium	0.5 BHI3 + 5% FBS
GC7	Verrucomicrobiota	*Akkermansiaceae*	*Akkermansia muciniphila*	BHI3 + 5% FBS

All starting ODs used were 0.01 except for *A. muciniphila*, which was at 0.05.

Supplementary Table 2. 3. **Bifidobacterium adolescentis *genomes statistics*.**

Strain	Total Length	Contigs	N50	N90
GC583	2501804	38	224495	74607
GC586	2497489	46	366474	82152
GC607	2497694	42	222992	50997
GC609	2276175	44	233136	77630
GC612	2402362	21	1713981	119958
GC622	2516778	29	290377	75763
GC632	2503453	40	233073	74614
GC641	2210700	16	1759187	107668
GC657	2519437	28	290376	83012
GC659	2277811	30	329698	82646
GC663	2497240	46	237378	80679
GC666	2502690	32	329228	82712
GC669	2496856	43	237380	81282
GC725	2278288	36	258359	74595
GC733	2159217	22	407194	75586
GC735	2159384	20	467062	89694
GC736	2159103	18	467134	89612
GC737	2159954	17	1239196	75586
GC749	2159493	19	467135	75657
GC808	2159459	21	467062	118530
GC809	2159460	21	467062	82538
GC810	2159452	19	467061	118529
GC814	2159610	22	467134	82543
GC815	2160502	21	467063	82538
GC816	2159397	23	467064	118080
GC817	2159461	23	467063	82538
GC819	2159300	22	467063	82538
GC821	2159569	22	467135	82538
GC854	2258482	30	480535	82390
GC855	2257389	27	1243519	82150
GC857	2244160	28	1243520	62909

Supplementary Table 2. 4. **Bifidobacterium adolescentis *and other* Bifidobacterium *species relative growth data*.**

ID	Species	Growth Relative to Vehicle Control
GC657	*B. adolescentis*	34.2
GC810	*B. adolescentis*	36.0
GC821	*B. adolescentis*	38.4
GC809	*B. adolescentis*	39.7
GC808	*B. adolescentis*	41.1
GC749	*B. adolescentis*	41.6
GC814	*B. adolescentis*	45.8
GC641	*B. adolescentis*	47.7
GC819	*B. adolescentis*	50.9
GC583	*B. adolescentis*	51.8
GC736	*B. adolescentis*	51.8
GC733	*B. adolescentis*	52.6
GC737	*B. adolescentis*	53.7
GC816	*B. adolescentis*	58.3
GC817	*B. adolescentis*	60.9
GC666	*B. adolescentis*	63.3
GC815	*B. adolescentis*	64.9
GC586	*B. adolescentis*	67.5
GC854	*B. adolescentis*	73.1
GC735	*B. adolescentis*	75.3
GC725	*B. adolescentis*	77.3
GC663	*B. adolescentis*	77.8
GC669	*B. adolescentis*	89.4
GC659	*B. adolescentis*	90.8
GC857	*B. adolescentis*	91.9
GC632	*B. adolescentis*	93.0
GC607	*B. adolescentis*	100
GC609	*B. adolescentis*	100
GC612	*B. adolescentis*	100
GC622	*B. adolescentis*	100
GC855	*B. adolescentis*	100
GC96	*B. breve*	64.2
GC1101	*B. catenulatum*	100
GC914	*B. catenulatum*	100

GC948	*B. dentium*	100
GC399	*B. longum*	80.6
GC899	*B. longum*	85.9
GC133	*B. longum*	100
GC134	*B. longum*	100
GC398	*B. longum*	100
GC462	*B. longum*	100
GC751	*B. longum*	100
GC95	*B. scardovii*	61.8
GC93	*B. scardovii*	73.0
GC92	*B. scardovii*	95.3
GC90	*B. scardovii*	97.5
GC89	*B. scardovii*	97.6
GC94	*B. scardovii*	99.3
GC87	*B. scardovii*	100
GC88	*B. scardovii*	100
GC91	*B. scardovii*	100

Supplementary Table 2. 5. RNAtag-seq adapters and primers used in this study.

Sequence	**Barcode**	**Purpose**
/5Phos/A ACATTATT AGATCGGAAGAGCGTCGTGTA /3SpC3/	ACATTATT	Ctrl_1
/5Phos/A CCCTACAG AGATCGGAAGAGCGTCGTGTA /3SpC3/	CCCTACAG	BPA_1
/5Phos/A TGGGAGAC AGATCGGAAGAGCGTCGTGTA /3SpC3/	TGGGAGAC	BPS_1
/5Phos/A ACCCATGT AGATCGGAAGAGCGTCGTGTA /3SpC3/	ACCCATGT	Ctrl_2
/5Phos/A CCGGTACC AGATCGGAAGAGCGTCGTGTA /3SpC3/	CCGGTACC	BPA_2
/5Phos/A CCAAGTCG AGATCGGAAGAGCGTCGTGTA /3SpC3/	CCAAGTCG	BPS_2
/5Phos/A AAGTGTTG AGATCGGAAGAGCGTCGTGTA /3SpC3/	AAGTGTTG	Ctrl_3
/5Phos/A CGGAGGGC AGATCGGAAGAGCGTCGTGTA /3SpC3/	CGGAGGGC	BPA_3
/5Phos/A CCCGTCTT AGATCGGAAGAGCGTCGTGTA /3SpC3/	CCCGTCTT	BPS_3
/5Phos/AGATCGGAAGAGCACACGTCTG /3SpC3/	-	3Tr3 adapter (3' linker) with 5'P and 3' C3 spacer
TACACGACGCTCTTCCGAT	-	AR2 primer for cDNA synthesis
/5Phos/A GAACGATT AGATCGGAAGAGCGTCGTGTA/36-FAM/	GAACGATT	Control Oligo Tag33FAM to confirm successful tag

Supplementary Table 2. 6. **Bifidobacterium adolescentis – *bisphenols RNA-seq statistics*.**

Sample	Total Reads	Assigned Reads (%)	rRNA Assigned (%)
BPA1	6567971	4037425 (61.5)	924 (0.01)
BPA2	5276262	3363307 (63.7)	1646 (0.03)
BPA3	5990677	3324909 (55.5)	3285 (0.05)
BPS1	7463237	4343437 (58.2)	11162 (0.15)
BPS2	10642395	6241202 (58.6)	3954 (0.04)
BPS3	8233342	4943038 (60.0)	1435 (0.02)
Ctrl1	4179057	2712926 (64.9)	6258 (0.15)
Ctrl2	6570854	4152804 (63.2)	1685 (0.02)
Ctrl3	8443760	5066238 (60.0)	4931 (0.06)

Chapter 3. Transcriptional regulation of human gastrointestinal microbiota species by agri-food chemicals

Preface

Research presented as part of this chapter has been prepared for publication as:

Syed SA, Rossi L, Shekkariz S, Derakshani H, Marko VA, Bernier SP, Barra NG, Schertzer JD, Khan WI, Steinberg GR, Morrison KM, Holloway AC, & Surette MG. Transcriptional regulation of human gastrointestinal microbiota species by agri-food chemicals. *In preparation*.

Author contributions: SAS, LR, SS, HD, NBG, ACH, JDS, WIK, GRS, KMM, and MGS contributed to the intellectual design of the study. SAS, performed all experiments. LR assisted with library preparation of RNA samples. Isolate collection and sequencing was performed by HD, VAM, and SPB. Data analysis was performed by SAS. SAS wrote the manuscript.

This publication is in preparation for publication and up to date as March 15, 2023.

Title page and author list

Transcriptional regulation of human gastrointestinal microbiota species by agri-food chemicals

Saad A. Syed[1], Laura Rossi[2], Shahrokh Shekkariz[1], Hooman Derakshani[1], Victoria A. Marko[1], Steve P. Bernier[1], Nicole G. Barra[1], Alison C. Holloway[1,3], Jonathan D. Schertzer[1], Waliul I. Khan[1], Gregory R. Steinberg[1,2], Morrison KM[1] & Michael G. Surette[1,2,*]

[1]Department of Biochemistry and Biomedical Sciences, McMaster University, Hamilton, Canada

[2]Department of Medicine, McMaster University, Hamilton, Canada

[3]Department of Obstetrics and Gynecology, McMaster University, Hamilton, Canada

* To whom correspondence should be addressed:

surette@mcmaster.ca

3.1. Abstract

Agricultural toxicants are known to be ingested by the general human population, where they are exposed to the human gastrointestinal tract, and the gastrointestinal microbiota. Little is known about how agri-food chemicals impact gene expression of gastrointestinal microbiota species. Here, to assess the impact of seven of the globally most commonly used food production and processing chemicals at doses relevant to a single exposure in food consumption on gene expression. we apply RNA sequencing to eight genetically diverse gastrointestinal microbiota species cultured from healthy humans. We find that azo dyes, namely Allura Red and Sunset Yellow, demonstrate the greatest degree of gene modulation with minimal detected impact by pesticides and bisphenols. Functional enrichment analysis of differentially expressed genes suggest changes to transcriptional factor expression relating to virulence and the bacterial cell wall. Together, this data provides insight into a previously uncharacterized gut microbial-xenobiotic relationship and raise questions for future investigations into the role of azo dyes on the human gut microbiome.

3.2. Introduction

Much of human exposure in the general public to agricultural toxicants is felt to be through oral ingestion and through the gastrointestinal tract (Djekkoun et al., 2021). The gastrointestinal microbiota response to toxicants is a relative unknown in chemical toxicologic profiles.

The interaction of xenobiotics, like agricultural toxicants, and human gastrointestinal microbiota species is a pivotal lever for bacterial function. For example, subtherapeutic dosages of antibiotics have previously been shown to impact the global expression profile of the gastrointestinal pathogen *Salmonella* Typhimurium and *Escherichia coli*, in the absence of growth impacts, to promote virulence and alter microbial metabolism (Goh et al., 2002; Yim et al., 2010). Notably, it has been shown that the pesticide glyphosate, at high concentrations, modulates transcription of *E. coli* with broad changes in genes responsible for both virulence and metabolism (Lu et al., 2013). A growing body of literature also links gut microbiota changes with agricultural chemical exposure and deleterious host impacts (Liang et al., 2019; Motta et al., 2018; Tian et al., 2020).

With respect to agricultural toxicants, each layer of food production adds more xenobiotics to the list of potential human exposures. The use of pesticides such as glyphosate, metolachlor, and deltamethrin are highly common in crop production in the developed world. Food processing of crops after harvest often involves the addition of colourants, such as the azo dyes like Allura Red and Sunset Yellow to enhance visual appeal. Finally, foods are stored in polycarbonate packaging, made with bisphenol A or more commonly now, alternatives, such as bisphenol S.

Little is known how these chemicals directly impact the gene regulation of gastrointestinal microbiota species. Notably, Allura Red has been shown to play a role in inducing colitis in mice through microbiome-associated mechanisms (Kwon et al., 2022). Similarly, case reports exist of Sunset Yellow associating it with adverse drug reactions when used as an excipient, including gastrointestinal symptoms (Gross et al., 1989; Jenkins et al., 1982; Taneja et al., 2021).

Until recently, previous challenges in culturing fastidious microbes of the gastrointestinal microbiome contributed to a limited understanding of xenobiotic-microbe interactions. Here, we utilize isolates from this culture collection to map the impact of seven of the most used pesticides and food processing compounds to assess their impact on gut microbial transcription.

3.3. Methods

3.3.1. Microbial strains and growth

All strains, except for *Akkermansia muciniphila* ATCC-BAA835, were isolated as previously described and grown as outlined in Chapter 2.3 (Derrien et al., 2004; Lau et al., 2016). Strains were selected based on prior screening (**Table 1**). Briefly, strains were grown from frozen stocks on BHI agar with 0.5g/L L-cysteine, 10mg/L hemin, 1mg/L vitamin K and then transferred to BHI broth (with the same supplements as above). All growth was conducted in a Coy Laboratory Vinyl Anaerobic Chamber (5 % CO_2, 2 % H_2, 93 % N_2) and incubations were done at 37°C. Media were pre-reduced in the anoxic environment for at least 4 hours before use.

Cell cultures were then diluted to an OD600 of 0.01 to achieve a final volume of 1ml in 2ml deep-well 96-well microplates.

3.3.2. Chemical selection and exposures

Chemicals were purchased from Toronto Research Chemicals Inc. (Toronto, CA) and suspended in dimethyl sulfoxide. Chemicals were selected based on inclusion in screening carried out in Chapter 2, as well as any of 1) involvement in at least one microbe-chemical pair with a growth impact (i.e. deltamethrin), 2) close structural similarity with a compound that did cause growth impacts (Bisphenol A as a structural analogue with Bisphenol S), or 3) common usage globally with keen public and scientific interest (i.e. glyphosate) (**Table 2**).

Chemicals were combined with culture inoculate such that chemical concentrations were 1uM and 1% DMSO. 1% DMSO served as vehicle control. Breathable membranes were overlayed to prevent evaporation. Growth occurred until an OD600 of 0.1-0.3, at which point chemicals were added for 2 hours before proceeding immediately to RNA isolation. All experiments were performed in triplicate. Batch effects were minimized by only one user performing all experiments and grouping each replicate for each microbe across all chemicals on each day.

3.3.3. Total RNA isolation and RNA-seq library preparation

Please see **Appendix File 1** for full details on extraction. Briefly, 1ml of culture was centrifuged at 4,000 x *g* at room temperature for 2 minutes. Cell pellets were rapidly resuspended in the extraction solution (95% formamide, 18 mM ethylenediaminetetraacetic acid, 0.025% sodium dodecyl sulphate and 1% B-mercaptoethanol) and incubated at 95°C for 7 minutes to lyse cells (Stead et al., 2012). The samples were then centrifuged at 16,000 x *g* for 5 minutes at room temperature and 200ul of the supernatant was transferred to a fresh tube for RNA clean up with the Zymo clean and concentrator kit (USA; #R1017 and #E1010) per manufacturer's

instructions. Total RNA concentrations were measured using the Qubit RNA HS Assay Kit (ThermoFisher Scientific, USA; Q32855). RNA integrity was confirmed for all samples on a 0.8% agarose gel in TBE buffer and a random subset of 15 samples were also assessed using the Tapestation (Agilent Technologies, USA).

3.3.4. RNA-seq library preparation

The RNA-seq libraries were prepared using RNAtag-Seq, with minor modifications, as detailed in **Appendix File 2** (Shishkin et al., 2015). Briefly, we combined the library preparation of three replicates from chemical exposure samples and vehicle control samples for each bacteria into a pool of 24 samples. Unique barcoded adaptors (**Supplementary Table 1**) were used to tag each sample.

Ribosomal RNA (rRNA) depletion was performed utilizing a previously described RNase H-based depletion protocol, with minor modifications, detailed in **Appendix File 3** (Huang et al., 2020). Probes were generated with 16S and 23S rRNA sequences extracted using barrnap from the sequenced genomes and are available in **Appendix File 4**. For each organism, probe pools were ordered as DNA oPools (Integrated DNA Technologies Inc.; Coralville, USA) at 50pmol per oligo and dissolved in DNase/RNase-free distilled water to achieve a final concentration of 1000ng/ul. Briefly, 500ng of whole RNA underwent annealing to ssDNA probes at a 1:10 ratio, followed by incubation with RNase H at 45°C for 30 minutes. Probes were removed using a 2X ratio of RNAClean XP beads to sample volume and output was utilized for first strand synthesis and subsequent RNAtag-seq library preparation. The RNAtag-seq library was sequenced by single-end (1x100) Illumina sequencing at McMaster Genomics Facility (Hamilton, Canada) on the NextSeq platform. To

minimize technical confounding, all samples of the same organism underwent library preparation together and all samples were sequenced on the same sequencing run.

3.3.5. RNA-seq data analysis

The pool was demultiplexed according to the unique 8nt ligated barcode adaptor for each sample using cutadapt (v3.4), retaining reads with a quality score > 20 and post-trimming lengths >25nt (Supplementary Table 2; Martin, 2011). Post-demultiplexing reads were assessed using multiQC (v1.14): The median sample read depth was 5,499,064 reads (IQR: 4157558.5 – 7112671.75) and no obvious bias in the number of final reads counted per sample was noted, with median assigned reads of 3,716,252 reads (IQR: 2863964.25 – 4765683.25 **Supplementary Table 3**) (Ewels et al., 2016).

The sequenced bacterial genome was annotated with bakta (Schwengers et al., 2021). Reads were mapped after demultiplexing to this reference genome using BWA, and indexed and sorted with SAMtools (H. Li et al., 2009; H. Li & Durbin, 2009). Successful rRNA depletion was confirmed using htseq-count by quantifying reads mapped to rRNAs, with <1% rRNA reads in all samples (**Supplementary Table 3**; Anders et al., 2015).

Differential gene expression analysis

RNA-seq analysis workflows were based on previously published workflows (Chen, Lun, et al., 2016; Love et al., 2016). Read counts per gene were generated using featureCounts in the subread package using single, reverse-stranded input and including all annotations within a mapped sequence (Y. Liao et al., 2014). All samples with less than 1.5 million reads mapped to the reference were removed (3/192). Unsupervised exploratory analysis was first completed to assess data structure and

identify any outliers for removal using principal component analysis plots generated with regularized log transformed count data. Genes with less than 11 reads across all samples and appearing in 2 or less samples were removed. RUVseq was used to identify hidden batch effects for inclusion in differential expression analysis with an iterative approach (Risso et al., 2014). Differential expression analysis was performed using DESeq2 with the Wald test and including sample replicate as a fixed effect. Differentially expressed genes were defined as those with a p value after Benjamin-Hochberg adjustment for multiple testing of <0.05 (Benjamini & Hochberg, 1995; Love et al., 2014). The shinyGO web app (version 0.77) was used to perform functional enrichment analysis using the STRING gene set library (version 11.5), the hypergeometric test for statistical enrichment calculations with false discovery rate corrections (Ge et al., 2020; Szklarczyk et al., 2023). The background list was specified as all genes that underwent modeling in DESeq2.

Phylogenetic tree generation

A phylogenetic tree of the included strains was generated with PhyloT (https://phylot.biobyte.de/) in Newick format using GTDB taxonomy(Parks et al., 2022). The visualization of the tree was achieved using iTol (Letunic & Bork, 2021).

Data visualization

Visualization was performed with DESeq2 and ggplot2 (Love et al., 2014; Wickham et al., 2019). Venn diagrams were calculated and created using the Venn Diagrams web tool (https://bioinformatics.psb.ugent.be/webtools/Venn/). All figures were finalized for publication using Inkscape (v1.2.1).

3.4. Results

Our previous work (detailed in Chapter 2) illustrated growth impacts of agricultural toxicants, leading us to seek to better characterize the transcriptome landscape of a panel of broadly representative gastrointestinal microbes (**Table 1**) exposed to a curated panel of agri-food chemicals (**Table 2**).

3.4.1. Bacterial-chemical selection

Bacteria were cultured from healthy adult human donor stool and were priority organisms for further study based on earlier described growth screening. Some selected strains were previously used in gastrointestinal microbiota research, such as *E. coli* and *A. muciniphila* although the majority were non-model bacteria (**Figure 1**). In total, these microbes consisted of at least one representative of the four major phyla of the gastrointestinal microbiota, and multiple of the two most predominant, the Firmicutes and Bacteroidota. We paired each of these eight bacteria with seven agri-food chemicals of interest. These chemicals were selected based of common usage globally and previous reports of possible impacts on gut microbiota. With a median of over 3.7 million assigned non-rRNA reads, the necessary 2-3 million non-rRNA reads to proceed with statistical testing for reliable differential gene expression testing were available for all 56 bacteria-toxicant combinations and for control conditions (**Supplementary Table 3**; Haas et al., 2012).

3.4.2. Differential gene expression profiles find subtle changes in expression in response to azo dyes and little response to other agri-food chemicals

Differential gene expression analysis showed heterogeneity in the degree of response to each condition (**Figure 2a;** all differentially expressed genes summarized in

Appendix File 4). For example, bisphenol A and deltamethrin elicited very little change in gene expression whereas both azo dyes were noted, on average, to elicit the most gene regulation across our eight bacteria. Interestingly, this azo dye gene regulation appeared to be noted more in gram-negative organisms (**Figure 2b**). No obvious differences were noted when data was analyzed by phyla (**Supplementary Figure 3**).

Notably, prior to proceeding with differential expression analysis, we generated unsupervised principal coordinate analysis plots to assess for possible outliers or overt sources of systematic bias in our samples (**Supplementary Figure 1**). We identified 3 outlier samples that were removed (**Supplementary Figure 2**). Furthermore, replicate samples for each condition within each bacterial strain were noted to be explain sample variation in most bacterial strains in unsupervised analysis plots. Therefore, replicate number was included in the statistical model for those organisms. We felt dispersion within each condition was within an acceptable range of similarity and proceeded with analyzing samples together rather than as individual groups versus control.

3.4.3. Differential gene regulation between azo dyes in impacted bacteria

We next focused our analysis on the azo dyes considering less gene regulation in our bacteria to the bisphenols or pesticides. We assessed the conservation of gene regulation between the two azo dyes we tested across bacteria with altered gene expression in the presence of both dyes (**Figure 3**). There was substantial overlap in differentially expressed genes in *Bacteroides* species and *A. muciniphila*, where the majority of differentially expressed genes were shared between the two azo dyes. Meanwhile, in

E. coli only Allura Red was noted to modulate gene expression with no differentially expressed genes when *E. coli* was exposed to Sunset Yellow.

3.4.4. Functional enrichment analysis suggests impact on cell wall and virulence regulation

To better understand whether these differences between azo dyes related to the function of differentially expressed genes, we undertook functional enrichment analysis (**Figure 4**). We noted functional enrichment of a distinct pathway in each of Allura Red and Sunset Yellow. In Allura Red exposed *E. coli*, pathways associated with the transcriptional regulator AraC were enriched. In *B. fragilis*, pathways associated with outer membrane function were enriched, although notably the quality of pathway annotation was noted to be largely uncharacterized. We did not find high-quality annotation databases for *A. muciniphila* or *B. xylanisolvens* but did proceed with testing against available databases – this analysis did not find any enriched pathways.

3.5. Discussion

The human gastrointestinal microbiota expands the genetic repertoire of the human gastrointestinal tract, yet much of the current field of research has focused on characterizing the taxonomic and genetic compositions rather than the expressed genes. While previous studies have explored the interaction of agricultural toxicants on microbial gene expression, little exists on the impact on gastrointestinal microbiota or at concentrations relevant to general population exposure (Lu et al., 2013). In this study, we apply RNAtag-seq to quantify the impact of seven commonly used agricultural toxicants at physiologically relevant concentrations on eight prevalent and diverse human gastrointestinal microbiota (Shishkin et al., 2015). We utilize RNAse-H

based depletion to successfully deplete the vast majority of rRNA in our samples; this allowed for sufficient reads mapping with only 5.5 million reads on average per sample (Huang et al., 2020).

We noted very little impact on gene regulation by glyphosate, deltamethrin, metolachlor, bisphenol A, and bisphenol S at our tested concentrations which were applied for two hours prior to proceeding with extraction. Notably, both azo dyes had the highest percentage of regulated genes and this response, at least partly, was found to relate to gene regulation related to the gram negative cell wall. In *E. coli*, where only Allura Red induced changes in gene expression, pathway enrichment analysis suggested an impact on transcriptional regulation relating to virulence.

Notably, xenobiotics are foreign to living organisms and so an evolutionary basis for their impacts has been hypothesized to more likely relate to toxicity or metabolism mediated by generally broadly applicable transcription factors. Our results align with this perspective as we also noted gene expression changes relating to cell wall function and transcription factors relating to virulence.

The lack of more broad changes in gene regulation in this study may relate to several factors. Real-life exposure may be more closely represented by intermittent exposures of higher concentrations over a wider period of time – this study focused on a slightly lower concentration and a single exposure. Further, impacts on gene expression may relate more to regulation earlier in exponential phase or in stationary phase and our experiment would have missed this 'window' of gene expression.

Our study is limited by several other factors. In our methodology, we did note systematic impact of replicates in our unsupervised PCA plots. Notably, this was felt to be relating to laboratory technique and, importantly, orthogonal in all PCA plots to

our variable of interest (i.e. unrelated to our covariates of interest). This bias was therefore not felt to confound differential gene expression analysis results. Our experimental design also has substantial complexity and includes comparison both between control samples and each toxicant but also between chemicals of the same class and through functional analysis, such as with the azo dyes. We assumed similar dispersion within conditions and although this was generally true across our analyses, there were some cases where increased dispersion within one condition could have impacted our statistical analysis. We also have limited statistical power considering our total number of samples per condition, which also limits our ability to detect smaller changes in gene expression. Notably, further inferential analysis from our sequencing results was limited by our choice of non-model bacteria as most functional enrichment tools rely on curated databases of lab organisms. Further, our experiments were all conducted in single organisms and with single toxicants whereas in more real-world cases, microbial communities and toxicant mixtures are the reality. Nonetheless, our present results still capture an essential component of bacterial-toxicant exposure and the associated transcriptomic landscape.

The advantages of our experimental design include a scalable and more customizable approach to bacterial screening, library preparation, and analysis in non-model bacteria that enables stream-lined whole transcriptome profiling of the diversity of human microbiota. In summary, the results presented here provide novel avenues for further research into toxicant-microbe interactions, particularly with respect to azo dyes and gastrointestinal microbial gene expression as it relates to microbial virulence and function.

3.6. Acknowledgements

We thank the staff of the Farncombe Metagenomic Facility (Hamilton, CA) for constructive discussions and support in sample preparations and library sequencing. We also thank Jonathan Livny and Yiming Huang for discussions on bacterial rRNA depletion in non-model bacteria. Lastly, we thank Jake Szamosi for many conversations on RNA-seq sample processing, analysis, and interpretation. This work was supported by funding from Canadian Institutes for Health Research.

3.7. Figures

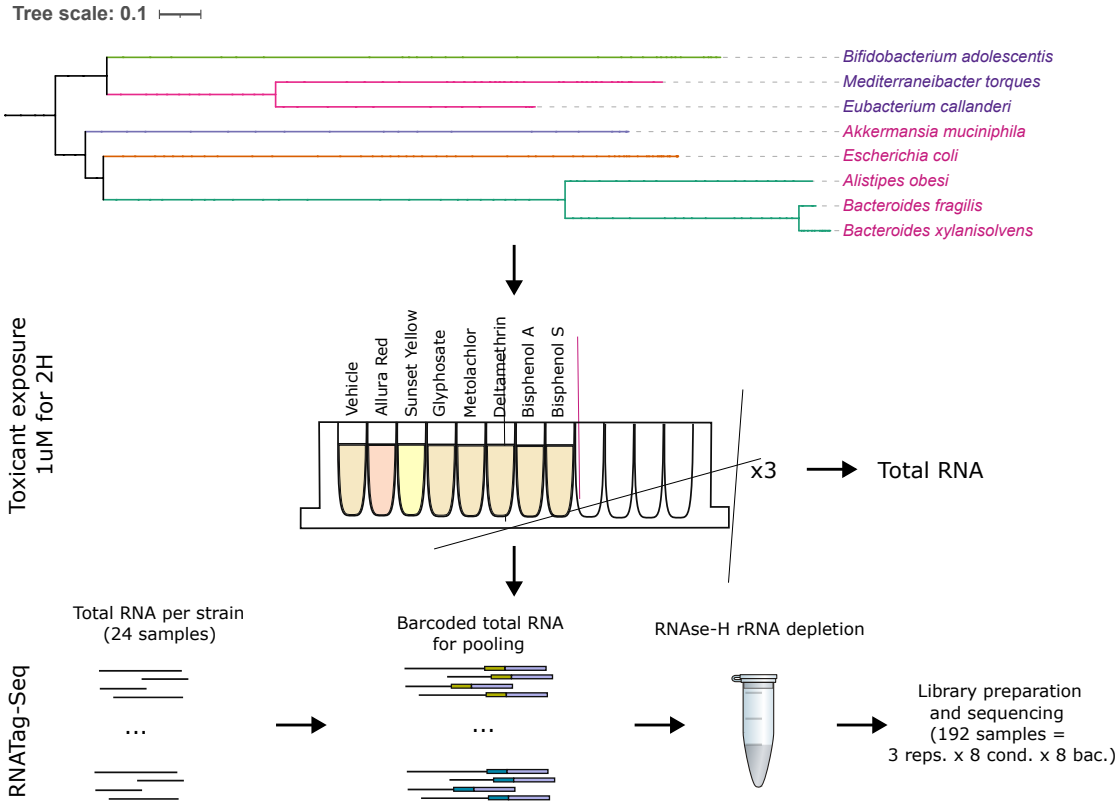

Figure 3. 1. Schematic of experimental design and phylogeny of organisms screened.

Phylogenetic tree with label colours indicating gram stain (pink – gram negative, purple – gram positive), and branches coloured by phyla (green – Actinobacteriota, red – Firmicutes, blue – Verrucomicrobiota, orange – Proteobacteria, and cyan – Bacteroidota) is shown. RNA-seq library preparation layout to generate 24 samples per species 98 conditions with 3 replicates) for RNAtag-Seq resulted in 192 total samples.

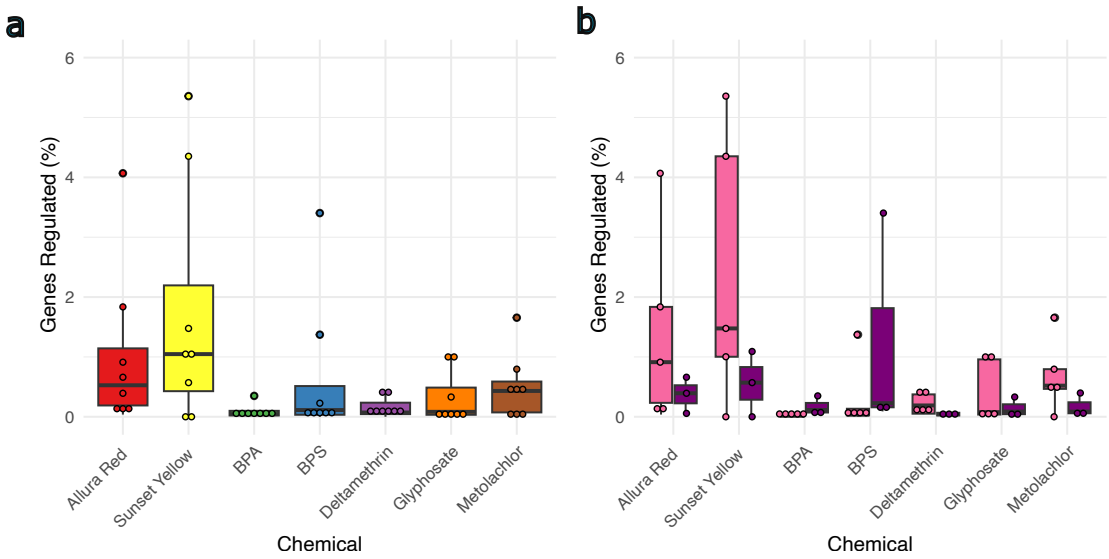

Figure 3. 2. Differential expression testing for transcriptomic profiles of each bacterial species across various chemical exposures (vs. control) summarized across all bacteria and by gram stain.

a) Screened chemicals are shown by colour and each dot represents one bacteria paired with that chemical and its percentage of differential gene expression across all tested genes. **b)** Gram-negative (n=5; pink) and gram-positive (n=3; purple) are shown by chemical.

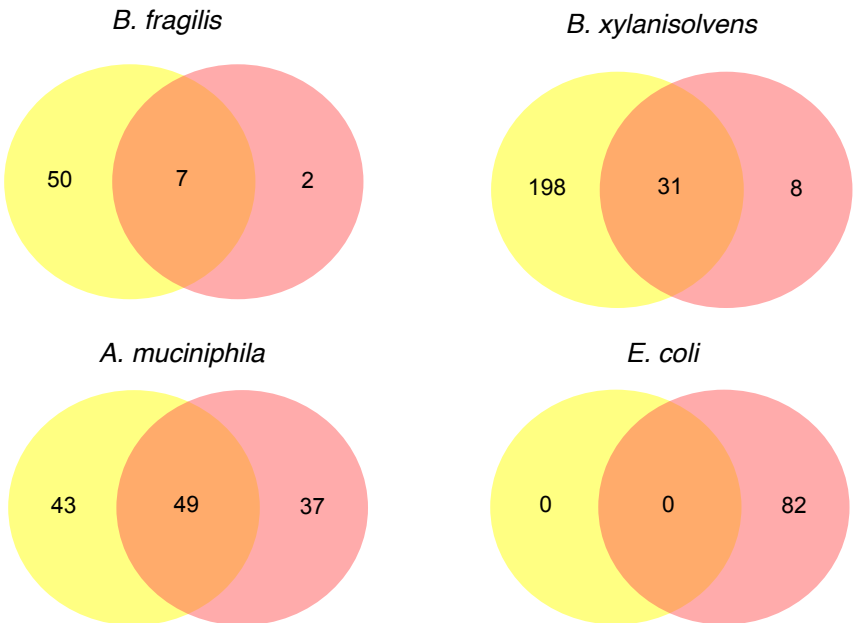

Figure 3. 3. Conserved responses to azo dyes across selected bacteria.

Bacteria with at least 50 differentially expressed genes under exposure conditions were selected for intersection analysis. Yellow circle indicates differential expressed genes in Sunset Yellow. Red circle indicates differentially expressed genes in Allura Red.

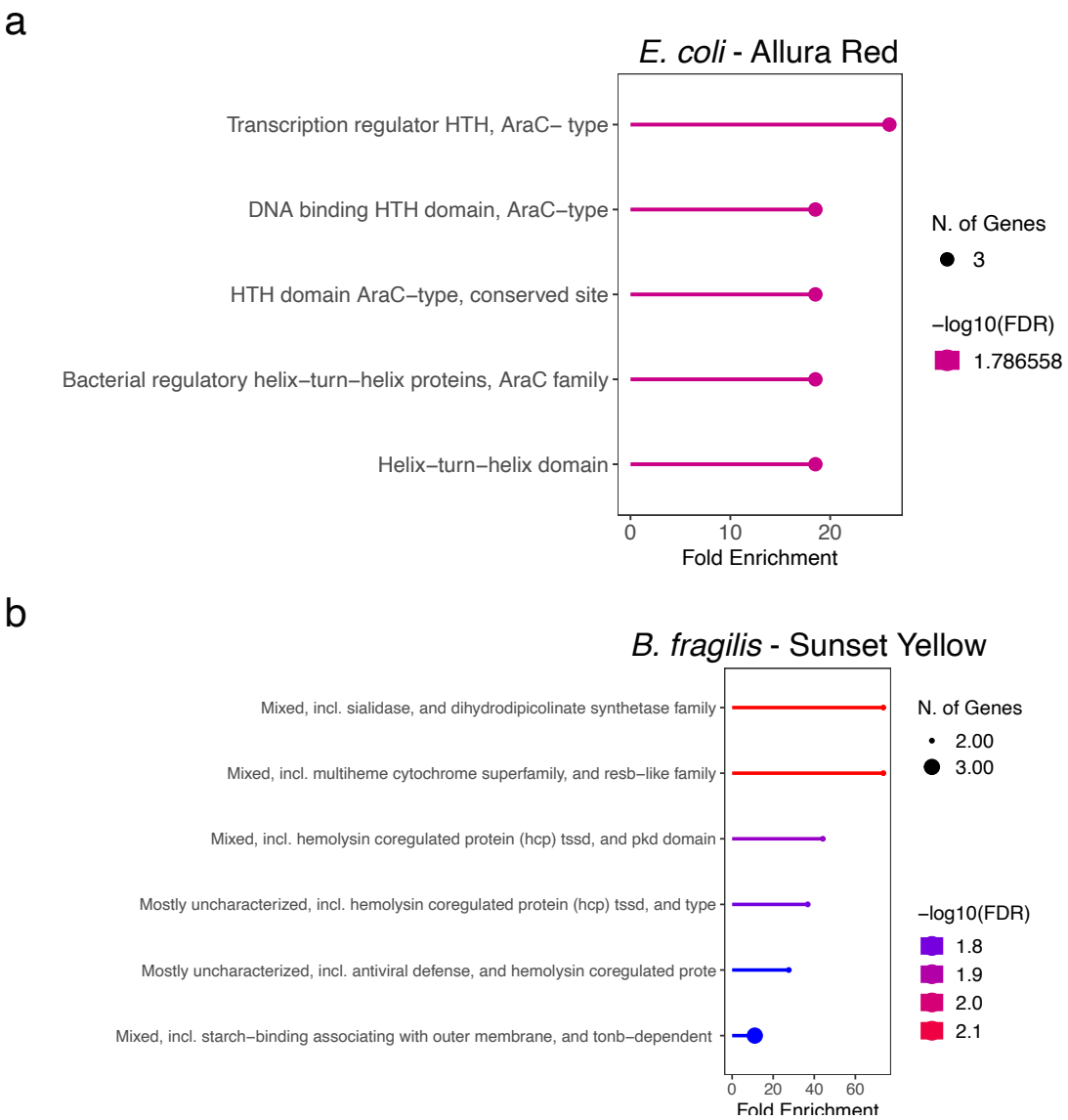

Figure 3. 4. Functional enrichment analysis of two different azo dye-bacterial pairs,* E. coli *and Allura Red, and* B. fragilis *and Sunset Yellow.

Functional categories are noted on the left-hand side with degree of fold-enrichment of that category shown. Size of the end of the line indicates number of genes within that category that were differentially regulated in the pair.

3.8. Tables

Table 3. 1. Strains utilized in this study.

Strain ID	**Taxonomy**	**Phylum**
GC641	*Bifidobacterium adolescentis*	Actinobacteriota
GC129	*Alistipes obesi*	Actinobacteriota
GC73	*Bacteroides fragilis*	Bacteroidota
GC187	*Bacteroides xylanisolvens*	Bacteroidota
GC811	*Eubacterium callanderi*	Firmicutes
GC450	*Mediterraneibacter torques*	Firmicutes
GC253	*Escherichia coli*	Proteobacteria
ATCC BAA-835	*Akkermansia muciniphila*	Verrucimicrobiota

All strains were sourced from this study except *A. muciniphila* which was from Derrien et al. (2004).

Table 3. 2. Agricultural toxicants screened in this study.

Chemical	**Class**
Allura Red	Food processing
Sunset Yellow	Food processing
Metolachlor	Pesticide
Glyphosate	Pesticide
Deltamethrin	Pesticide
Bisphenol A	Food packaging
Bisphenol S	Food packaging

3.9. Supplementary Material

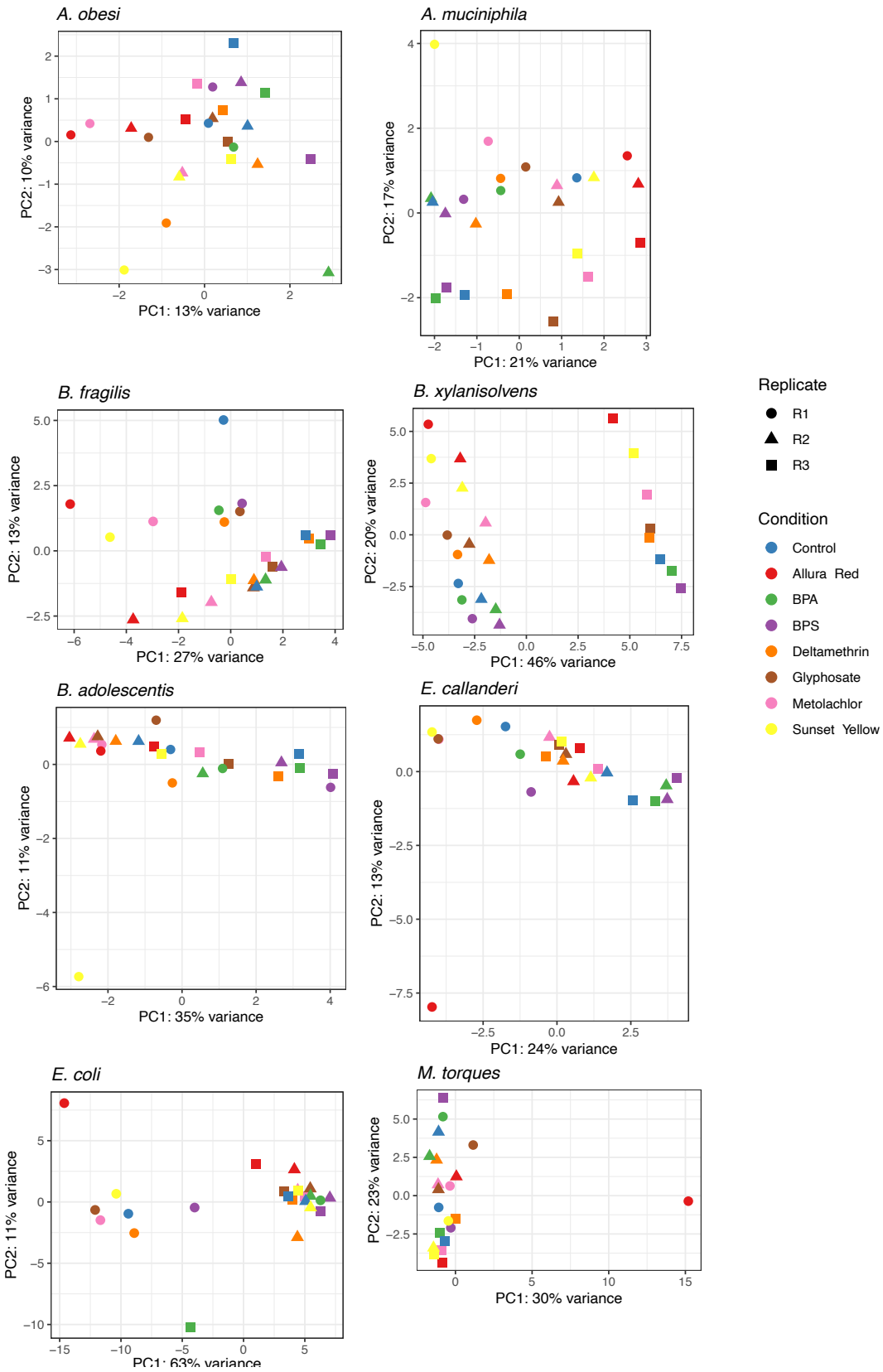

Supplementary Figure 3. 1. Unsupervised exploratory principal component analysis plots of all samples by species.

Percent variance explained and axis number is indicated in axis labels. Shapes indicate replicates and colours indicate agricultural toxicant exposure.

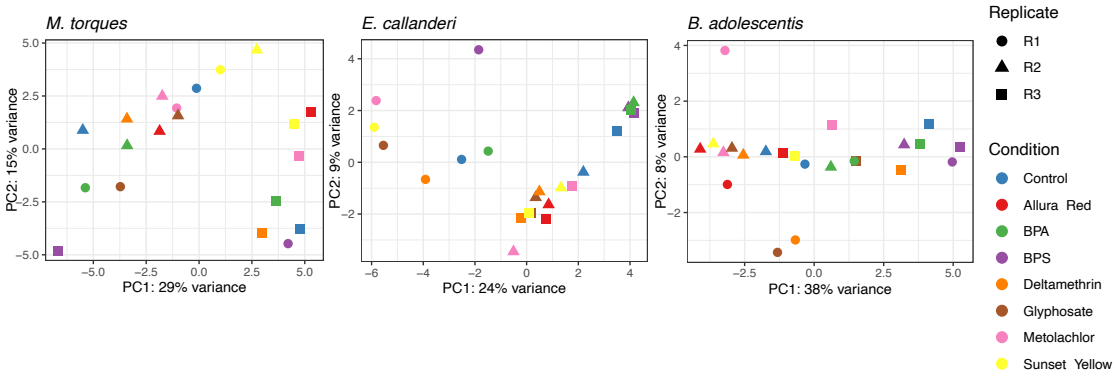

Supplementary Figure 3. 2. Principal component analysis plots of three bacteria after removal of an outlier for each bacterial strain.

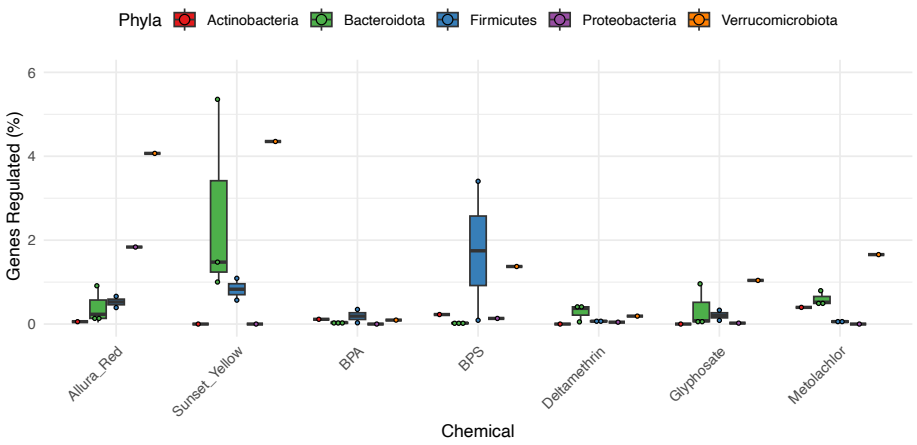

Supplementary Figure 3. 3. Differential expression testing for transcriptomic profiles of each bacterial summarized by phylum.

2.10 Supplementary Tables

Supplementary Table 3. 1. RNATag-Seq primers and barcodes utilized in this study.

Name	**Sequence (5' to 3')**
Adapt_1	/5Phos/ A ACATTATT AGATCGGAAGAGCACACGTCTGAACTC /3SpC3/
Adapt_2	/5Phos/ A AAGTGTTG AGATCGGAAGAGCACACGTCTGAACTC/3SpC3/
Adapt_3	/5Phos/ A AGAATTAT AGATCGGAAGAGCACACGTCTGAACTC/3SpC3/
Adapt_4	/5Phos/ A ATATGGAC AGATCGGAAGAGCACACGTCTGAACTC/3SpC3/
Adapt_5	/5Phos/ A ATCACTTG AGATCGGAAGAGCACACGTCTGAACTC/3SpC3/
Adapt_6	/5Phos/ A CCAAGTCG AGATCGGAAGAGCACACGTCTGAACTC/3SpC3/
Adapt_7	/5Phos/ A CAACTCGC AGATCGGAAGAGCACACGTCTGAACTC/3SpC3/
Adapt_8	/5Phos/ A CCCGTCTT AGATCGGAAGAGCACACGTCTGAACTC/3SpC3/
Adapt_9	/5Phos/ A CCCTACAG AGATCGGAAGAGCACACGTCTGAACTC/3SpC3/
Adapt_10	/5Phos/ A CCCTCGGC AGATCGGAAGAGCACACGTCTGAACTC/3SpC3/
Adapt_11	/5Phos/ A CCGGTACC AGATCGGAAGAGCACACGTCTGAACTC/3SpC3/
Adapt_12	/5Phos/ A CGGAGGGC AGATCGGAAGAGCACACGTCTGAACTC/3SpC3/
Adapt_13	/5Phos/ A CTCGGTAC AGATCGGAAGAGCACACGTCTGAACTC/3SpC3/
Adapt_14	/5Phos/ A CGGCACTT AGATCGGAAGAGCACACGTCTGAACTC/3SpC3/
Adapt_15	/5Phos/ A CTCTAACT AGATCGGAAGAGCACACGTCTGAACTC/3SpC3/
Adapt_16	/5Phos/ A CTGGATCG AGATCGGAAGAGCACACGTCTGAACTC/3SpC3/
Adapt_17	/5Phos/ A GCAGCCAC AGATCGGAAGAGCACACGTCTGAACTC/3SpC3/
Adapt_18	/5Phos/ A GAGATTGT AGATCGGAAGAGCACACGTCTGAACTC/3SpC3/
Adapt_19	/5Phos/ A GAGCCATC AGATCGGAAGAGCACACGTCTGAACTC/3SpC3/
Adapt_20	/5Phos/ A GTAACTGC AGATCGGAAGAGCACACGTCTGAACTC/3SpC3/
Adapt_21	/5Phos/ A GGCCCAAG AGATCGGAAGAGCACACGTCTGAACTC/3SpC3/
Adapt_22	/5Phos/ A GTCTGGCG AGATCGGAAGAGCACACGTCTGAACTC/3SpC3/
Adapt_23	/5Phos/ A GGTCCTCT AGATCGGAAGAGCACACGTCTGAACTC/3SpC3/
Adapt_24	/5Phos/ A TCATCGTG AGATCGGAAGAGCACACGTCTGAACTC/3SpC3/
adap_second	/5Phos/ AGATCGGAAGAGCGTCGTGTAGG /3SpC3/
primer_RT	GAGTTCAGACGTGTGCTCTTCC

Supplementary Table 3. 2. Quality filtering and demultiplexing statistics of RNA-seq samples.

	Akkermansia muciniphila	***Alistipes obesi***	***Bifidobacterium adolescentis***	***Bacteroides fragilis***	***Bacteroides xylanisolvens***	***Escherichia coli***	***Eubacterium callanderi***	***Mediterraneibacter torques***
Raw reads	170079685	147235885	165755349	119258288	142183223	155938445	139201085	147363257
Adapter-trimmed reads	166317824	139344253	163742314	118108907	139984010	153720944	137553056	142018293
Ambiguous reads	3259162	4201084	3671547	2616801	3225931	3108211	2800914	3854548
Demultiplexed reads	163058662	135143169	160070767	115492106	136758079	150612733	134752142	138163745

Supplementary Table 3. 3. RNAtag-seq individual sample statistics.

Sample	Condition	Rep.	Tot. Reads	Tot. Reads Assigned (%)	Tot. rRNA Reads (%)
Akkermansia muciniphila	Allura Red	1	6471858	4294269 (66.35)	1454 (0.03)
		2	9402686	6067499 (64.53)	1759 (0.03)
		3	4519049	3077045 (68.09)	654 (0.02)
	Bisphenol A	1	6700005	4781836 (71.37)	1679 (0.04)
		2	4631252	3192287 (68.93)	597 (0.02)
		3	11813722	7923203 (67.07)	3635 (0.05)
	Bisphenol S	1	7509232	5016446 (66.80)	2021 (0.04)
		2	6223375	4340686 (69.75)	1663 (0.04)
		3	4812220	3576808 (74.33)	407 (0.01)
	Control	1	6236127	4275069 (68.55)	1236 (0.03)
		2	9945985	6722190 (67.59)	2323 (0.03)
		3	12675880	8315933 (65.60)	3434 (0.04)
	Deltamethrin	1	4538554	3149140 (69.39)	703 (0.02)
		2	6640492	4468104 (67.29)	927 (0.02)
		3	4868780	3234167 (66.43)	1830 (0.06)
	Glyphosate	1	5856231	4056557 (69.27)	1301 (0.03)
		2	7149445	4781860 (66.88)	1834 (0.04)
		3	3331387	2521620 (75.69)	1485 (0.06)
	Metolachlor	1	8157366	5768196 (70.71)	2178 (0.04)
		2	6100732	4379049 (71.78)	958 (0.02)
		3	5888546	4156037 (70.58)	1796 (0.04)
	Sunset Yellow	1	4470839	3215638 (71.92)	592 (0.02)
		2	4755223	3299515 (69.39)	737 (0.02)
		3	7649897	5568115 (72.79)	656 (0.01)
Alistipes obesi	Allura Red	1	8588720	6392804 (74.43)	6419 (0.10)
		2	3182475	2427662 (76.28)	2892 (0.12)
		3	3441242	2637105 (76.63)	1487 (0.06)
	Bisphenol A	1	4056485	3061049 (75.46)	4529 (0.15)
		2	2423012	1812491 (74.80)	6429 (0.35)
		3	5290815	3755371 (70.98)	20333 (0.54)
	Bisphenol S	1	10559161	7978238 (75.56)	13591 (0.17)
		2	5679187	4188331 (73.75)	32104 (0.77)
		3	3106463	2332383 (75.08)	688 (0.03)
	Control	1	7461214	5650312 (75.73)	5721 (0.10)
		2	3835512	2806967 (73.18)	5326 (0.19)
		3	9284449	6889178 (74.20)	13463 (0.20)
	Deltamethrin	1	5078689	3843672 (75.68)	1592 (0.04)
		2	3168727	2345682 (74.03)	4636 (0.20)
		3	4234484	2912116 (68.77)	24314 (0.83)
	Glyphosate	1	7147286	5166404 (72.28)	4250 (0.08)
		2	6119841	4526115 (73.96)	38155 (0.84)
		3	3807655	2811313 (73.83)	12409 (0.44)
	Metolachlor	1	9478189	6594879 (69.58)	9022 (0.14)

		2	5884003	4357052 (74.05)	24669 (0.57)
		3	5940425	4343022 (73.11)	15538 (0.36)
	Sunset Yellow	1	6617356	4760299 (71.94)	3511 (0.07)
		2	4639014	3517583 (75.83)	3161 (0.09)
		3	3704279	2895296 (78.16)	1664 (0.06)
Bifidobacterium adolescentis	Allura Red	1	4161428	2780090 (66.81)	1257 (0.05)
		2	5739263	3584437 (62.45)	890 (0.02)
		3	4383228	2647226 (60.39)	568 (0.02)
	Bisphenol A	1	6567971	4037425 (61.47)	924 (0.02)
		2	5276262	3363307 (63.74)	1646 (0.05)
		3	5990677	3324909 (55.50)	3285 (0.10)
	Bisphenol S	1	7463237	4343437 (58.20)	11162 (0.26)
		2	10642395	6241202 (58.64)	3954 (0.06)
		3	8233342	4943038 (60.04)	1435 (0.03)
	Control	1	4179057	2712926 (64.92)	6258 (0.23)
		2	6570854	4152804 (63.20)	1685 (0.04)
		3	8443760	5066238 (60.00)	4931 (0.10)
	Deltamethrin	1	3945543	2549869 (64.63)	706 (0.03)
		2	5127206	3067612 (59.83)	997 (0.03)
		3	9604173	5680534 (59.15)	5708 (0.10)
	Glyphosate	1	4101018	2606543 (63.56)	930 (0.04)
		2	7126076	4354649 (61.11)	1110 (0.03)
		3	6732513	4222981 (62.73)	1299 (0.03)
	Metolachlor	1	8328800	5373408 (64.52)	2323 (0.04)
		2	9099103	5638856 (61.97)	4214 (0.07)
		3	7260238	4246860 (58.49)	3415 (0.08)
	Sunset Yellow	1	4826127	3072803 (63.67)	647 (0.02)
		2	7379562	4503742 (61.03)	908 (0.02)
		3	6547662	4172327 (63.72)	526 (0.01)
Bacteroides fragilis	Allura Red	1	5756710	4293213 (74.58)	13484 (0.31)
		2	7125712	5306690 (74.47)	11795 (0.22)
		3	3680389	2792706 (75.88)	1899 (0.07)
	Bisphenol A	1	2732021	2116857 (77.48)	18067 (0.85)
		2	3813481	2840333 (74.48)	3837 (0.14)
		3	4928470	3005512 (60.98)	15089 (0.50)
	Bisphenol S	1	5158765	3713905 (71.99)	13538 (0.36)
		2	6681538	4687706 (70.16)	17555 (0.37)
		3	3855194	2760462 (71.60)	1065 (0.04)
	Control	1	3744005	2796268 (74.69)	4275 (0.15)
		2	5867361	4328127 (73.77)	11628 (0.27)
		3	5824906	3787169 (65.02)	20387 (0.54)
	Deltamethrin	1	2043611	1650648 (80.77)	977 (0.06)
		2	7069776	4972408 (70.33)	15293 (0.31)
		3	4788665	3397182 (70.94)	10385 (0.31)
	Glyphosate	1	4145950	3129653 (75.49)	5593 (0.18)
		2	5272639	3850262 (73.02)	4975 (0.13)

		3	3996278	3077435 (77.01)	2339 (0.08)
	Metolachlor	1	4194360	3204639 (76.40)	3448 (0.11)
		2	5123459	3908672 (76.29)	1618 (0.04)
		3	5118632	3490721 (68.20)	6934 (0.20)
	Sunset Yellow	1	3415053	2589763 (75.83)	1971 (0.08)
		2	6661795	4937808 (74.12)	5236 (0.11)
		3	2521141	1951403 (77.40)	530 (0.03)
Bacteroides xylanisolvens	Allura Red	1	5490905	4324178 (78.75)	655 (0.02)
		2	3980839	3098969 (77.85)	323 (0.01)
		3	5436124	4274608 (78.63)	371 (0.01)
	Bisphenol A	1	5373065	4277238 (79.61)	15209 (0.36)
		2	4437333	3487131 (78.59)	349 (0.01)
		3	8580404	6232438 (72.64)	2104 (0.03)
	Bisphenol S	1	8230079	6109148 (74.23)	4082 (0.07)
		2	6408226	4655929 (72.66)	1967 (0.04)
		3	4737287	3638926 (76.81)	129 (0.00)
	Control	1	4480738	3572416 (79.73)	490 (0.01)
		2	6159060	4549150 (73.86)	1429 (0.03)
		3	9048015	6392032 (70.65)	2300 (0.04)
	Deltamethrin	1	5696444	4579396 (80.39)	631 (0.01)
		2	6153156	4666301 (75.84)	1145 (0.02)
		3	3261853	2444208 (74.93)	3482 (0.14)
	Glyphosate	1	4758137	3745836 (78.72)	644 (0.02)
		2	5880801	4455243 (75.76)	621 (0.01)
		3	3657364	2874654 (78.60)	367 (0.01)
	Metolachlor	1	5587968	4471985 (80.03)	559 (0.01)
		2	6441949	5086206 (78.95)	608 (0.01)
		3	3834815	2866586 (74.75)	364 (0.01)
	Sunset Yellow	1	4030176	3276466 (81.30)	451 (0.01)
		2	6536240	5146280 (78.73)	399 (0.01)
		3	6192053	5021258 (81.09)	217 (0.00)
Escherichia coli	Allura Red	1	2811143	1978075 (70.37)	486 (0.02)
		2	7867724	5583942 (70.97)	1236 (0.02)
		3	7108325	5235889 (73.66)	571 (0.01)
	Bisphenol A	1	3294414	2340317 (71.04)	313 (0.01)
		2	5465966	3866778 (70.74)	1231 (0.03)
		3	10471484	5756102 (54.97)	1643 (0.03)
	Bisphenol S	1	3003624	2029579 (67.57)	833 (0.04)
		2	7601741	5233324 (68.84)	2987 (0.06)
		3	5939409	4032692 (67.90)	455 (0.01)
	Control	1	4324416	2923716 (67.61)	1904 (0.07)
		2	6736024	4830017 (71.70)	537 (0.01)
		3	9531546	6147634 (64.50)	2795 (0.05)
	Deltamethrin	1	3164137	2237694 (70.72)	278 (0.01)
		2	8855226	6238447 (70.45)	2008 (0.03)
		3	6421056	4092852 (63.74)	1236 (0.03)

	Glyphosate	1	5047016	3284459 (65.08)	747 (0.02)
		2	5519668	3740157 (67.76)	1228 (0.03)
		3	5676895	4124803 (72.66)	958 (0.02)
	Metolachlor	1	4237452	2856099 (67.40)	507 (0.02)
		2	8526232	5744512 (67.37)	1026 (0.02)
		3	7872843	5288094 (67.17)	1278 (0.02)
	Sunset Yellow	1	3873441	2767943 (71.46)	336 (0.01)
		2	7766283	5376873 (69.23)	901 (0.02)
		3	7787966	5453842 (70.03)	705 (0.01)
Eubacterium callanderi	Allura Red	1	7183087	3307033 (46.04)	910 (0.03)
		2	6432998	3383999 (52.60)	1109 (0.03)
		3	3065524	1765030 (57.58)	275 (0.02)
	Bisphenol A	1	5969748	3689357 (61.80)	683 (0.02)
		2	4066201	2370452 (58.30)	363 (0.02)
		3	4424705	2335784 (52.79)	1478 (0.06)
	Bisphenol S	1	8131294	4605557 (56.64)	1489 (0.03)
		2	6261834	3756195 (59.99)	711 (0.02)
		3	5046062	3138607 (62.20)	425 (0.01)
	Control	1	5298775	3235746 (61.07)	769 (0.02)
		2	6767182	3668460 (54.21)	1011 (0.03)
		3	7694993	4148407 (53.91)	1922 (0.05)
	Deltamethrin	1	3672539	2373948 (64.64)	286 (0.01)
		2	5650898	3277972 (58.01)	813 (0.02)
		3	6008647	3363943 (55.99)	935 (0.03)
	Glyphosate	1	5409506	3192877 (59.02)	917 (0.03)
		2	5706347	3224324 (56.50)	591 (0.02)
		3	4491481	2788080 (62.07)	676 (0.02)
	Metolachlor	1	6274699	3718598 (59.26)	953 (0.03)
		2	5400172	3321457 (61.51)	956 (0.03)
		3	5541995	3113854 (56.19)	1345 (0.04)
	Sunset Yellow	1	4721649	2784068 (58.96)	356 (0.01)
		2	5036890	2943002 (58.43)	593 (0.02)
		3	4654878	2812366 (60.42)	388 (0.01)
Mediterraneibacter torques	Allura Red	1	3182602	2298784 (72.23)	959 (0.04)
		2	7352121	5434830 (73.92)	1522 (0.03)
		3	7292073	5022774 (68.88)	224 (0.00)
	Bisphenol A	1	3412484	2457716 (72.02)	558 (0.02)
		2	3670459	2597457 (70.77)	1065 (0.04)
		3	8928597	5453611 (61.08)	2234 (0.04)
	Bisphenol S	1	9672219	6245942 (64.58)	6456 (0.10)
		2	*685190*	*379389 (55.37)*	*2806 (0.74)*
		3	3007451	1918688 (63.80)	223 (0.01)
	Control	1	4459632	3346831 (75.05)	504 (0.02)
		2	3945154	2822059 (71.53)	862 (0.03)
		3	11019788	6882552 (62.46)	3154 (0.05)
	Deltamethrin	*1*	*683259*	*504988 (73.91)*	*192 (0.04)*

		2	4558861	3278807 (71.92)	532 (0.02)
		3	8926867	5351460 (59.95)	3677 (0.07)
	Glyphosate	1	5507223	3587652 (65.14)	907 (0.03)
		2	7386836	5063837 (68.55)	1493 (0.03)
		3	*1445668*	*900321 (62.28)*	*362 (0.04)*
	Metolachlor	1	5387291	3843779 (71.35)	789 (0.02)
		2	5104414	3661142 (71.73)	639 (0.02)
		3	8064337	4976645 (61.71)	1586 (0.03)
	Sunset Yellow	1	7741491	4394181 (56.76)	1021 (0.02)
		2	8394310	5963475 (71.04)	748 (0.01)
		3	5451719	3928348 (72.06)	221 (0.01)

Chapter 4. Impact of azo dyes and short chain fatty acids on a *Salmonella* Typimirium promoter library

Preface

Research presented as part of this chapter has been prepared for publication as:

Syed SA, Shekarriz S, Derakshani H, and Surette MG. Identification and validation of biosensors for azo dyes and short chain fatty acids. 2023.

Contributions:
SAS, SS, DH, and MGS contributed to the intellectual design of the experiments, analyzed the data, and wrote the manuscript. SAS performed all experiments.

This publication is in preparation for publication and up to date as of March 19, 2023.

Title page and author list

Identification and validation of biosensors for short chain fatty acids

Saad A. Syed[1], Shahrokh Shekkariz[1], Hooman Derakshani[1], & Michael G. Surette[1,2,*]

[1]Department of Biochemistry and Biomedical Sciences, McMaster University, Hamilton, Canada

[2]Department of Medicine, McMaster University, Hamilton, Canada

* To whom correspondence should be addressed:

surette@mcmaster.ca

4.1. Abstract

The ability to monitor bacterial function as a response to xenobiotics in vivo provides unique perspective for improving the understanding of environment-microbe interactions. Here, we apply a random promoter library of *Salmonella enterica* serovar Typhimurium to establish a global, rapid, and real-time platform for assessing the bacterial transcriptional response to pervasive food additives, the azo food dyes. We found that approximately 9% of unique promoter clones were modulated in their expression by Allura Red and that this pattern was unique from other azo dyes and included altered expression of genes involved in invasion, motility, and metabolism. Recognizing the utility of this transcriptional response as a 'fingerprint' for small molecules, we applied the same screening approach to identify candidate biosensors for butyrate, a key short chain fatty acid produced by the gut microbiota. Finally, we leveraged high-throughput sequencing to identify the majority of our random promoter library clones, enabling 1) identification of our differentially expressed promoter clones and 2) ordering of the library for more rapid screening for future global expression analysis or biosensor identification. By applying high throughput sequencing to in vitro global gene expression analysis methodology, we characterized unique microbial expression profiles in response to a pervasive food additive, increasing understanding of diet-microbe interactions. Our ordered promoter library provides a consolidated platform for future gene expression analysis.

4.2. Introduction

Despite the considerable interest in the impact of diet on intestinal microbiota, only recently has data begun to emerge on the impact of agri-food chemicals on the function of the intestinal microbiome.

One microarray study in *Escherichia coli* found glyphosate, the active ingredient in the herbicide RoundUp, induced alterations in the expression of hundreds of genes, including those involved in the biosynthesis, transport, and regulation of tryptophan (Lu et al., 2013). Tryptophan is the precursor of serotonin, a key metabolite in gastrointestinal function and tryptophan metabolites such as indole acetate and kynurenine are important signalling molecules in humans (Haq et al. 2021). This study, however, used a level of glyphosate well above typical dietary exposure. For instance, we previously showed much more subtle effects upon glyphosate exposure in the previous chapter.

Microbiota-mediated effects of agri-food chemicals have also been demonstrated in human health - following epidemiological data that correlated organophosphate exposure and diabetes in a rural Indian population, researchers treated mice with the organophosphate monocrotophos (MCP) and found an onset of glucose intolerance over the course of 180 days (Velmurugan et al., 2017). This correlated with a shift in the metatranscriptomic and metabolomics profiles of the gut microbiota towards xenobiotic metabolism and an enrichment of acetate. Short chain fatty acids (SCFAs), like butyrate, propionate, acetate, are secondary metabolites produced by the gastrointestinal microbiota with key roles in host-microbiota interactions related to metabolic, immune, and gastrointestinal function (Tan et al., 2022). The increase in

the SCFA acetate was necessary for MCP-dependent induction of glucose intolerance (Velmurugan et al., 2017).

While sequencing and in vivo studies on microbiome communities and agri-food chemicals can inform what organisms are present and what a community may be doing, they do not provide high-resolution or rapid information on how specific microbes are functioning. In the intestinal tract, for example, wide changes in pH, nutrient availability, and interspecies and intraspecies competition drive a dynamic community. All of these stimuli activate transcription factors that promote the activation or repression of genes. This allows bacteria to survive hostile interactions with compounds and this response has been fine-tuned and evolved over millennia. Such dynamic behavior is not captured in typical high-throughput sequencing based profiling, such as amplicon or metagenomic profiling. Even whole transcriptome shotgun sequencing only provides a 'snapshot' of what is a dynamic, real-time event. In vitro experiments are needed to develop mechanistic understandings of intestinal microbiota function.

Notably, one major contribution of intestinal microbiota to host health is via modulation of peripheral serotonin by short chain fatty acid metabolites. For example, recently with collaborators, we showed that one azo dye, Allura Red, caused colitis in mice models via modulation of peripheral serotonin (Kwon et al., 2022). Yet, studies quantifying short chain fatty acids are limited by current mass spectrometry-based techniques that are the gold standard for detecting and quantifying metabolites in fecal samples. Whole-cell biosensors, with the ability to detect SCFAs offer advantages to the current gold standard techniques due to their portability, sensing of the bioavailable fraction, self-replication, and low cost. Whole-cell biosensors leverage the

evolved machinery in bacterial cells to detect environmental cues. For example, in the intestinal tract, wide changes in pH, oxygen levels, and nutrient availability drive microbial activities. These stimuli activate transcription factors that promote the activation or repression of genes.

Previously, our group used a random promoter library in *Salmonella enterica* serovar Typhimurium strain ATCC14028 for global, sensitive, real-time, high-throughput analysis of bacterial gene expression in a variety of physiologically and medically relevant environments (Bjarnason et al., 2003). *S.* Typhimurium was utilized because of its ability to colonize the majority of the gastrointestinal tract and its relatively large genome and transcriptional systems that senses a wide range of gastrointestinal stimuli and enacts appropriate responses to promote survival. This organism was transformed with a *luxCDABE* reporter incorporated into a low-copy number vector, the pCS26-Pac vector, with strong transcriptional terminators. This system was used to comprehensively map iron regulation, the response to sub-inhibitory antibiotics and aminosalicylates (used to treat inflammatory bowel disease), the coordinated changes in gene expression in swarming bacteria, and to define high resolution temporal patterns associated with aggregation behaviours (Bjarnason et al., 2003; Kaufman et al., 2009; W. Kim & Surette, 2003; White et al., 2008). The original reporter library was lost in a freezer failure, so I reconstructed a new reporter library with subtle modifications to increase library size, for example, by inclusion of anaerobic screening. Here, we systematically screen this library to: 1) obtain profiles of microbial gene expression upon exposure to azo dyes and 2) obtain profiles against the three most prevalent SCFAs in the gastrointestinal tract – butyrate, propionate, and acetate – at physiologically relevant concentrations to identify SCFA-responsive biosensors.

Our results provide insight into the transcriptional response of a gastrointestinal pathogen to highly pervasive dietary additives and novel direction for SCFA quantification.

4.3. Methods

4.3.1. Bacterial strains and growth conditions

Salmonella enterica serovar Typhimurium strain ATCC14028 was grown aerobically in Luria-Bertani (LB) broth at 37°C. For screening assays, 10% LB broth + 50mM MOPS buffer was used. Butyrate, propionate, or acetate were added to growth medium at a final concentration of 10mM, unless otherwise noted. Azo dyes (Allura Red, Brilliant Blue, Sunset Yellow, and Tartazine; Toronto Research Chemical) were added at 1uM, unless otherwise noted. Distilled water or DMSO was added as vehicle control, as appropriate. When appropriate, kanamycin (50 ug/ml) was added. Strains used are detailed in **Supplementary Table 1**.

For the disk diffusion assay, disks were saturated with 10mM of vehicle control and each of the SCFA, and the compounds were allowed to diffuse through the solid agar media overnight before imaging.

4.3.2. Library construction

The *Salmonella* Typhimurium random promoter library was constructed as previously described with the following modifications (Bjarnason et al., 2003): 1) An additional screening condition of anaerobic growth (37°C in an anaerobic chamber (5% CO2, 5% H2, 90% N2, Shel Labs)) was added. All anaerobic plates were read within 30 minutes of removal from the anaerobic environment. 2) 16 wells in each screening plate were used as sterility and background luminescence controls. Clones were

determined to exhibit promoter activity if in any of the screening conditions the given well had a luminescence value greater than the level of quantification, defined as:

$$(SD_{\text{background wells}} \times 5) + \text{mean}_{\text{background wells}}$$

All clones between this level of quantification and the level of detection, defined as:

$$(SD_{\text{background wells}} \times 1.5) + \text{mean}_{\text{background wells}}$$

were re-arrayed for rescreening with longer read times to confirm for activity. Background was defined as the luminescence read from wells containing culture media but not bacterial growth. The final library constitutes approximately 6% of all colonies assayed and totaled 6,528 clones (17 X 384 microtiter plates; **Table 1**).

4.3.3. Screening for promoters activated by azo dyes and SCFAs

A 384-pin replicator (V&P Scientific) was used to grow the library from frozen stock and overnight cultures were pin replicated into black 384-well clear-bottom plates (Corning) for initial screening. Plates were incubated and light production was measured in a microplate reader (Biotek Synergy Neo2) at 5 and 20 hours. Clones showing >3X differential luminescence expression compared to vehicle control were re-arrayed into 384-well plates and screened again, this time with readings taken at 2, 4, 6, and 20 or 24 hours.

Clones giving a positive response to only one of the tested SCFAs were re-arrayed into 96-well plates. Consistently positive clones were again screened, this time by diluting overnight cultures 1:10,000 and performing kinetic assays with reads every 30 minutes for OD_{600} and luminescence for a total of 20 hours. A constitutive growth promoter was also screened for normalization. Consistent positive responses were deemed to be candidate biosensors for each respective chemical.

4.3.4. Sequencing of the random promoter library

To enable identification of hits and of all clones in the library, we adapted existing methodology for miniaturized, cost-effective, multiplexed shallow Illumina sequencing (Derakhshani et al., 2020).

Library amplification and sequencing

Briefly, promoter regions are PCR amplified using primers flanking the BamHI cloning site. Each primer contains a partial Illumina adapter and one of 24 unique barcodes (**Supplementary Table 2**). Promoter library clones are pinned directly into PCR reaction mixtures with a 384-pin replicator. After completion of the first round of PCR, each set of 24 barcoded amplicons are pooled and undergo Illumina library preparation with primers containing the complete Illumina adapters and unique barcodes. The samples are pooled together, size selected, and mixed in appropriate volumes to adjust for Illumina sequencer size bias. The final library is sequenced on an Illumina MiSeq platform with paired-end 2x250-bp reads.

Sequence processing and analysis

After sequencing, reads are demultiplexed, trimmed of all plasmid or primer-associated sequences, and quality filtered using cutadapt (Martin, 2011). Processed reads were then read mapped to the *Salmonella* serovar Typhimurium 14028 reference genome and mapping information is combined with the directionality of the plasmid lux operon to extract the associated promoter for each clone, using samtools (H. Li et al., 2009). If any other genes were within 50 base pairs and in the same directionality of the original identified gene for each clone, an operon was predicted for that clone. Data was analyzed further and visualized using tidyverse (Wickham et al., 2019) on

RStudio (R version 4.2.1) (Rstudio Team, 2020). Scripts and sequencing data are available upon request.

4.4. Results

4.4.1. Effects of azo dyes on *S.* Typhimurium growth and transcription

None of the dyes (**Figure 1A**) impacted the growth of S. Typhimurium ATCC14028 (**Figure 1B**). After both an initial screen of the entire library and a secondary confirmation screen (**Supplementary Figure 1**), several hundred 1-250 promoter reporter clones were differentially expressed across the screened food dyes (**Figure 2B-D**). We then focused on Allura Red considering recent findings for its role in colitis in a mouse model (Kwon et al., 2022). Of the clones, 128 were differentially expressed after a tertiary screen in Allura Red (**Figure 2A**). Notably, several genes involved in virulence associated functions, including invasion, motility, and adhesion were differentially expressed (**Supplementary Table 3**).

4.4.2. Identification of random promoter clones

To identify differentially expressed promoters, we conducted miniaturized, cost-effective, multiplexed shallow Illumina sequencing of the entire random promoter library (**Appendix File 5; Supplementary Figure 2A**). This enabled identification of the majority of the library (~70%) at a fraction of the cost of more traditional Sanger sequencing (**Supplementary Figure 2B**), albeit with some size bias, secondary to sequencing technique, towards inserts smaller than 1000bp. Sequencing results identified 1437 unique gene identities representing a wide range of promoters, representing the majority of predicted promoters in the genome (**Table 1; Appendix File 6**).

4.4.3. Effects of SCFAs on Salmonella growth and transcription

To assess whether promoter-reporter clones may function as candidate biosensors for bacterial secondary metabolites, we first screened for growth impacts by SCFAs on *S.* Typhimurium. SCFAs (butyrate, propionate, and acetate) impacted growth of *S.* Typhimurium in liquid cultures. Notably, growth impact was observed in the kinetics of growth, although growth in the butyrate condition eventually reached levels of growth similar to vehicle control by stationary phase, unlike propionate and acetate (**Figure 3A**). Similarly, confluence on solid agar was notably diminished when *S.* Typhimurium was grown with exposure to SCFAs (**Figure 3B**).

We screened our random promoter library agnostically of any growth impacts, reasoning that it would be difficult to monitor biosensor growth and turbidity when using the biosensors for human fecal samples and so luminescence relative to control was the key variable to focus on.

We observed 298 clones responsive to all three SCFAs, 118 promoters differentially expressed with butyrate, 216 promoters with propionate, and 288 with acetate (**Figure 4**). From this, we manually curated a panel of 10 candidate biosensors for butyrate (**Table 3**). This panel was selected by clustering normalized temporal expression data (**Supplementary Figure 3**) and selecting for the cluster with clones with single-tailed increases (i.e. always increased or always decreased) in differential expression by both raw luminescence measures and as a ratio compared to control conditions.

4.5. Discussion

Recent studies on azo dyes have highlighted several key deleterious effects on host biology and related these to the gastrointestinal microbiota. Zou et al. (2020) illustrated the ability of azo dyes to impair drug absorption by inhibiting OATP2B1, a key intestinal transporter, and found that this function is rescued by gut microbe metabolism of azo dyes by bacterial azoreductases. Two other studies demonstrated Allura Red causes both gut microbiome-independent and -dependent colitis in mice via peripheral serotonin and IL23 (Z. He et al., 2021; Kwon et al., 2022). Despite these implications for host biology, how food colourants modulate the gut microbiota is less understood.

Here, we report the usage of a random promoter library to characterize the bacterial transcriptional response to azo dyes at physiologically relevant concentrations. In this study, we found that despite no impact on *S.* Typhimurium growth, azo dyes impacted the microbial transcriptional profile. This expression profile correlated in a manner that supports previous findings of microbiota-mediated colitis (Kwon et al., 2022), likely by altered expression of various virulence genes as noted in our results.

Notably peripheral serotonin is also impacted by SCFAs produced by the gut microbiome. This led us to wonder whether we could apply our promoter library to identify biosensors for key gut microbiota metabolites.

The advantages of our methodology, real-time and rapid quantification, allowed for the assessment of transcriptional effects across various stages of microbial growth. The promoter library is estimated to be constituted of >99% of all promoters in the genome and provides highly sensitive characterization of low expression promoters with minimal crosstalk across wells. Our group has previously applied this

methodology to a range of biologic questions, including the impact of pharmacotherapy on gastrointestinal bacterial expression.

For example, to improve understanding of the mechanism of aminosalicylates on inflammatory bowel diseases, aminosalicylates had no impact on the growth of *Salmonella* at high concentrations but increased the expression of genes involved in antibiotic and stress resistance, invasion, and metabolism (Kaufman et al., 2009). This past study highlighted that isolates not experiencing growth inhibition may still have altered transcription in response to chemical exposure.

We applied high-throughput sequencing to identify the clones in our random promoter library. This methodology took advantage of multiplexing techniques and shallow sequences to identify most of our promoter library, thus enabling ordering of the library for even more rapid screening in the future.

While our methodology offered significant advantages, our results are limited by the usage of *S.* Typhimurium in light of emerging technologies that may make molecular biology in gut microbes more amenable (L. Zheng et al., 2022). Further, our results are limited by our choice of sequencing platform, as the Illumina platform was unable to characterize approximately 30% of our promoter clones, likely due to insert sizes being >1000 base pairs (Ross et al., 2013); this can be circumvented by performing long-read sequencing with the PacBio platform, which is currently underway. Finally, our candidate biosensors will require further testing in various environments, including in the presence of other SCFAs, although we anticipate cross-activation or suppression will be minimal as evidenced by our usage of reporters only activated by one of acetate, propionate, or butyrate. Our candidate biosensors are also lacking validation in whole cell culture, culture supernatant, and human stool and serum

samples, to better ascertain their utility, and will need to be compared to the gold standard of mass-spectrometry based techniques. These reporters provide promising candidate biosensors for butyrate which could serve as an affordable and scalable screening tool to identify a key metabolite of interest in a collection of bacterial strains or stool samples across many conditions.

4.6. Acknowledgements

We thank the staff of the Farncombe Metagenomic Facility (Hamilton, CA), the Center for Microbial Chemical Biology (Hamilton, CA) and all members of the Surette laboratory, particularly Laura Rossi, for constructive discussions and support in sample preparations and library sequencing. We thank Jean-Philippe Côté and Carolyn Southward for key discussions regarding construction of the random promoter library. We thank the Holloway and Khan laboratories for providing azo dye chemicals. This work was supported by funding from Canadian Institutes for Health Research.

4.7. Figures

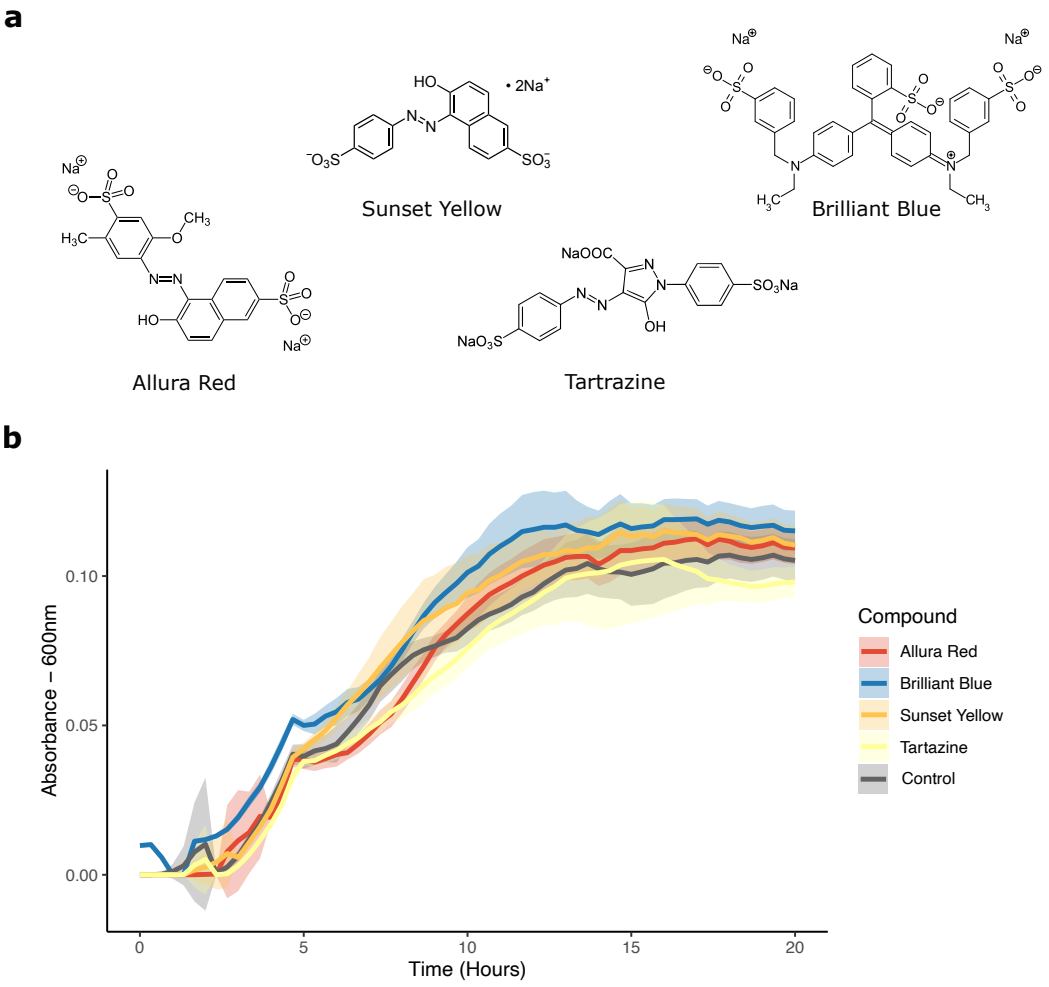

Figure 4. 1. Azo dyes do not impact the growth of* S. *Typhimurium ATCC14028 grown in random promoter library assay conditions.

a) Chemical structures of the four azo dyes included in this screen. **b)** Growth curves of *S.* Typhimurium S14028 grown in 10% LB and 1uM of the respective dye. Lines represent averages of replicates and shaded areas around the line represent standard deviation. Overnight culture of the organism was diluted 1/3000 at the start of this assay and added to each condition.

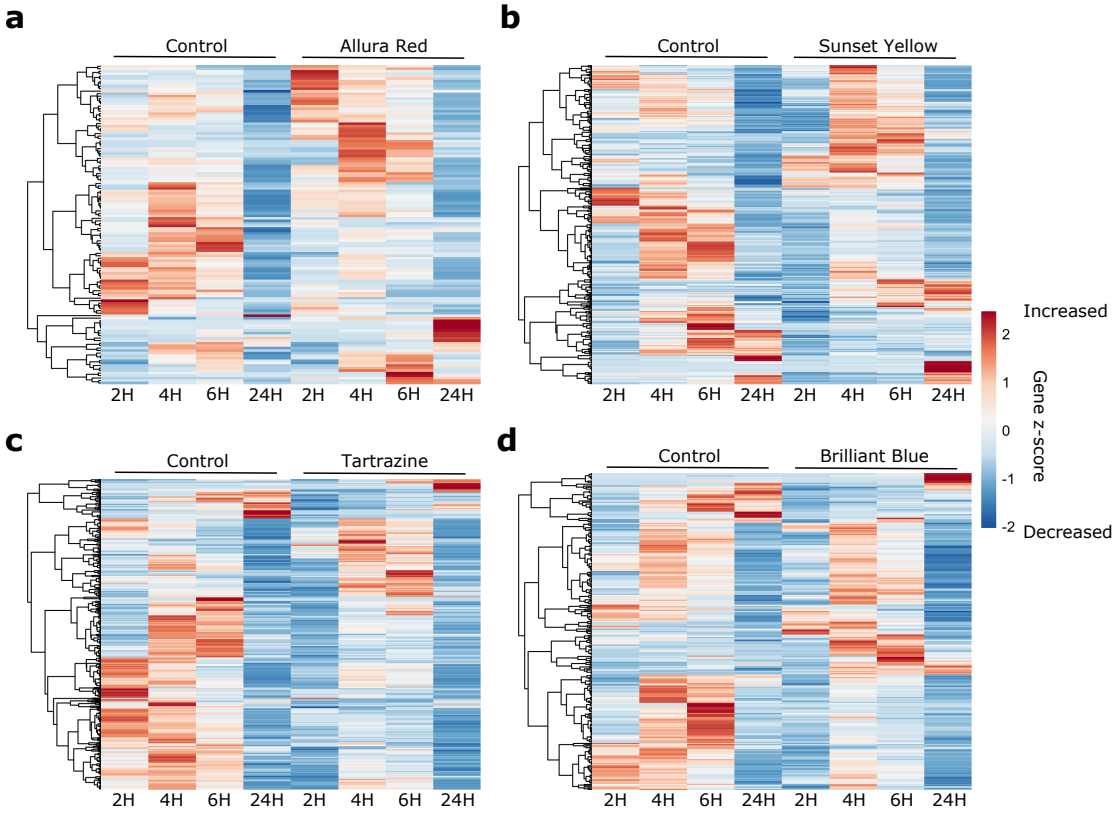

Figure 4. 2. Distinct gene expression signatures in* S. *Typhimurium in response to azo dyes.

The four azo dyes approved for usage in food, Allura Red (**a**), Sunset Yellow (**b**), Tartazine (**c**), and Brilliant Blue (**d**) were screened at 1uM against the random promoter library. Results from the secondary screen are shown where each row represents a promoter reporter clone and each column is a different condition/time point. Reads were taken at 2, 4, 6, and 24 hours and only those wells showing >3-fold differences in expression between the dye conditions and control were visualized. Data was transformed by mean centering each gene and normalizing the expression with gene z-scores. A high gene z-score represents high luminescence and is shown in red whereas low scores and luminescence are shown in blue. Genes are hierarchically clustered using correlation as a similarity measure.

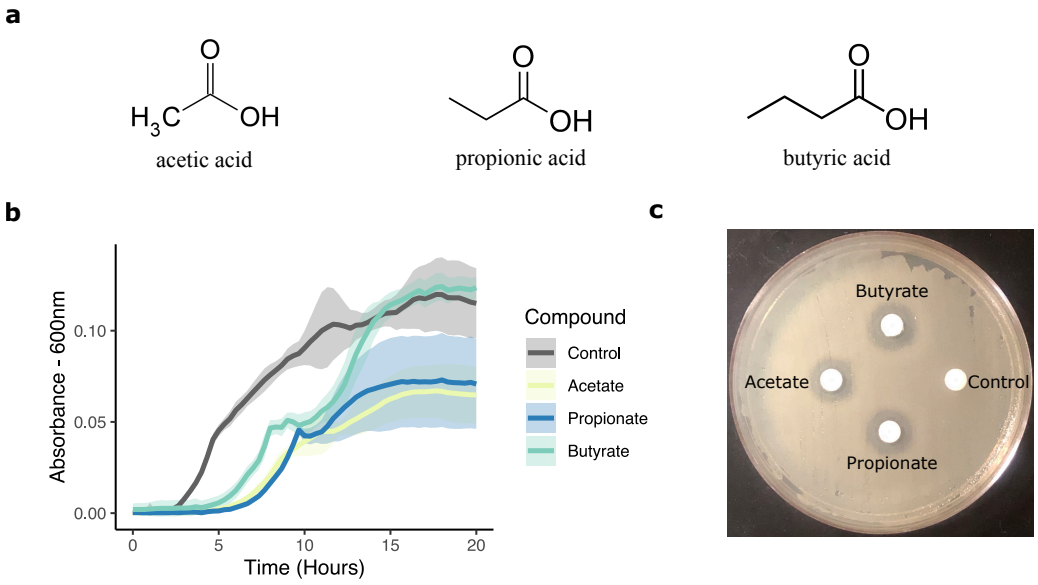

Figure 4. 3. Impact of SCFAs on* S. *Typhimurium growth.

a) Chemical structures of the three short chain fatty acids included in this screen. **b)** Growth curves of *S.* Typhimurium S14028 grown in 10% LB with 50mM MOPS and 10mM of the respective fatty acid. Lines represent averages of replicates and shaded areas around the line represent standard deviation. Overnight culture of the organism was diluted 1/3000 at the start of this assay and added to each condition. **c)** Disk diffusion growth assay of *S.* Typhirmirium in the presence of vehicle control, acetate, propionate, and butyrate on LB agar with 50mM MOPS. Clear gradient zones around discs indicate zones of killing.

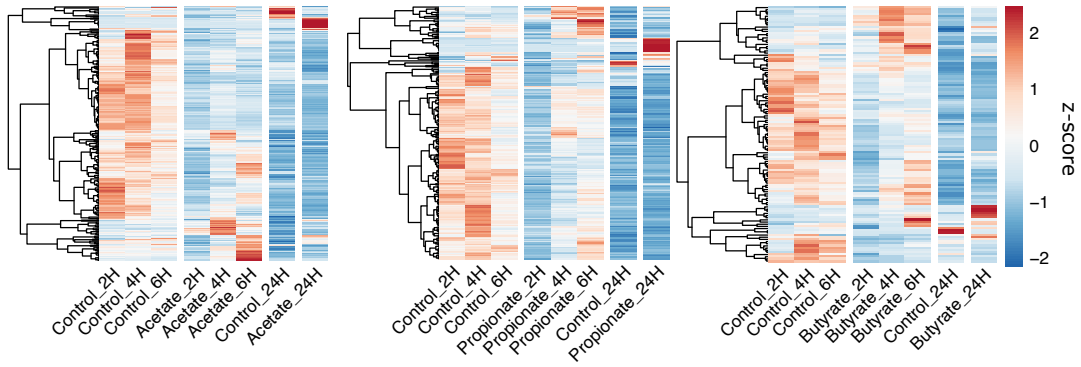

Figure 4. 4. Identification of SCFA-specific promoter reporter clones.

Acetate, propionate, and butyrate were screened at 10mM in 10% LB broth with 50mM MOPS buffer. Results from the secondary screen are shown where each row represents a promoter reporter clone and each column is a different condition/time point. Reads were taken at 2, 4, 6, and 24 hours and only those wells showing >3-fold differences in expression between the dye conditions and control were visualized. Data was transformed by mean centering each gene and normalizing the expression with gene z-scores. A high gene z-score represents high luminescence and is shown in red whereas low scores and luminescence are shown in blue. Genes are hierarchically clustered using correlation as a similarity measure.

4.8. Tables

Table 4. 1. Promoter library statistics.

Characteristics	**Results for Salmonella**
Genome Size (kb)	4,857
Clones Screened	106,905
Number of Predicted Promoters	2,430
Size of Library	6,626
Estimated Fold Coverage	2.73
Percent Positivity of Clones Screened	6.2%
Successful ID	4122
Unique Annotations	1437
Fold Coverage of Annotations	2.89
Fold Coverage of Predicted Promoters	0.59

Table 4. 2. Sequence analysis of Allura Red responsive clones.

Group	Operon	Expression	Function
Invasion-associated	*phoPQ*	-9.2	Two component regulatory system proteins essential for virulence
	corA	-4.3	Magnesium transport protein
	mipA	-3.6	MltA-interacting protein A
Metabolism	*pdxY*	-47.9	Pyridoxal kinase involved in the salvage pathway of pyridoxal 5'-phosphate (PLP).
	cysK	-24.5	Cysteine synthase
	aroL	-4.8	Shikimate kinase
	gudT	-4.1	D-glucarate permease
	argD_2	-4.1	Acetylornithine/succinyldiaminopimelate aminotransferase
	wecF	-3.9	TDP-N-acetylfucosamine:lipid II N-acetylfucosaminyltransferase
	plsB	-3.8	Glycerol-3-phosphate acyltransferase
	serB	-3.6	Phosphoserine phosphatase
	pgtC	-3.5	Phosphoglycerate transport regulatory protein
	ygjU	-3.5	Serine/threonine transporter
	glmU	-3.3	Bifunctional protein catalyzing reactions in the de novo biosynthetic pathway for UDP-GlcNAc
	btuC	-3.0	Vitamin B12 import system permease protein
	nifJ	3.5	pyruvate-flavodoxin oxidoreductase
	fhlA	3.3	Formate hydrogen-lyase transcriptional activator
	ndh	3.6	Respiratory NADH dehydrogenase
Motility	*flgK*	-6.1	Flagellar hook associated protein
	rtn	-4.1	Anti-FlhC(2)FlhD(4) factor
	fliK	9.1	Flagellar hook-length control protein
	fimAICDHF	4.9	Type 1 fimbriae
Uncharacterized	*yabI*	-13.9	Putative plasma membrane protein
	ygbJ	-11.9	Putative organic acid catabolism protein
	STM14_3769	-7.2	Putative metal binding protein
	STM14_0256	-5.6	Putative ribosomal protein
	yjfN	-4.7	Putative inner membrane protein
	STM14_3301	-3.5	Uncharacterized
	yehS	-3.5	Putative cytoplasmic protein
	yeeF	-3.4	Putative amino acid transport protein
	slp	-3.4	Putative outer membrane protein
	STM14_4861	-3.2	HTH cro/C1-type domain-containing protein
	ynfC	-3.2	Putative lipoprotein
	yaaA	-3.0	Putative lipoprotein
	STM14_0347	4.4	Uncharacterized
	yccD	3.5	Putative modulation of DnaK chaperone system
	STM14_1751	3.3	Uncharacterized

Table 4. 3. Candidate butyrate biosensors.

ID	Operon	Expression	Peak luminescence (time)
P7D05	*modF*	67.8	714 (6H)
P4B03	*adhE*	32.2	4460 (14.5H)
P3L09	*lysP*	32.2	1105(4.5H)
P6H04	*marR*	28	974 (5H)
P5K18	*STM14_4446*	22.6	207 (5.5H)
P11L24	*Unknown*	17.8	11413 (20H)
P11E23	*Unknown*	9.5	192 (3.5H)
P3P10	*Unknown*	7.4	471 (5H
P2L02	*Unknown*	5.6	778 (4.5H)
P3D06	*Unknown*	11.4	559 (4.5H)

4.9. Supplementary Materials

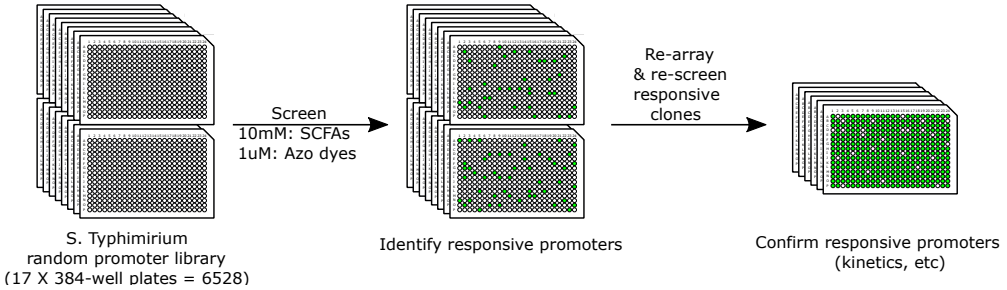

Supplementary Figure 4. 1. Primary screening strategy for promoter library gene expression experiments.

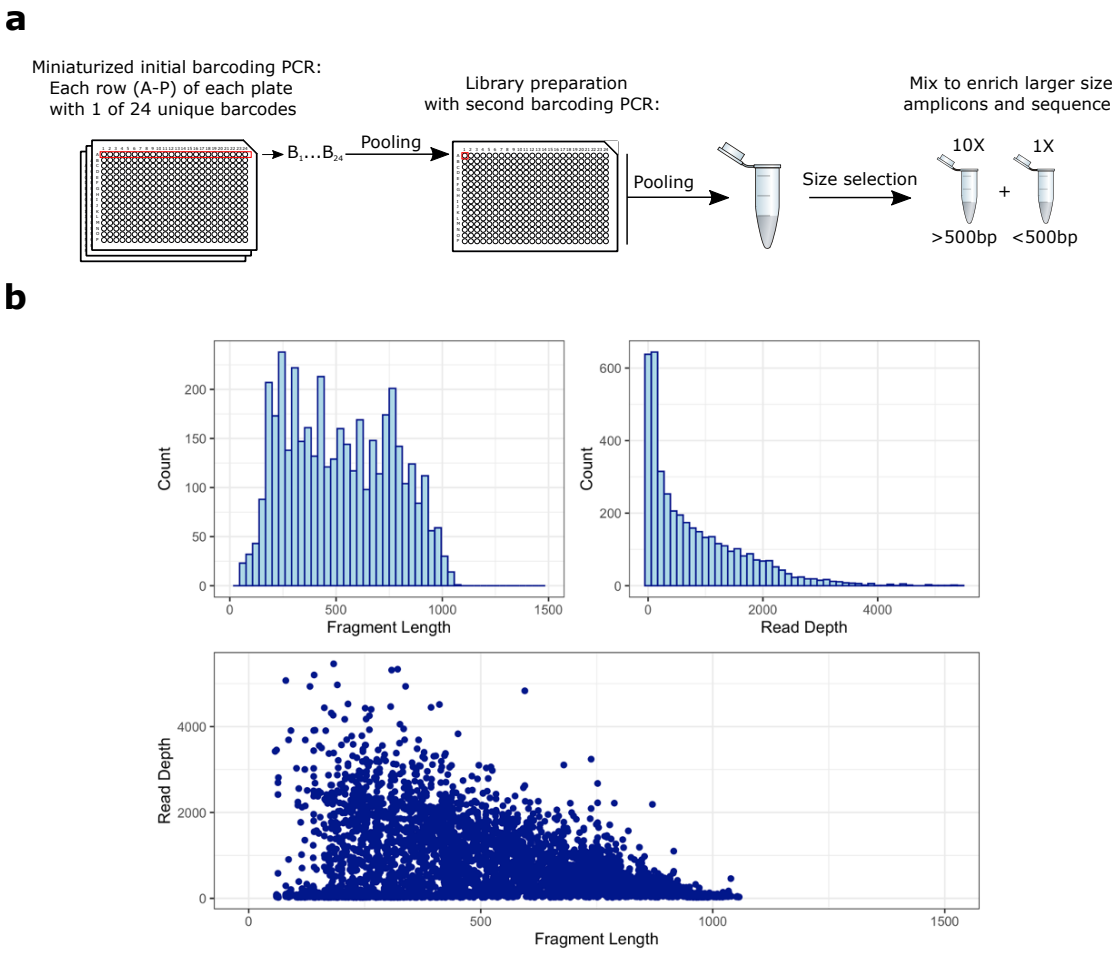

Supplementary Figure 4. 2. Sequencing strategy for identification of promoter library clones provides annotations for over 4000 wells, albeit in a size-biased manner.

a) Schematic of the high-throughput, multiplexed amplification, and sequencing strategy for identification of promoter library clones. **b)** Of the 4122 wells that were successfully identified, the average fragment length was approximately 600bp. Read depth ranged from as low as twenty to almost 5000 reads for certain wells. Smaller fragments tended to constitute the higher read depth samples.

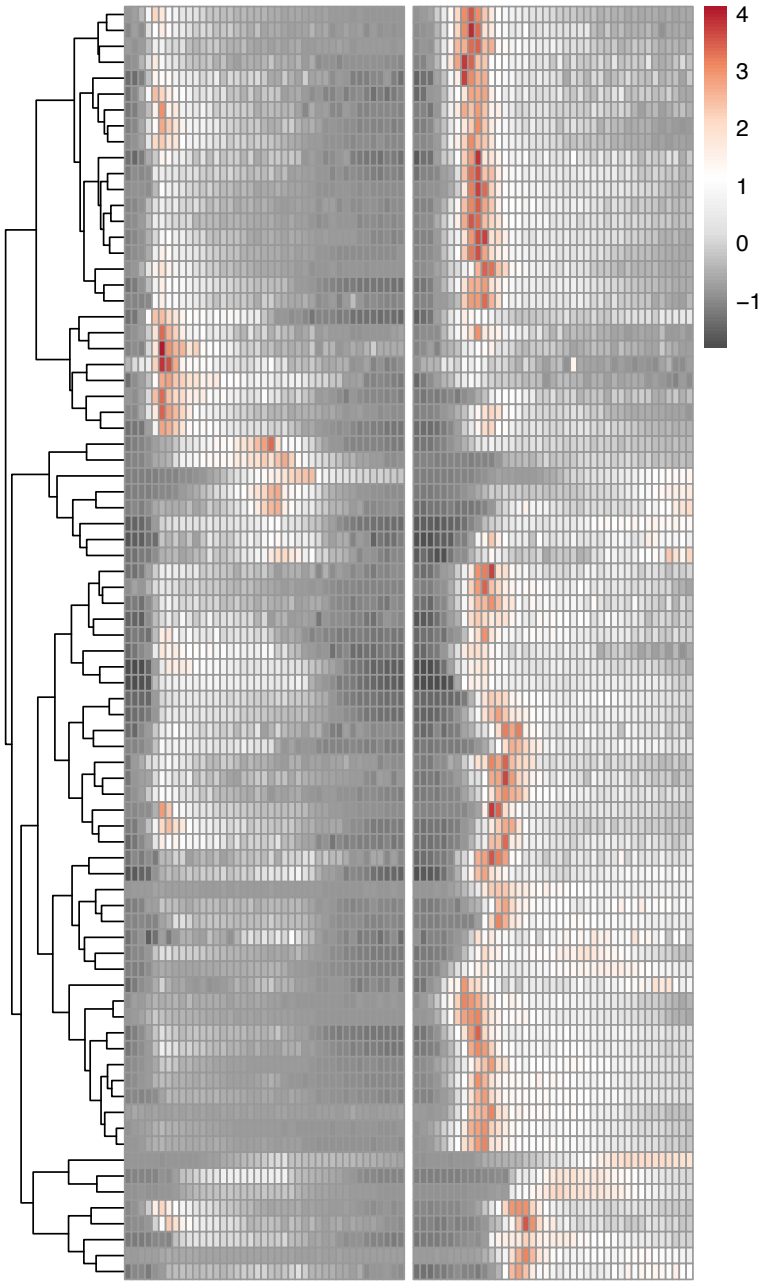

Supplementary Figure 4. 3. Hierarchical clustering of temporal expression data comparing vehicle control to butyrate exposure.

Normalized luminescence data is shown across the x-axis and separated by vehicle control on the left and butyrate on the right. Each differentially expressed clone is represented as a row. Clones are hierarchically clustered.

Supplementary Table 4. 1. Strains used in this study.

Strain	**Characteristics**	**Source and/or ref.**
S. Typhimurium C35 sigma70	Constitutively expressed sigma70 promoter	Kim & Surette, 2006
S. Typhimurium S14028	Wild type strain	ATCC 14028S

Supplementary Table 4. 2. Primers used in this study.

Name	Partial Adaptor	Barcode	Plasmid Primer
pZE.05	N/A	N/A	CCAGCTGGCAATTCCGA
pZE.06	N/A	N/A	GCACTAAATCATCACTTTCG
pZE.06_ID	GTGACTGGAGTTCAGACGTGTGCTCTTCCGATCT	N/A	GCACTAAATCATCACTTTCG
pZE.05_ID1	ACACTCTTTCCCTACACGACGCTCTTCCGATCTNNNN	CCCGTCTT	CCAGCTGGCAATTCCGA
pZE.05_ID2	ACACTCTTTCCCTACACGACGCTCTTCCGATCTNNNN	CGGCACTT	CCAGCTGGCAATTCCGA
pZE.05_ID3	ACACTCTTTCCCTACACGACGCTCTTCCGATCTNNNN	ACATTATT	CCAGCTGGCAATTCCGA
pZE.05_ID4	ACACTCTTTCCCTACACGACGCTCTTCCGATCTNNNN	GAGATTGT	CCAGCTGGCAATTCCGA
pZE.05_ID5	ACACTCTTTCCCTACACGACGCTCTTCCGATCTNNNN	GGTCCTCT	CCAGCTGGCAATTCCGA
pZE.05_ID6	ACACTCTTTCCCTACACGACGCTCTTCCGATCTNNNN	CTCTAACT	CCAGCTGGCAATTCCGA
pZE.05_ID7	ACACTCTTTCCCTACACGACGCTCTTCCGATCTNNNN	AGAATTAT	CCAGCTGGCAATTCCGA
pZE.05_ID8	ACACTCTTTCCCTACACGACGCTCTTCCGATCTNNNN	TACAACAT	CCAGCTGGCAATTCCGA
pZE.05_ID9	ACACTCTTTCCCTACACGACGCTCTTCCGATCTNNNN	AAGTGTTG	CCAGCTGGCAATTCCGA
pZE.05_ID10	ACACTCTTTCCCTACACGACGCTCTTCCGATCTNNNN	ATCACTTG	CCAGCTGGCAATTCCGA
pZE.05_ID11	ACACTCTTTCCCTACACGACGCTCTTCCGATCTNNNN	TCATCGTG	CCAGCTGGCAATTCCGA
pZE.05_ID12	ACACTCTTTCCCTACACGACGCTCTTCCGATCTNNNN	TACAGATG	CCAGCTGGCAATTCCGA
pZE.05_ID13	ACACTCTTTCCCTACACGACGCTCTTCCGATCTNNNN	TCCCGCGG	CCAGCTGGCAATTCCGA
pZE.05_ID14	ACACTCTTTCCCTACACGACGCTCTTCCGATCTNNNN	CCAAGTCG	CCAGCTGGCAATTCCGA
pZE.05_ID15	ACACTCTTTCCCTACACGACGCTCTTCCGATCTNNNN	CTGGATCG	CCAGCTGGCAATTCCGA
pZE.05_ID16	ACACTCTTTCCCTACACGACGCTCTTCCGATCTNNNN	GTCTGGCG	CCAGCTGGCAATTCCGA
pZE.05_ID17	ACACTCTTTCCCTACACGACGCTCTTCCGATCTNNNN	TTACCACG	CCAGCTGGCAATTCCGA
pZE.05_ID18	ACACTCTTTCCCTACACGACGCTCTTCCGATCTNNNN	TGAACCAG	CCAGCTGGCAATTCCGA
pZE.05_ID19	ACACTCTTTCCCTACACGACGCTCTTCCGATCTNNNN	CCCTACAG	CCAGCTGGCAATTCCGA
pZE.05_ID20	ACACTCTTTCCCTACACGACGCTCTTCCGATCTNNNN	GGCCCAAG	CCAGCTGGCAATTCCGA
pZE.05_ID21	ACACTCTTTCCCTACACGACGCTCTTCCGATCTNNNN	GAGCCATC	CCAGCTGGCAATTCCGA
pZE.05_ID22	ACACTCTTTCCCTACACGACGCTCTTCCGATCTNNNN	GTAACTGC	CCAGCTGGCAATTCCGA
pZE.05_ID23	ACACTCTTTCCCTACACGACGCTCTTCCGATCTNNNN	CGGAGGGC	CCAGCTGGCAATTCCGA
pZE.05_ID24	ACACTCTTTCCCTACACGACGCTCTTCCGATCTNNNN	CCCTCGGC	CCAGCTGGCAATTCCGA

Chapter 5. Conclusions

In this dissertation, I have applied molecular and culture-based techniques to probe the relationship between gastrointestinal bacteria and agri-food chemicals. By doing so, I established a platform for reproducibly screening gastrointestinal microbiota for profiling bacterial in vitro growth in a number of different growth conditions anaerobically.

Applying this approach, I was able to identify a strain-specific relationship between *Bifidobacterium adolescentis* growth impacts by bisphenol S (**Chapter 2**). I applied genomic and transcriptomic approaches to probe this relationship further. This analysis suggested upregulation in the expression of bacterial stress responses and an enrichment of growth impact in strains with phage-associated genetic elements, although I was unable to definitively identify a mechanism.

I then built on my screening platform and these findings to apply high-throughput sequencing to better understand the impact of agri-food chemicals on the transcriptome of key gastrointestinal bacteria (**Chapter 3**). This involved establishing a platform for bulk RNA-seq of gastrointestinal microbiota species using previously published protocols for multiplexing and rRNA depletion. A considerable focus was on ensuring our methodology would apply to our non-model organisms as commercial kits were not applicable to our strains. Our results did not detect substantial differences in expression for many bacterial strain- agri-food chemical pairs, which suggested that either our experimental design lacked sensitivity, missed the key transcriptional window for effect for some or many of our bacteria-agrochemical pairs, or a true lack of biological effect exists at the low concentrations we tested. We nonetheless noted transcriptional regulation by azo dyes in multiple species. Notably,

our analysis to better characterize this regulation was limited by the availability of methods for functional analysis in non-model organisms.

We sought to better characterize bacterial transcriptional regulation by azo dyes through leveraging a random promoter library in a lab strain of *S.* Typhimurium (**Chapter 4**). From this, we noted Allura Red altered expression of invasion and metabolism- associated genes. To provide a platform for better understanding how agri-food chemicals may impact secondary metabolite production from gastrointestinal microbiota, we generated candidate whole-cell biosensors although further characterization of their activity is still needed.

My doctoral research program was centred on the idea that access to newly culturable gastrointestinal bacteria allowed for a better understanding of environmental factors, such as agri-food chemicals, and their direct impact on gastrointestinal bacteria growth and function. Specifically, I aimed to push beyond correlation-based culture-independent methods to test the hypotheses that agri-food chemicals directly impact growth of certain microbiota species and that even at sub-inhibitory concentrations, there are transcriptional effects which suggest an impact on bacterial physiology. With respect to my first hypothesis, I did find growth impacts by several agri-food chemicals and suggest a possible mechanism for one noted effect; however there remain a number of interactions still to be understood. My ability to further probe these findings was limited by several factors. One substantial issue was the fastidious nature of growth for some human-isolated anaerobic bacteria and their resultant lack of suitability to high-throughput screening techniques. These challenges often paired with limited molecular and computational tools for mining high-throughput sequencing data from these non-model organisms, resulting in homebrewed

techniques and usage of sub-optimal quality annotations. While this has inevitably slowed my progress in mining both the in vitro functions of my strains and the in silico data associated, it has been a meaningful challenge to develop my own approach to these problems I recognize are an inevitability in a nascent field.

Despite this, the results to date from my growth screening provide exciting future opportunities for investigations from specific questions such as searching for the ability of agri-food chemicals to trigger bacteriophage or further characterization of species of interest, such as *Eubacterium callanderi*. Both examples will require even further expanded, high-quality, gut microbiota strain culture collections to better capture the diversity of the human gastrointestinal microbiota across the span of human health, age, and geography. Such collections will also require leveraging ever-increasing capabilities in high-throughput screening and sequencing of gastrointestinal bacteria. For example, with regards to my findings regarding *B. adolescentis* and BPS, one possible mechanism related to enrichment of phage-related genetic elements. Considering the often strain-specific nature of phage host selection, it is only through deep culture collections with tens if not hundreds, of strains, that interactions with agri-food chemicals would be determined.

There is considerable excitement around the role of phage in diseases, such as inflammatory bowel diseases, and improved collections of strains and data will be essential to probing this relationship and whether there is any relationship with agrochemical exposure. Such collections would also provide ample opportunities for downstream experiments in axenic mice to solidify mechanism. With the advent of more readily available molecular and computational tools for gastrointestinal microbiota species, the ability to better probe such interactions will also improve.

In answering my second hypothesis regarding the role of agri-food chemicals in gene regulation, I found, through both molecular and in vitro methods, that azo dyes impact the expression of virulence and stress machinery in gastrointestinal bacteria. This provides some connection to hypotheses that azo dyes play a role in disease via a direct agrochemical-bacteria impact in response to a sporadic or intermittent pulsation in concentration of agri-food chemicals. In such a case, this agrochemical exposure would be sufficient to trigger increased virulence- or invasion-associated response in the microbe, thus contributing to enteroinvasive phenotypes. Such phenotypes are observed to be enriched in various gastrointestinal diseases and there is emerging evidence for such pathologic findings in one recent trial of emulsifiers and colitis in humans (Chassaing et al., 2022). Similarly, while our collaborators have shown some microbiome-mediated impacts on colitis in mice relating to Allura Red administration, further studies in axenic mice using monoculture with strains from our study may provide more definitive and stronger evidence to this effect (Kwon et al., 2022). While addressing my second hypothesis regarding bacterial gene regulation and agri-food chemicals has provided novel insight into the relationship between gastrointestinal bacteria and agri-food chemicals, it has also highlighted several gaps to be addressed in the toolbox of microbiome research. The limitations of our in vitro and sequencing approaches are essential to the planning of future experiments with gut microbiome species – without consideration of the growth needs of certain strains in high-throughput settings, the tools available to deplete rRNA, and the computational tools available to perform meaningful analysis, even the most well-designed theoretical experiment could fail.

The development of improved anaerobic screening technologies, molecular tools, and bioinformatic tools will undoubtedly improve targeting for such work in the future. If this work was repeated, further selection of genetically diverse strains from larger culture collections would enable more representative bacterial strain screening panels. More information on intraluminal concentrations of agri-food chemicals would enable improved concentration selection of chemicals for screening and even testing combinations of typically co-used chemicals. Interrogation of how growth is assessed could include testing of different growth conditions by trialling several different media that more closely mirror the colonic environment. For example, the usage of rich media, such as BHI and mGAM in these studies limits the ability to assess impacts of certain agricultural chemicals, such as glyphosate. In minimal media with less or no available aromatic amines, it would be hypothesized that more profound effects would be observed of glyphosate inhibition of the shikimate pathway.

Despite improved tools, it will still be human decisions that guide what we are able to glean from such large-scale data. For example, even though I detected minimal changes in my RNA-seq experiment, I made several decisions which another reasonable analyst may not make. Specifically, I elected to group all samples for each organism into one model even though there were cases within the analysis where such an approach may be thought to wash out valuable findings from dispersion-based statistics applied. Similarly, in the detection and modelling of unwanted variation, the inclusion or exclusion of each dimension of variation is a human decision. Even comparing my choices for the modelling of unwanted variation from day to day, I realized the degree of subjectivity in such decisions and their ability to 'bend the needle' on findings.

Such experiences, not only in computation analyses but also in how experiments are conducted in the laboratory, suggest that the ability of the scientific method is limited not by our ability to use the tools available to us, but to communicate how we went about using them. When it comes to the scale of data now generated in the field of microbiome research, doing so is the only way to improve reliability.

In the clinic, there is substantial excitement about microbial-based therapies. In my few years so far, I've seen questions about probiotics from patients become more commonplace and the number of clinicians becoming aware of and interested in the microbiota increase in popularity. Yet how our understanding of the gastrointestinal microbiota is impacting human health is just beginning. So far, this impact has taken the form of directed therapies, such as FMT for recurrent *C. difficile* or in patients refractory to anti-PD-1 therapy (Sivan et al., 2015; Walter & Shanahan, 2023).

I do believe the greatest impacts for microbiome on human health are yet to come. These impacts will come from an understanding of how we may prevent disease through improving the environment for the general population. This will be much like the rise of epidemiology and large cohort studies that occurred in the 20th century, such as the Avon Longitudinal Study that identified lotions with peanut oil were causing subsequent oral peanut allergy in children (Lack et al., 2003). Much like those studies however, it will require a strong commitment to longitudinal and deep data collection from scientists, driven by curiosity. I hope the research presented here has embodied this curiosity and provided the groundwork for future studies on xenobiotic-microbiome relationships that may help improve environmental health.

Chapter 6. Bibliography

Alipour, M., Zaidi, D., Valcheva, R., Jovel, J., Martínez, I., Sergi, C., Walter, J., Mason, A. L., Ka-Shu Wong, G., Dieleman, L. A., Carroll, M. W., Huynh, H. Q., & Winea, E. (2016). Mucosal Barrier Depletion and Loss of Bacterial Diversity are Primary Abnormalities in Paediatric Ulcerative Colitis. *Journal of Crohn's and Colitis*, *10*(4), 462–471. https://doi.org/10.1093/ECCO-JCC/JJV223

Allen, R. W., Barn, P. K., & Lanphear, B. P. (2015). Randomized Controlled Trials in Environmental Health Research: Unethical or Underutilized? *PLoS Medicine*, *12*(1), 1–5. https://doi.org/10.1371/JOURNAL.PMED.1001775

Altschul, S. F., Madden, T. L., Schäffer, A. A., Zhang, J., Zhang, Z., Miller, W., & Lipman, D. J. (1997). Gapped BLAST and PSI-BLAST: a new generation of protein database search programs. *Nucleic Acids Research*, *25*(17), 3389–3402. https://doi.org/10.1093/NAR/25.17.3389

Anders, S., Pyl, P. T., & Huber, W. (2015). HTSeq—a Python framework to work with high-throughput sequencing data. *Bioinformatics*, *31*(2), 166. https://doi.org/10.1093/BIOINFORMATICS/BTU638

Andrews, S. (2010). *FastQC: a quality control tool for high throughput sequence data.*

Atkinson, M. A., & Chervonsky, A. (2012). Does the gut microbiota have a role in type 1 diabetes? Early evidence from humans and animal models of the disease. *Diabetologia*, *55*(11), 2868–2877. https://doi.org/10.1007/S00125-012-2672-4/FIGURES/3

Bäckhed, F., Ding, H., Wang, T., Hooper, L. V., Gou, Y. K., Nagy, A., Semenkovich, C. F., & Gordon, J. I. (2004). The gut microbiota as an environmental factor that regulates fat storage. *Proceedings of the National Academy of Sciences of the United States of America*, *101*(44), 15718–15723. https://doi.org/10.1073/PNAS.0407076101/SUPPL_FILE/07076TABLE4.PDF

Bäckhed, F., Ley, R. E., Sonnenburg, J. L., Peterson, D. A., & Gordon, J. I. (2005). Host-bacterial mutualism in the human intestine. *Science*, *307*(5717), 1915–1920. https://doi.org/10.1126/SCIENCE.1104816/SUPPL_FILE/BACKHED.SOM.PDF

Bartram, A. K., Lynch, M. D. J., Stearns, J. C., Moreno-Hagelsieb, G., & Neufeld, J. D. (2011). Generation of multimillion-sequence 16S rRNA gene libraries from complex microbial communities by assembling paired-end illumina reads. *Applied and Environmental Microbiology*, *77*(11), 3846–3852. https://doi.org/10.1128/AEM.02772-10

Baruch, E. N., Youngster, I., Ben-Betzalel, G., Ortenberg, R., Lahat, A., Katz, L., Adler, K., Dick-Necula, D., Raskin, S., Bloch, N., Rotin, D., Anafi, L., Avivi, C., Melnichenko, J., Steinberg-Silman, Y., Mamtani, R., Harati, H., Asher, N., Shapira-Frommer, R., … Boursi, B. (2021). Fecal microbiota transplant promotes response in immunotherapy-refractory melanoma patients. *Science*, *371*(6529), 602 LP – 609. https://doi.org/10.1126/science.abb5920

Bashiardes, S., Zilberman-Schapira, G., & Elinav, E. (2016). Use of Metatranscriptomics in Microbiome Research. *Bioinformatics and Biology Insights*, *10*, 19. https://doi.org/10.4137/BBI.S34610

Bauer, H., Horowitz, R. E., Levenson, S. M., & Popper, H. (1963). The response of the lymphatic tissue to the microbial flora. Studies on germfree mice. *The American Journal of Pathology*, *42*, 471–483.

Benedict, M. N., Henriksen, J. R., Metcalf, W. W., Whitaker, R. J., & Price, N. D. (2014). ITEP: An integrated toolkit for exploration of microbial pan-genomes. *BMC Genomics*, *15*(1), 1–11. https://doi.org/10.1186/1471-2164-15-8/FIGURES/5

Benjamini, Y., & Hochberg, Y. (1995). Controlling the False Discovery Rate: A Practical and Powerful Approach to Multiple Testing. *Journal of the Royal Statistical Society. Series B (Methodological)*, *57*(1), 289–300. http://www.jstor.org/stable/2346101

Bhatt, A. P., Pellock, S. J., Biernat, K. A., Walton, W. G., Wallace, B. D., Creekmore, B. C., Letertre, M. M., Swann, J. R., Wilson, I. D., Roques, J. R., Darr, D. B., Bailey, S. T., Montgomery, S. A., Roach, J. M., Azcarate-Peril, M. A., Sartor, R. B., Gharaibeh, R. Z., Bultman, S. J., & Redinbo, M. R. (2020). Targeted inhibition of gut bacterial β-glucuronidase activity enhances anticancer drug efficacy. *Proceedings of the National Academy of Sciences*, 201918095. https://doi.org/10.1073/pnas.1918095117

Bian, X., Chi, L., Gao, B., Tu, P., Ru, H., & Lu, K. (2017). Gut microbiome response to sucralose and its potential role in inducing liver inflammation in mice. *Frontiers in Physiology*, *8*(JUL), 487. https://doi.org/10.3389/FPHYS.2017.00487/BIBTEX

Binns, T. B. (1956). GASTRO-INTESTINAL COMPLICATIONS OF ORAL ANTIBIOTICS. *The Lancet*, *267*(6917), 336–338. https://doi.org/10.1016/S0140-6736(56)91667-1

Bisanz, J. E., Soto-Perez, P., Noecker, C., Aksenov, A. A., Lam, K. N., Kenney, G. E., Bess, E. N., Haiser, H. J., Kyaw, T. S., Yu, F. B., Rekdal, V. M., Ha, C. W. Y., Devkota, S., Balskus, E. P., Dorrestein, P. C., Allen-Vercoe, E., & Turnbaugh, P. J. (2020). A Genomic Toolkit for the Mechanistic Dissection of Intractable Human Gut Bacteria. *Cell Host & Microbe*, *27*(6), 1001-1013.e9. https://doi.org/10.1016/j.chom.2020.04.006

Bjarnason, J., Southward, C. M., & Surette, M. G. (2003). Genomic profiling of iron-responsive genes in Salmonella enterica serovar typhimurium by high-throughput screening of a random promoter library. *Journal of Bacteriology*, *185*(16), 4973–4982. https://doi.org/10.1128/JB.185.16.4973

Bolger, A. M., Lohse, M., & Usadel, B. (2014). Trimmomatic: a flexible trimmer for Illumina sequence data. *Bioinformatics*, *30*(15), 2114. https://doi.org/10.1093/BIOINFORMATICS/BTU170

Brotons, J. A., Olea-Serrano, M. F., Villalobos, M., Pedraza, V., & Olea, N. (1995). Xenoestrogens released from lacquer coatings in food cans. *Environmental Health Perspectives*, *103*(6), 608–612. https://doi.org/10.1289/EHP.95103608

Browne, H. P., Forster, S. C., Anonye, B. O., Kumar, N., Neville, B. A., Stares, M. D., Goulding, D., & Lawley, T. D. (2016). Culturing of "unculturable" human microbiota reveals novel taxa and extensive sporulation. *Nature*, *533*(7604), 543–546. https://doi.org/10.1038/nature17645

Burrows, A. (2009). Palette of Our Palates: A Brief History of Food Coloring and Its Regulation. *Comprehensive Reviews in Food Science and Food Safety*, *8*(4), 394–408. https://doi.org/10.1111/J.1541-4337.2009.00089.X

Byndloss, M. X., Olsan, E. E., Rivera-Chávez, F., Tiffany, C. R., Cevallos, S. A., Lokken, K. L., Torres, T. P., Byndloss, A. J., Faber, F., Gao, Y., Litvak, Y., Lopez, C. A., Xu, G., Napoli, E., Giulivi, C., Tsolis, R. M., Revzin, A., Lebrilla,

C. B., & Bäumler, A. J. (2017). Microbiota-activated PPAR-γ signaling inhibits dysbiotic Enterobacteriaceae expansion. *Science*, *357*(6351), 570 LP – 575. https://doi.org/10.1126/science.aam9949

Callahan, B. J., McMurdie, P. J., Rosen, M. J., Han, A. W., Johnson, A. J. A., & Holmes, S. P. (2016). DADA2: High-resolution sample inference from Illumina amplicon data. *Nature Methods*, *13*(7), 581–583. https://doi.org/10.1038/nmeth.3869

Capella-Gutiérrez, S., Silla-Martínez, J. M., & Gabaldón, T. (2009). trimAl: a tool for automated alignment trimming in large-scale phylogenetic analyses. *Bioinformatics*, *25*(15), 1972. https://doi.org/10.1093/BIOINFORMATICS/BTP348

Caporaso, J. G., Lauber, C. L., Walters, W. A., Berg-Lyons, D., Lozupone, C. A., Turnbaugh, P. J., Fierer, N., & Knight, R. (2011). Global patterns of 16S rRNA diversity at a depth of millions of sequences per sample. *Proceedings of the National Academy of Sciences of the United States of America*, *108*(SUPPL. 1), 4516–4522. https://doi.org/10.1073/PNAS.1000080107/SUPPL_FILE/PNAS.201000080SI.PDF

Carey, J. N., Mettert, E. L., Fishman-Engel, D. R., Roggiani, M., Kiley, P. J., & Goulian, M. (2019). Phage integration alters the respiratory strategy of its host. *ELife*, *8*. https://doi.org/10.7554/ELIFE.49081

Cash, H. L., Whitham, C. V., Behrendt, C. L., & Hooper, L. V. (2006). Symbiotic bacteria direct expression of an intestinal bactericidal lectin. *Science*, *313*(5790), 1126–1130. https://doi.org/10.1126/SCIENCE.1127119/SUPPL_FILE/CASH_SOM.PDF

Catron, T. R., Keely, S. P., Brinkman, N. E., Zurlinden, T. J., Wood, C. E., Wright, J. R., Phelps, D., Wheaton, E., Kvasnicka, A., Gaballah, S., Lamendella, R., & Tal, T. (2019). Host Developmental Toxicity of BPA and BPA Alternatives Is Inversely Related to Microbiota Disruption in Zebrafish. *Toxicological Sciences : An Official Journal of the Society of Toxicology*, *167*(2), 468–483. https://doi.org/10.1093/TOXSCI/KFY261

Chassaing, B., Compher, C., Bonhomme, B., Liu, Q., Tian, Y., Walters, W., Nessel, L., Delaroque, C., Hao, F., Gershuni, V., Chau, L., Ni, J., Bewtra, M., Albenberg, L., Bretin, A., McKeever, L., Ley, R. E., Patterson, A. D., Wu, G. D., … Lewis, J. D. (2022). Randomized Controlled-Feeding Study of Dietary Emulsifier Carboxymethylcellulose Reveals Detrimental Impacts on the Gut Microbiota and Metabolome. *Gastroenterology*, *162*(3), 743–756. https://doi.org/10.1053/J.GASTRO.2021.11.006/ATTACHMENT/0B4A6042-BF13-4A37-B0AF-BAAD02D00A3E/MMC2.PDF

Chassaing, B., Koren, O., Goodrich, J. K., Poole, A. C., Srinivasan, S., Ley, R. E., & Gewirtz, A. T. (2015). Dietary emulsifiers impact the mouse gut microbiota promoting colitis and metabolic syndrome. *Nature*, *519*(7541), 92–96. https://doi.org/10.1038/nature14232

Chen, Y., Lun, A. T. L., & Smyth, G. K. (2016). From reads to genes to pathways: differential expression analysis of RNA-Seq experiments using Rsubread and the edgeR quasi-likelihood pipeline. *F1000Research*, *5*, 1438. https://doi.org/10.12688/f1000research.8987.1

Chen, Y., Shu, L., Qiu, Z., Lee, D. Y., Settle, S. J., Que Hee, S., Telesca, D., Yang, X., & Allard, P. (2016). Exposure to the BPA-Substitute Bisphenol S Causes

Unique Alterations of Germline Function. *PLOS Genetics*, *12*(7), e1006223. https://doi.org/10.1371/JOURNAL.PGEN.1006223

Chiu, K., Warner, G., Nowak, R. A., Flaws, J. A., & Mei, W. (2020). The Impact of Environmental Chemicals on the Gut Microbiome. *Toxicological Sciences*.

Cohn, B. A., La Merrill, M., Krigbaum, N. Y., Yeh, G., Park, J. S., Zimmermann, L., & Cirillo, P. M. (2015). DDT Exposure in Utero and Breast Cancer. *The Journal of Clinical Endocrinology & Metabolism*, *100*(8), 2865–2872. https://doi.org/10.1210/JC.2015-1841

Cummings, J. H., Pomare, E. W., Branch, H. W. J., Naylor, E., & Macfarlane, G. T. (1987). *Short chain fatty acids in human large intestine, portal, hepatic and venous blood*. *28*, 122–123. https://doi.org/10.1136/gut.28.10.1221

Davar, D., Dzutsev, A. K., McCulloch, J. A., Rodrigues, R. R., Chauvin, J. M., Morrison, R. M., Deblasio, R. N., Menna, C., Ding, Q., Pagliano, O., Zidi, B., Zhang, S., Badger, J. H., Vetizou, M., Cole, A. M., Fernandes, M. R., Prescott, S., Costa, R. G. F., Balaji, A. K., … Zarour, H. M. (2021). Fecal microbiota transplant overcomes resistance to anti-PD-1 therapy in melanoma patients. *Science*, *371*(6529), 595–602. https://doi.org/10.1126/SCIENCE.ABF3363/SUPPL_FILE/ABF3363_MDAR_REPRODUCIBILITY_CHECKLIST.PDF

Davis, C. P., & Savage, D. C. (1974). Habitat, Succession, Attachment, and Morphology of Segmented, Filamentous Microbes Indigenous to the Murine Gastrointestinal Tract. *Infection and Immunity*, *10*(4), 948–956. https://doi.org/10.1128/IAI.10.4.948-956.1974

Deorowicz, S., Debudaj-Grabysz, A., & Gudys, A. (2016). FAMSA: Fast and accurate multiple sequence alignment of huge protein families. *Scientific Reports 2016 6:1*, *6*(1), 1–13. https://doi.org/10.1038/srep33964

Derakhshani, H., Bernier, S. P., Marko, V. A., & Surette, M. G. (2020). Completion of draft bacterial genomes by long-read sequencing of synthetic genomic pools. *BMC Genomics*, *21*(1), 519. https://doi.org/10.1186/s12864-020-06910-6

Derrien, M., Vaughan, E. E., Plugge, C. M., & de Vos, W. M. (2004). Akkermansia muciniphila gen. nov., sp. nov., a human intestinal mucin-degrading bacterium. *International Journal of Systematic and Evolutionary Microbiology*, *54*(Pt 5), 1469–1476. https://doi.org/10.1099/IJS.0.02873-0

De Vadder, F., Kovatcheva-Datchary, P., Goncalves, D., Vinera, J., Zitoun, C., Duchampt, A., Bäckhed, F., & Mithieux, G. (2014). Microbiota-Generated Metabolites Promote Metabolic Benefits via Gut-Brain Neural Circuits. *Cell*, *156*(1), 84–96. https://doi.org/10.1016/j.cell.2013.12.016

Djekkoun, N., Lalau, J. D., Bach, V., Depeint, F., & Khorsi-Cauet, H. (2021). Chronic oral exposure to pesticides and their consequences on metabolic regulation: role of the microbiota. In *European Journal of Nutrition* (Vol. 60, Issue 8, pp. 4131–4149). Springer Science and Business Media Deutschland GmbH. https://doi.org/10.1007/s00394-021-02548-6

Dobkin, J. F., Saha, J. R., Butler, V. P., Neu, H. C., & Lindenbaum, J. (1983). Digoxin-Inactivating Bacteria: Identification in Human Gut Flora. *Science*, *220*(4594), 325–327. https://doi.org/10.1126/SCIENCE.6836275

Douthwaite, A. H., & Lintott, G. A. M. (1938). GASTROSCOPIC OBSERVATION OF THE EFFECT OF ASPIRIN AND CERTAIN OTHER SUBSTANCES

ON THE STOMACH. *The Lancet*, *232*(6013), e1. https://doi.org/10.1016/S0140-6736(00)78970-7

Duranti, S., Milani, C., Lugli, G. A., Mancabelli, L., Turroni, F., Ferrario, C., Mangifesta, M., Viappiani, A., Sanchez, B., Margolles, A., van Sinderen, D., & Ventura, M. (2016). Evaluation of genetic diversity among strains of the human gut commensal Bifidobacterium adolescentis. *Scientific Reports*, *6*. https://doi.org/10.1038/SREP23971

Duranti, S., Turroni, F., Lugli, G. A., Milani, C., Viappiani, A., Mangifesta, M., Gioiosa, L., Palanza, P., van Sinderen, D., & Ventura, M. (2014). Genomic Characterization and Transcriptional Studies of the Starch-Utilizing Strain Bifidobacterium adolescentis 22L. *Applied and Environmental Microbiology*, *80*(19), 6080. https://doi.org/10.1128/AEM.01993-14

Eckburg, P. B., Bik, E. M., Bernstein, C. N., Purdom, E., Dethlefsen, L., Sargent, M., Gill, S. R., Nelson, K. E., & Relman, D. A. (2005). Microbiology: Diversity of the human intestinal microbial flora. *Science*, *308*(5728), 1635–1638. https://doi.org/10.1126/SCIENCE.1110591/SUPPL_FILE/ECKBURG_SOM.PDF

Eren, A. M., Esen, O. C., Quince, C., Vineis, J. H., Morrison, H. G., Sogin, M. L., & Delmont, T. O. (2015). Anvi'o: An advanced analysis and visualization platformfor 'omics data. *PeerJ*, *2015*(10). https://doi.org/10.7717/PEERJ.1319/SUPP-5

Ericsson, A. C., & Franklin, C. L. (2015). Manipulating the Gut Microbiota: Methods and Challenges. *ILAR Journal*, *56*(2), 205–217. https://doi.org/10.1093/ILAR/ILV021

Ewels, P., Magnusson, M., Lundin, S., & Käller, M. (2016). MultiQC: summarize analysis results for multiple tools and samples in a single report. *Bioinformatics*, *32*(19), 3047–3048. https://doi.org/10.1093/BIOINFORMATICS/BTW354

Finegold, S. M., Attebery, H. R., & Sutter, V. L. (1974). Effect of diet on human fecal flora: comparison of Japanese and American diets. *The American Journal of Clinical Nutrition*, *27*(12), 1456–1469. https://doi.org/10.1093/AJCN/27.12.1456

Flowers, S. A., Evans, S. J., Ward, K. M., McInnis, M. G., & Ellingrod, V. L. (2017). Interaction Between Atypical Antipsychotics and the Gut Microbiome in a Bipolar Disease Cohort. *Pharmacotherapy: The Journal of Human Pharmacology and Drug Therapy*, *37*(3), 261–267. https://doi.org/10.1002/PHAR.1890

Forslund, K., Sunagawa, S., Kultima, J. R., Mende, D. R., Arumugam, M., Typas, A., & Bork, P. (2013). Country-specific antibiotic use practices impact the human gut resistome. *Genome Research*, *23*(7), 1163–1169. https://doi.org/10.1101/gr.155465.113

Frost, G., Sleeth, M. L., Sahuri-Arisoylu, M., Lizarbe, B., Cerdan, S., Brody, L., Anastasovska, J., Ghourab, S., Hankir, M., Zhang, S., Carling, D., Swann, J. R., Gibson, G., Viardot, A., Morrison, D., Thomas, E. L., & Bell, J. D. (2014). The short-chain fatty acid acetate reduces appetite via a central homeostatic mechanism. *Nature Communications 2014 5:1*, *5*(1), 1–11. https://doi.org/10.1038/ncomms4611

Ge, S. X., Jung, D., & Yao, R. (2020). ShinyGO: a graphical gene-set enrichment tool for animals and plants. *Bioinformatics*, *36*(8), 2628–2629. https://doi.org/10.1093/bioinformatics/btz931

Gilbert, J. A., Blaser, M. J., Caporaso, J. G., Jansson, J. K., Lynch, S. V., & Knight, R. (2018). Current understanding of the human microbiome. *Nature Medicine*, *24*(4), 392–400. https://doi.org/10.1038/nm.4517

Gilbert, J. A., & Dupont, C. L. (2010). Microbial Metagenomics: Beyond the Genome. *Http://Dx.Doi.Org/10.1146/Annurev-Marine-120709-142811*, *3*, 347–371. https://doi.org/10.1146/ANNUREV-MARINE-120709-142811

Glöckner, F. O., Yilmaz, P., Quast, C., Gerken, J., Beccati, A., Ciuprina, A., Bruns, G., Yarza, P., Peplies, J., Westram, R., & Ludwig, W. (2017). 25 years of serving the community with ribosomal RNA gene reference databases and tools. *Journal of Biotechnology*, *261*, 169–176. https://doi.org/https://doi.org/10.1016/j.jbiotec.2017.06.1198

Goh, E.-B., Yim, G., Tsui, W., McClure, J., Surette, M. G., & Davies, J. (2002). Transcriptional modulation of bacterial gene expression by subinhibitory concentrations of antibiotics. *Proceedings of the National Academy of Sciences*, *99*(26), 17025–17030. https://doi.org/10.1073/pnas.252607699

Gordon, H. A. (1960). The germ-free animal. *The American Journal of Digestive Diseases 1960 5:10*, *5*(10), 841–867. https://doi.org/10.1007/BF02232187

Gross, P. A., Lance, K., Whitlock, R. J., & Blume, R. S. (1989). Additive Allergy: Allergic Gastroenteritis Due to Yellow Dye #6. *Annals of Internal Medicine*, *111*(1), 87–88. https://doi.org/10.7326/0003-4819-111-1-87

Guardia-Escote, L., Basaure, P., Biosca-Brull, J., Cabré, M., Blanco, J., Pérez-Fernández, C., Sánchez-Santed, F., Domingo, J. L., & Colomina, M. T. (2020). APOE genotype and postnatal chlorpyrifos exposure modulate gut microbiota and cerebral short-chain fatty acids in preweaning mice. *Food and Chemical Toxicology : An International Journal Published for the British Industrial Biological Research Association*, *135*. https://doi.org/10.1016/J.FCT.2019.110872

Gurevich, A., Saveliev, V., Vyahhi, N., & Tesler, G. (2013). QUAST: quality assessment tool for genome assemblies. *Bioinformatics*, *29*(8), 1072–1075. https://doi.org/10.1093/BIOINFORMATICS/BTT086

Haas, B. J., Chin, M., Nusbaum, C., Birren, B. W., & Livny, J. (2012). How deep is deep enough for RNA-Seq profiling of bacterial transcriptomes? *BMC Genomics*, *13*(1), 734. https://doi.org/10.1186/1471-2164-13-734

Haiser, H. J., Seim, K. L., Balskus, E. P., & Turnbaugh, P. J. (2014). Mechanistic insight into digoxin inactivation by Eggerthella lenta augments our understanding of its pharmacokinetics. *Https://Doi.Org/10.4161/Gmic.27915*, *5*(2), 233–238. https://doi.org/10.4161/GMIC.27915

Hashem, M. M., Atta, A. H., Arbid, M. S., Nada, S. A., & Asaad, G. F. (2010). Immunological studies on Amaranth, Sunset Yellow and Curcumin as food colouring agents in albino rats. *Food and Chemical Toxicology*, *48*(6), 1581–1586. https://doi.org/10.1016/J.FCT.2010.03.028

Hayashi, H., Sakamoto, M., & Benno, Y. (2002). Phylogenetic analysis of the human gut microbiota using 16S rDNA clone libraries and strictly anaerobic culture-based methods. *Microbiology and Immunology*, *46*(8), 535–548. https://doi.org/10.1111/J.1348-0421.2002.TB02731.X

He, M., Urban, M. W., & Bauer, R. S. (1993). Exudation processes in hydrogenated bisphenol-a-based epoxy coatings: Spectroscopic study. *Journal of Applied Polymer Science*, *49*(2), 345–359. https://doi.org/10.1002/APP.1993.070490215

He, Z., Chen, L., Catalan-Dibene, J., Bongers, G., Faith, J. J., Suebsuwong, C., DeVita, R. J., Shen, Z., Fox, J. G., Lafaille, J. J., Furtado, G. C., & Lira, S. A. (2021). Food colorants metabolized by commensal bacteria promote colitis in mice with dysregulated expression of interleukin-23. *Cell Metabolism*, *33*(7), 1358-1371.e5. https://doi.org/10.1016/J.CMET.2021.04.015

Hertz-Picciotto, I., Sass, J. B., Engel, S., Bennett, D. H., Bradman, A., Eskenazi, B., Lanphear, B., & Whyatt, R. (2018). Organophosphate exposures during pregnancy and child neurodevelopment: Recommendations for essential policy reforms. *PLOS Medicine*, *15*(10), e1002671. https://doi.org/10.1371/JOURNAL.PMED.1002671

Huang, Y., Sheth, R. U., Kaufman, A., & Wang, H. H. (2020). Scalable and cost-effective ribonuclease-based rRNA depletion for transcriptomics. *Nucleic Acids Research*, *48*(4), e20–e20. https://doi.org/10.1093/NAR/GKZ1169

Huttenhower, C., Kostic, A. D., & Xavier, R. J. (2014). Inflammatory Bowel Disease as a Model for Translating the Microbiome. *Immunity*, *40*(6), 843–854. https://doi.org/10.1016/J.IMMUNI.2014.05.013

Imhann, F., Bonder, M. J., Vila, A. V., Fu, J., Mujagic, Z., Vork, L., Tigchelaar, E. F., Jankipersadsing, S. A., Cenit, M. C., Harmsen, H. J. M., Dijkstra, G., Franke, L., Xavier, R. J., Jonkers, D., Wijmenga, C., Weersma, R. K., & Zhernakova, A. (2016). Proton pump inhibitors affect the gut microbiome. *Gut*, *65*(5), 740–748. https://doi.org/10.1136/GUTJNL-2015-310376

Jackson, M. A., Goodrich, J. K., Maxan, M. E., Freedberg, D. E., Abrams, J. A., Poole, A. C., Sutter, J. L., Welter, D., Ley, R. E., Bell, J. T., Spector, T. D., & Steves, C. J. (2016). Proton pump inhibitors alter the composition of the gut microbiota. *Gut*, *65*(5), 749–756. https://doi.org/10.1136/GUTJNL-2015-310861/-/DC1

Jenkins, P., Michelson, R., & Emerson, PeterA. (1982). ADVERSE DRUG REACTION TO SUNSET-YELLOW IN RIFAMPICIN/ISONIAZID TABLET. *The Lancet*, *320*(8294), 385. https://doi.org/10.1016/S0140-6736(82)90575-X

Jonsson, H., Hugerth, L. W., Sundh, J., Lundin, E., & Andersson, A. F. (2020). Genome sequence of segmented filamentous bacteria present in the human intestine. *Communications Biology 2020 3:1*, *3*(1), 1–9. https://doi.org/10.1038/s42003-020-01214-7

Juul, F. E., Garborg, K., Bretthauer, M., Skudal, H., Øines, M. N., Wiig, H., Rose, Ø., Seip, B., Lamont, J. T., Midtvedt, T., Valeur, J., Kalager, M., Holme, Ø., Helsingen, L., Løberg, M., & Adami, H.-O. (2018). Fecal Microbiota Transplantation for Primary Clostridium difficile Infection. *New England Journal of Medicine*, *378*(26), 2535–2536. https://doi.org/10.1056/NEJMc1803103

Kamada, N., Kim, Y. G., Sham, H. P., Vallance, B. A., Puente, J. L., Martens, E. C., & Núñez, G. (2012). Regulated virulence controls the ability of a pathogen to compete with the gut microbiota. *Science*, *336*(6086), 1325–1329. https://doi.org/10.1126/SCIENCE.1222195/SUPPL_FILE/PAPV3.PDF

Kaufman, J., Griffiths, T. A., Surette, M. G., Ness, S., & Rioux, K. P. (2009). Effects of mesalamine (5-Aminosalicylic Acid) on bacterial gene expression. *Inflammatory Bowel Diseases*, *15*(7), 985–996. https://doi.org/10.1002/ibd.20876

Kim, K. H., Kabir, E., & Jahan, S. A. (2017). Exposure to pesticides and the associated human health effects. *Science of The Total Environment*, *575*, 525–535. https://doi.org/10.1016/J.SCITOTENV.2016.09.009

Kim, S. G., Becattini, S., Moody, T. U., Shliaha, P. V., Littmann, E. R., Seok, R., Gjonbalaj, M., Eaton, V., Fontana, E., Amoretti, L., Wright, R., Caballero, S., Wang, Z. M. X., Jung, H. J., Morjaria, S. M., Leiner, I. M., Qin, W., Ramos, R. J. J. F., Cross, J. R., … Pamer, E. G. (2019). Microbiota-derived lantibiotic restores resistance against vancomycin-resistant Enterococcus. *Nature*, *572*(7771), 665–669. https://doi.org/10.1038/s41586-019-1501-z

Kim, W., & Surette, M. G. (2003). Swarming populations of Salmonella represent a unique physiological state coupled to multiple mechanisms of antibiotic resistance. *Biological Procedures Online*, *5*(1), 189–196. https://doi.org/10.1251/bpo61

Kobylewski, S., & Jacobson, M. F. (2013). Toxicology of food dyes. *Http://Dx.Doi.Org/10.1179/1077352512Z.00000000034*, *18*(3), 220–246. https://doi.org/10.1179/1077352512Z.00000000034

Konstantinidis, K. T., & Tiedje, J. M. (2005). Genomic insights that advance the species definition for prokaryotes. *Proceedings of the National Academy of Sciences of the United States of America*, *102*(7), 2567–2572. https://doi.org/10.1073/PNAS.0409727102

Koopman, J. P., Stadhouders, A. M., Kennis', H. M., & De Boer, H. (1987). The attachment of filamentous segmented micro-organisms to the distal ileum wall of the mouse: a scanning and transmission electron microscopy study. *Laboratory Animals*, *21*, 48–52.

Koppel, N., Rekdal, V. M., & Balskus, E. P. (2017). Chemical transformation of xenobiotics by the human gut microbiota. *Science*, *356*(6344), 1246–1257. https://doi.org/10.1126/SCIENCE.AAG2770/ASSET/7F3BFA3D-4441-425F-A5E7-A8C2BB8E8AEF/ASSETS/GRAPHIC/356_AAG2770_F4.JPEG

Kuchina, A., Brettner, L. M., Paleologu, L., Roco, C. M., Rosenberg, A. B., Carignano, A., Kibler, R., Hirano, M., William DePaolo, R., & Seelig, G. (2021). Microbial single-cell RNA sequencing by split-pool barcoding. *Science*, *5257*. https://doi.org/10.1101/869248

Kwok, Y. Y., Tally, F. P., Sutter, V. L., & Finegold, S. M. (1975). Disk Susceptibility Testing of Slow-Growing Anaerobic Bacteria. *Antimicrobial Agents and Chemotherapy*, *7*(1), 1–7. https://doi.org/10.1128/AAC.7.1.1

Kwon, Y. H., Banskota, S., Wang, H., Rossi, L., Grondin, J. A., Syed, S. A., Yousefi, Y., Schertzer, J. D., Morrison, K. M., Wade, M. G., Holloway, A. C., Surette, M. G., Steinberg, G. R., & Khan, W. I. (2022). Chronic exposure to synthetic food colorant Allura Red AC promotes susceptibility to experimental colitis via intestinal serotonin in mice. *Nature Communications 2022 13:1*, *13*(1), 1–18. https://doi.org/10.1038/s41467-022-35309-y

Lack, G., Fox, D., Northstone, K., & Golding, J. (2003). Factors Associated with the Development of Peanut Allergy in Childhood. *New England Journal of Medicine*, *348*(11), 977–985. https://doi.org/10.1056/NEJMoa013536

Lagier, J. C., Khelaifia, S., Alou, M. T., Ndongo, S., Dione, N., Hugon, P., Caputo, A., Cadoret, F., Traore, S. I., Seck, E. H., Dubourg, G., Durand, G., Mourembou, G., Guilhot, E., Togo, A., Bellali, S., Bachar, D., Cassir, N., Bittar, F., … Raoult, D. (2016). Culture of previously uncultured members of the

human gut microbiota by culturomics. *Nature Microbiology*, *1*. https://doi.org/10.1038/nmicrobiol.2016.203

Landrigan, P. J., Fuller, R., Acosta, N. J. R., Adeyi, O., Arnold, R., Basu, N. (Nil), Baldé, A. B., Bertollini, R., Bose-O'Reilly, S., Boufford, J. I., Breysse, P. N., Chiles, T., Mahidol, C., Coll-Seck, A. M., Cropper, M. L., Fobil, J., Fuster, V., Greenstone, M., Haines, A., … Zhong, M. (2018). The Lancet Commission on pollution and health. *The Lancet*, *391*(10119), 462–512. https://doi.org/10.1016/S0140-6736(17)32345-0

Lane, D. J., Pace, B., Olsen, G. J., Stahl, D. A., Sogin, M. L., & Pace, N. R. (1985). Rapid determination of 16S ribosomal RNA sequences for phylogenetic analyses. *Proceedings of the National Academy of Sciences of the United States of America*, *82*(20), 6955–6959. https://doi.org/10.1073/PNAS.82.20.6955

Lapébie, P., Lombard, V., Drula, E., Terrapon, N., & Henrissat, B. (2019). Bacteroidetes use thousands of enzyme combinations to break down glycans. *Nature Communications 2019 10:1*, *10*(1), 1–7. https://doi.org/10.1038/s41467-019-10068-5

Lau, J. T., Whelan, F. J., Herath, I., Lee, C. H., Collins, S. M., Bercik, P., & Surette, M. G. (2016). Capturing the diversity of the human gut microbiota through culture-enriched molecular profiling. *Genome Medicine*, *8*(1), 72. https://doi.org/10.1186/s13073-016-0327-7

Lee, M. D. (2019). GToTree: a user-friendly workflow for phylogenomics. *Bioinformatics*, *35*(20), 4162–4164. https://doi.org/10.1093/BIOINFORMATICS/BTZ188

Lehto, S., Buchweitz, M., Klimm, A., Straßburger, R., Bechtold, C., & Ulberth, F. (2017). Comparison of food colour regulations in the EU and the US: a review of current provisions. *Https://Doi.Org/10.1080/19440049.2016.1274431*, *34*(3), 335–355. https://doi.org/10.1080/19440049.2016.1274431

Letunic, I., & Bork, P. (2021). Interactive Tree Of Life (iTOL) v5: an online tool for phylogenetic tree display and annotation. *Nucleic Acids Research*, *49*(W1), W293–W296. https://doi.org/10.1093/NAR/GKAB301

Li, H., & Durbin, R. (2009). Fast and accurate short read alignment with Burrows–Wheeler transform. *Bioinformatics*, *25*(14), 1754–1760. https://doi.org/10.1093/BIOINFORMATICS/BTP324

Li, H., Handsaker, B., Wysoker, A., Fennell, T., Ruan, J., Homer, N., Marth, G., Abecasis, G., & Durbin, R. (2009). The Sequence Alignment/Map format and SAMtools. *Bioinformatics*, *25*(16), 2078–2079. https://doi.org/10.1093/BIOINFORMATICS/BTP352

Li, J., Jia, H., Cai, X., Zhong, H., Feng, Q., Sunagawa, S., Arumugam, M., Kultima, J. R., Prifti, E., Nielsen, T., Juncker, A. S., Manichanh, C., Chen, B., Zhang, W., Levenez, F., Wang, J., Xu, X., Xiao, L., Liang, S., … Mende, D. R. (2014). An integrated catalog of reference genes in the human gut microbiome. *Nature Biotechnology*, *32*(8), 834–841. https://doi.org/10.1038/NBT.2942

Liang, Y., Zhan, J., Liu, D., Luo, M., Han, J., Liu, X., Liu, C., Cheng, Z., Zhou, Z., & Wang, P. (2019). Organophosphorus pesticide chlorpyrifos intake promotes obesity and insulin resistance through impacting gut and gut microbiota. *Microbiome*, *7*(1). https://doi.org/10.1186/S40168-019-0635-4

Liao, C., Liu, F., Alomirah, H., Loi, V. D., Mohd, M. A., Moon, H. B., Nakata, H., & Kannan, K. (2012). Bisphenol S in urine from the United States and seven Asian

countries: Occurrence and human exposures. *Environmental Science and Technology*, *46*(12), 6860–6866. https://doi.org/10.1021/ES301334J/SUPPL_FILE/ES301334J_SI_001.PDF

Liao, Y., Smyth, G. K., & Shi, W. (2014). featureCounts: an efficient general purpose program for assigning sequence reads to genomic features. *Bioinformatics*, *30*(7), 923–930. https://doi.org/10.1093/bioinformatics/btt656

Linares, R., Fernández, M. F., Gutiérrez, A., García-Villalba, R., Suárez, B., Zapater, P., Martínez-Blázquez, J. A., Caparrós, E., Tomás-Barberán, F. A., & Francés, R. (2021). Endocrine disruption in Crohn's disease: Bisphenol A enhances systemic inflammatory response in patients with gut barrier translocation of dysbiotic microbiota products. *FASEB Journal : Official Publication of the Federation of American Societies for Experimental Biology*, *35*(7). https://doi.org/10.1096/FJ.202100481R

Love, M. I., Anders, S., Kim, V., & Huber, W. (2016). RNA-Seq workflow: Gene-level exploratory analysis and differential expression. *F1000Research*, *4*. https://doi.org/10.12688/f1000research.7035.2

Love, M. I., Huber, W., & Anders, S. (2014). Moderated estimation of fold change and dispersion for RNA-seq data with DESeq2. *Genome Biology*, *15*(12), 550. https://doi.org/10.1186/s13059-014-0550-8

Lu, W., Li, L., Chen, M., Zhou, Z., Zhang, W., Ping, S., Yan, Y., Wang, J., & Lin, M. (2013). Genome-wide transcriptional responses of Escherichia coli to glyphosate, a potent inhibitor of the shikimate pathway enzyme 5-enolpyruvylshikimate-3-phosphate synthase. *Molecular BioSystems*, *9*(3), 522–530. https://doi.org/10.1039/c2mb25374g

Luchi, R. J., & Gruber, J. W. (1968). Unusually large digitalis requirements: A study of altered digoxin metabolism. *The American Journal of Medicine*, *45*(2), 322–328. https://doi.org/10.1016/0002-9343(68)90049-1

Maggi, F., Tang, F. H. M., la Cecilia, D., & McBratney, A. (2019). PEST-CHEMGRIDS, global gridded maps of the top 20 crop-specific pesticide application rates from 2015 to 2025. *Scientific Data*, *6*(1), 1–20. https://doi.org/10.1038/s41597-019-0169-4

Maier, L., Pruteanu, M., Kuhn, M., Zeller, G., Telzerow, A., Anderson, E. E., Brochado, A. R., Fernandez, K. C., Dose, H., Mori, H., Patil, K. R., Bork, P., & Typas, A. (2018). Extensive impact of non-antibiotic drugs on human gut bacteria. *Nature*, *555*(7698), 623–628. https://doi.org/10.1038/nature25979

Marchesi, J. R., & Ravel, J. (2015). The vocabulary of microbiome research: a proposal. *Microbiome*, *3*(1), 1–3. https://doi.org/10.1186/S40168-015-0094-5

Marshall, B. J., & Warren, J. R. (1984). UNIDENTIFIED CURVED BACILLI IN THE STOMACH OF PATIENTS WITH GASTRITIS AND PEPTIC ULCERATION. *The Lancet*, *323*(8390), 1311–1315. https://doi.org/10.1016/S0140-6736(84)91816-6

Martin, M. (2011). Cutadapt removes adapter sequences from high-throughput sequencing reads. *EMBnet.Journal*, *17*(1), 10–12. https://doi.org/10.14806/EJ.17.1.200

Maruvada, P., Leone, V., Kaplan, L. M., & Chang, E. B. (2017). The Human Microbiome and Obesity: Moving beyond Associations. *Cell Host & Microbe*, *22*(5), 589–599. https://doi.org/10.1016/J.CHOM.2017.10.005

Matthiessen, P., Wheeler, J. R., & Weltje, L. (2017). A review of the evidence for endocrine disrupting effects of current-use chemicals on wildlife populations. *Https://Doi.Org/10.1080/10408444.2017.1397099*, *48*(3), 195–216. https://doi.org/10.1080/10408444.2017.1397099

Maurice, C. F., Haiser, H. J., & Turnbaugh, P. J. (2013). Xenobiotics shape the physiology and gene expression of the active human gut microbiome. *Cell*, *152*(1–2), 39–50. https://doi.org/10.1016/j.cell.2012.10.052

McCann, D., Barrett, A., Cooper, A., Crumpler, D., Dalen, L., Grimshaw, K., Kitchin, E., Lok, K., Porteous, L., Prince, E., Sonuga-Barke, E., Warner, J. O., & Stevenson, J. (2007). Food additives and hyperactive behaviour in 3-year-old and 8/9-year-old children in the community: a randomised, double-blinded, placebo-controlled trial. *The Lancet*, *370*(9598), 1560–1567. https://doi.org/10.1016/S0140-6736(07)61306-3

McDonald, L. C., Gerding, D. N., Johnson, S., Bakken, J. S., Carroll, K. C., Coffin, S. E., Dubberke, E. R., Garey, K. W., Gould, C. V, Kelly, C., Loo, V., Shaklee Sammons, J., Sandora, T. J., & Wilcox, M. H. (2018). Clinical Practice Guidelines for Clostridium difficile Infection in Adults and Children: 2017 Update by the Infectious Diseases Society of America (IDSA) and Society for Healthcare Epidemiology of America (SHEA). *Clinical Infectious Diseases*, *66*(7), e1–e48. https://doi.org/10.1093/cid/cix1085

McDonough, C. M., Xu, H. S., & Guo, T. L. (2021). Toxicity of bisphenol analogues on the reproductive, nervous, and immune systems, and their relationships to gut microbiome and metabolism: insights from a multi-species comparison. *Critical Reviews in Toxicology*, *51*(4), 283–300. https://doi.org/10.1080/10408444.2021.1908224

Mehta, R. S., Mayers, J. R., Zhang, Y., Bhosle, A., Glasser, N. R., Nguyen, L. H., Ma, W., Bae, S., Branck, T., Song, K., Sebastian, L., Pacheco, J. A., Seo, H. S., Clish, C., Dhe-Paganon, S., Ananthakrishnan, A. N., Franzosa, E. A., Balskus, E. P., Chan, A. T., & Huttenhower, C. (2023). Gut microbial metabolism of 5-ASA diminishes its clinical efficacy in inflammatory bowel disease. *Nature Medicine*. https://doi.org/10.1038/s41591-023-02217-7

Meighen, E. A. (1991). Molecular biology of bacterial bioluminescence. *Microbiological Reviews*, *55*(1), 123–142. https://doi.org/10.1128/MR.55.1.123-142.1991

Meighen, E. A. (1993). Bacterial bioluminescence: organization, regulation, and application of the lux genes. *FASEB Journal : Official Publication of the Federation of American Societies for Experimental Biology*, *7*(11), 1016–1022. https://doi.org/10.1096/FASEBJ.7.11.8370470

Mesnage, R., & Antoniou, M. N. (2020). Computational modelling provides insight into the effects of glyphosate on the shikimate pathway in the human gut microbiome. *Current Research in Toxicology*, *1*, 25–33. https://doi.org/10.1016/j.crtox.2020.04.001

Motta, E. V. S., Raymann, K., & Moran, N. A. (2018). Glyphosate perturbs the gut microbiota of honey bees. *Proceedings of the National Academy of Sciences*, *115*(41), 10305–10310. https://doi.org/10.1073/pnas.1803880115

Müller, P. (1946). 204. Über Zusammenhänge zwischen Konstitution und insektizider Wirkung I (Dichlordiphenyl-trichlor-äthan-Derivate und verwandte Verbindungen). *Helvetica Chimica Acta*, *29*(6), 1560–1580. https://doi.org/10.1002/HLCA.19460290626

Nasuti, C., Coman, M. M., Olek, R. A., Fiorini, D., Verdenelli, M. C., Cecchini, C., Silvi, S., Fedeli, D., & Gabbianelli, R. (2016). Changes on fecal microbiota in rats exposed to permethrin during postnatal development. *Environmental Science and Pollution Research International*, *23*(11), 10930–10937. https://doi.org/10.1007/S11356-016-6297-X

Natividad, J. M. M., Hayes, C. L., Motta, J. P., Jury, J., Galipeau, H. J., Philip, V., Garcia-Rodenas, C. L., Kiyama, H., Bercik, P., & Verdú, E. F. (2013). Differential induction of antimicrobial REGIII by the intestinal microbiota and Bifidobacterium breve NCC2950. *Applied and Environmental Microbiology*, *79*(24), 7745–7754. https://doi.org/10.1128/AEM.02470-13/SUPPL_FILE/ZAM999104954SO1.PDF

Navaranjan, G., Diamond, M. L., Harris, S. A., Jantunen, L. M., Bernstein, S., Scott, J. A., Takaro, T. K., Dai, R., Lefebvre, D. L., Azad, M. B., Becker, A. B., Mandhane, P. J., Moraes, T. J., Simons, E., Turvey, S. E., Sears, M. R., Subbarao, P., & Brook, J. R. (2021). Early life exposure to phthalates and the development of childhood asthma among Canadian children. *Environmental Research*, *197*, 110981. https://doi.org/10.1016/J.ENVRES.2021.110981

Nguyen, L. T., Schmidt, H. A., von Haeseler, A., & Minh, B. Q. (2015). IQ-TREE: A Fast and Effective Stochastic Algorithm for Estimating Maximum-Likelihood Phylogenies. *Molecular Biology and Evolution*, *32*(1), 268. https://doi.org/10.1093/MOLBEV/MSU300

Ni, Y., Hu, L., Yang, S., Ni, L., Ma, L., Zhao, Y., Zheng, A., Jin, Y., & Fu, Z. (2021). Bisphenol A impairs cognitive function and 5-HT metabolism in adult male mice by modulating the microbiota-gut-brain axis. *Chemosphere*, *282*. https://doi.org/10.1016/J.CHEMOSPHERE.2021.130952

Pace, N. R., Sapp, J., & Goldenfeld, N. (2012). Phylogeny and beyond: Scientific, historical, and conceptual significance of the first tree of life. *Proceedings of the National Academy of Sciences of the United States of America*, *109*(4), 1011–1018. https://doi.org/10.1073/PNAS.1109716109

Park, J. S., Lee, W. C., Yeo, K. J., Ryu, K.-S., Kumarasiri, M., Hesek, D., Lee, M., Mobashery, S., Song, J. H., Kim, S. il, Lee, J. C., Cheong, C., Jeon, Y. H., & Kim, H.-Y. (2012). Mechanism of anchoring of OmpA protein to the cell wall peptidoglycan of the gram-negative bacterial outer membrane. *The FASEB Journal*, *26*(1), 219. https://doi.org/10.1096/FJ.11-188425

Parks, D. H., Chuvochina, M., Rinke, C., Mussig, A. J., Chaumeil, P.-A., & Hugenholtz, P. (2022). GTDB: an ongoing census of bacterial and archaeal diversity through a phylogenetically consistent, rank normalized and complete genome-based taxonomy. *Nucleic Acids Research*, *50*(D1), D785–D794. https://doi.org/10.1093/nar/gkab776

Paseiro Losada, P., Simal Lozano, J., Paz Abuín, S., López Mahía, P., & Simal Gándara, J. (1993). Kinetics of the hydrolysis of bisphenol A diglycidyl ether (BADGE) in water-based food simulants. *Fresenius' Journal of Analytical Chemistry 1993 345:7*, *345*(7), 527–532. https://doi.org/10.1007/BF00326345

Pingali, P. L. (2012). Green revolution: Impacts, limits, andthe path ahead. *Proceedings of the National Academy of Sciences of the United States of America*, *109*(31), 12302–12308. https://doi.org/10.1073/PNAS.0912953109

Polic, I. I. (2018). *Evaluation of the Impact of Azo Dyes on the Metabolism of Stabilized Fecal Communities and In Vitro Cell Culture ABSTRACT EVALUATION OF THE IMPACT*

OF AZO DYES ON THE METABOLISM OF STABILIZED FECAL COMMUNITIES AND IN VITRO CELL CULTURE. *May*.

Price, M. N., Dehal, P. S., & Arkin, A. P. (2010). FastTree 2 – Approximately Maximum-Likelihood Trees for Large Alignments. *PLOS ONE*, *5*(3), e9490. https://doi.org/10.1371/JOURNAL.PONE.0009490

Pritchard, L., Glover, R. H., Humphris, S., Elphinstone, J. G., & Toth, I. K. (2015). Genomics and taxonomy in diagnostics for food security: soft-rotting enterobacterial plant pathogens. *Analytical Methods*, *8*(1), 12–24. https://doi.org/10.1039/C5AY02550H

Pruesse, E., Peplies, J., & Glöckner, F. O. (2012). SINA: Accurate high-throughput multiple sequence alignment of ribosomal RNA genes. *Bioinformatics*, *28*(14), 1823–1829. https://doi.org/10.1093/BIOINFORMATICS/BTS252

Pruesse, E., Quast, C., Knittel, K., Fuchs, B. M., Ludwig, W., Peplies, J., & Glöckner, F. O. (2007). SILVA: a comprehensive online resource for quality checked and aligned ribosomal RNA sequence data compatible with ARB. *Nucleic Acids Research*, *35*(21), 7188–7196. https://doi.org/10.1093/nar/gkm864

Rea, M. C., Sit, C. S., Clayton, E., O'Connor, P. M., Whittal, R. M., Zheng, J., Vederas, J. C., Ross, R. P., & Hill, C. (2010). Thuricin CD, a posttranslationally modified bacteriocin with a narrow spectrum of activity against Clostridium difficile. *Proceedings of the National Academy of Sciences of the United States of America*, *107*(20), 9352–9357. https://doi.org/10.1073/PNAS.0913554107/SUPPL_FILE/PNAS.200913554SI.PDF

Reese, A. T., Pereira, F. C., Schintlmeister, A., Berry, D., Wagner, M., Hale, L. P., Wu, A., Jiang, S., Durand, H. K., Zhou, X., Premont, R. T., Diehl, A. M., O'Connell, T. M., Alberts, S. C., Kartzinel, T. R., Pringle, R. M., Dunn, R. R., Wright, J. P., & David, L. A. (2018). Microbial nitrogen limitation in the mammalian large intestine. *Nature Microbiology*, *3*(12), 1441–1450. https://doi.org/10.1038/s41564-018-0267-7

Rekdal, V. M., Bess, E. N., Bisanz, J. E., Turnbaugh, P. J., & Balskus, E. P. (2019). Discovery and inhibition of an interspecies gut bacterial pathway for Levodopa metabolism. *Science*, *364*(6445), 1055. https://doi.org/10.1126/SCIENCE.AAU6323/SUPPL_FILE/AAU6323_MAINI-REKDAL_DATA-FILE-S1.XLSX

Risso, D., Ngai, J., Speed, T. P., & Dudoit, S. (2014). Normalization of RNA-seq data using factor analysis of control genes or samples. *Nature Biotechnology*, *32*(9), 896–902. https://doi.org/10.1038/nbt.2931

Robin Warren, J., & Marshall, B. (1983). UNIDENTIFIED CURVED BACILLI ON GASTRIC EPITHELIUM IN ACTIVE CHRONIC GASTRITIS. *The Lancet*, *321*(8336), 1273–1275. https://doi.org/10.1016/S0140-6736(83)92719-8

Rogers, M. A. M., & Aronoff, D. M. (2016). The influence of non-steroidal anti-inflammatory drugs on the gut microbiome. *Clinical Microbiology and Infection*, *22*(2), 178.e1-178.e9. https://doi.org/10.1016/J.CMI.2015.10.003

Roingeard, C., Monnereau, A., Goujon, S., Orazio, S., Bouvier, G., & Vacquier, B. (2021). Passive environmental residential exposure to agricultural pesticides and hematological malignancies in the general population: a systematic review. *Environmental Science and Pollution Research International*, *28*(32), 43190–43216. https://doi.org/10.1007/S11356-021-14789-3

Ross, M. G., Russ, C., Costello, M., Hollinger, A., Lennon, N. J., Hegarty, R., Nusbaum, C., & Jaffe, D. B. (2013). Characterizing and measuring bias in sequence data. *Genome Biology*, *14*(5), R51. https://doi.org/10.1186/gb-2013-14-5-r51

Round, J. L., & Mazmanian, S. K. (2009). The gut microbiota shapes intestinal immune responses during health and disease. *Nature Reviews Immunology 2009 9:5*, *9*(5), 313–323. https://doi.org/10.1038/nri2515

RStudio Team. (2020). *RStudio: Integrated Development for R*. http://www.rstudio.com/

Rubio-Rivas, M., Moreno, R., & Corbella, X. (2017). Occupational and environmental scleroderma. Systematic review and meta-analysis. *Clinical Rheumatology*, *36*(3), 569–582. https://doi.org/10.1007/S10067-016-3533-1

Rufus, I. B., Shah, H., & Hoyle, C. E. (1994). Identification of fluorescent products produced by the thermal treatment of bisphenol-A-based polycarbonate. *Journal of Applied Polymer Science*, *51*(9), 1549–1558. https://doi.org/10.1002/APP.1994.070510904

Sapone, A., Lammers, K. M., Casolaro, V., Cammarota, M., Giuliano, M. T., De Rosa, M., Stefanile, R., Mazzarella, G., Tolone, C., Russo, M. I., Esposito, P., Ferraraccio, F., Cartenì, M., Riegler, G., de Magistris, L., & Fasano, A. (2011). Divergence of gut permeability and mucosal immune gene expression in two gluten-associated conditions: Celiac disease and gluten sensitivity. *BMC Medicine*, *9*(1), 1–11. https://doi.org/10.1186/1741-7015-9-23/COMMENTS

Savage, D. C., Siegel, J. E., Snellen, J. E., & Whitt, D. D. (1981). Transit time of epithelial cells in the small intestines of germfree mice and ex-germfree mice associated with indigenous microorganisms. *Applied and Environmental Microbiology*, *42*(6), 996–1001. https://doi.org/10.1128/AEM.42.6.996-1001.1981

Schnupf, P., Gaboriau-Routhiau, V., Sansonetti, P. J., & Cerf-Bensussan, N. (2017). Segmented filamentous bacteria, Th17 inducers and helpers in a hostile world. *Current Opinion in Microbiology*, *35*, 100–109. https://doi.org/10.1016/J.MIB.2017.03.004

Schroven, K., Aertsen, A., & Lavigne, R. (2021). Bacteriophages as drivers of bacterial virulence and their potential for biotechnological exploitation. *FEMS Microbiology Reviews*, *45*(1), 1–15. https://doi.org/10.1093/FEMSRE/FUAA041

Schwengers, O., Jelonek, L., Dieckmann, M. A., Beyvers, S., Blom, J., & Goesmann, A. (2021). Bakta: Rapid and standardized annotation of bacterial genomes via alignment-free sequence identification. *Microbial Genomics*, *7*(11). https://doi.org/10.1099/MGEN.0.000685

Seemann, T. (n.d.). *barrnap 0.9: rapid ribosomal RNA prediction*.

Sender, R., Fuchs, S., & Milo, R. (2016). Revised Estimates for the Number of Human and Bacteria Cells in the Body. *PLOS Biology*, *14*(8), e1002533. https://doi.org/10.1371/JOURNAL.PBIO.1002533

Seshadri, R., Leahy, S. C., Attwood, G. T., Teh, K. H., Lambie, S. C., Cookson, A. L., Eloe-Fadrosh, E. A., Pavlopoulos, G. A., Hadjithomas, M., Varghese, N. J., Paez-Espino, D., Perry, R., Henderson, G., Creevey, C. J., Terrapon, N., Lapebie, P., Drula, E., Lombard, V., Rubin, E., … Cerón Cucchi, M. (2018). Cultivation and sequencing of rumen microbiome members from the Hungate1000 Collection. *Nature Biotechnology 2018 36:4*, *36*(4), 359–367. https://doi.org/10.1038/nbt.4110

Shaiber, A., Willis, A. D., Delmont, T. O., Roux, S., Chen, L. X., Schmid, A. C., Yousef, M., Watson, A. R., Lolans, K., Esen, Ö. C., Lee, S. T. M., Downey, N., Morrison, H. G., Dewhirst, F. E., Mark Welch, J. L., & Eren, A. M. (2020). Functional and genetic markers of niche partitioning among enigmatic members of the human oral microbiome. *Genome Biology*, *21*(1), 1–35. https://doi.org/10.1186/S13059-020-02195-W/METRICS

Shapiro, S. S., & Wilk, M. B. (1965). An analysis of variance test for normality (complete samples). *Biometrika*, *52*(3–4), 591–611. https://doi.org/10.1093/biomet/52.3-4.591

Sharma, P., Bilkhiwal, N., Chaturvedi, P., Kumar, S., & Khetarpal, P. (2021). Potential environmental toxicant exposure, metabolizing gene variants and risk of PCOS-A systematic review. *Reproductive Toxicology (Elmsford, N.Y.)*, *103*, 124–132. https://doi.org/10.1016/J.REPROTOX.2021.06.005

Shelton, C. D., Yoo, W., Shealy, N. G., Torres, T. P., Zieba, J. K., Calcutt, M. W., Foegeding, N. J., Kim, D., Kim, J., Ryu, S., & Byndloss, M. X. (2022). Salmonella enterica serovar Typhimurium uses anaerobic respiration to overcome propionate-mediated colonization resistance. *Cell Reports*, *38*(1), 110180. https://doi.org/10.1016/J.CELREP.2021.110180/ATTACHMENT/E01126A9-E0BA-4E95-AF96-0575CE2D329D/MMC1.PDF

Shishkin, A. A., Giannoukos, G., Kucukural, A., Ciulla, D., Busby, M., Surka, C., Chen, J., Bhattacharyya, R. P., Rudy, R. F., Patel, M. M., Novod, N., Hung, D. T., Gnirke, A., Garber, M., Guttman, M., & Livny, J. (2015). Simultaneous generation of many RNA-seq libraries in a single reaction. *Nature Methods 2015 12:4*, *12*(4), 323–325. https://doi.org/10.1038/nmeth.3313

Shoemaker, N. B., Vlamakis, H., Hayes, K., & Salyers, A. A. (2001). Evidence for Extensive Resistance Gene Transfer amongBacteroides spp. and among Bacteroides and Other Genera in the Human Colon. *Applied and Environmental Microbiology*, *67*(2), 561–568. https://doi.org/10.1128/AEM.67.2.561-568.2001

Sibley, C. D., Grinwis, M. E., Field, T. R., Eshaghurshan, C. S., Faria, M. M., Dowd, S. E., Parkins, M. D., Rabin, H. R., & Surette, M. G. (2011). Culture enriched molecular profiling of the cystic fibrosis airway microbiome. *PloS One*, *6*(7). https://doi.org/10.1371/JOURNAL.PONE.0022702

Sivan, A., Corrales, L., Hubert, N., Williams, J. B., Aquino-Michaels, K., Earley, Z. M., Benyamin, F. W., Lei, Y. M., Jabri, B., Alegre, M. L., Chang, E. B., & Gajewski, T. F. (2015). Commensal Bifidobacterium promotes antitumor immunity and facilitates anti-PD-L1 efficacy. *Science*, *350*(6264), 1084–1089. https://doi.org/10.1126/SCIENCE.AAC4255/SUPPL_FILE/PAPV2.PDF

Sorbara, M. T., Littmann, E. R., Fontana, E., Moody, T. U., Kohout, C. E., Gjonbalaj, M., Eaton, V., Seok, R., Leiner, I. M., & Pamer, E. G. (2020). Functional and Genomic Variation between Human-Derived Isolates of Lachnospiraceae Reveals Inter- and Intra-Species Diversity. *Cell Host and Microbe*, *28*(1), 134-146.e4. https://doi.org/10.1016/j.chom.2020.05.005

Stamboulian, M., Canderan, J., & Ye, Y. (2022). Metaproteomics as a tool for studying the protein landscape of human-gut bacterial species. *PLOS Computational Biology*, *18*(3), e1009397. https://doi.org/10.1371/JOURNAL.PCBI.1009397

Stead, M. B., Agrawal, A., Bowden, K. E., Nasir, R., Mohanty, B. K., Meagher, R. B., & Kushner, S. R. (2012). RNA snap ™: a rapid, quantitative and

inexpensive, method for isolating total RNA from bacteria. *Nucleic Acids Research*, *40*(20), e156–e156. https://doi.org/10.1093/NAR/GKS680

Storey, J. D., & Tibshirani, R. (2003). Statistical significance for genomewide studies. *Proceedings of the National Academy of Sciences of the United States of America*, *100*(16), 9440–9445. https://doi.org/10.1073/PNAS.1530509100/ASSET/25537429-365C-4D06-977A-86C871368513/ASSETS/GRAPHIC/PQ1530509003.JPEG

Swagata Sarkar, Juliana Dias Bernardes Gil, James Keeley, Nicklas Mohring, & Kees Jansen. (2021). *The use of pesticides in developing countries and their impact on health and the right to food | Think Tank | European Parliament*.

Szklarczyk, D., Kirsch, R., Koutrouli, M., Nastou, K., Mehryary, F., Hachilif, R., Gable, A. L., Fang, T., Doncheva, N. T., Pyysalo, S., Bork, P., Jensen, L. J., & von Mering, C. (2023). The STRING database in 2023: protein–protein association networks and functional enrichment analyses for any sequenced genome of interest. *Nucleic Acids Research*, *51*(D1), D638–D646. https://doi.org/10.1093/nar/gkac1000

Tan, T. G., Sefik, E., Geva-Zatorsky, N., Kua, L., Naskar, D., Teng, F., Pasman, L., Ortiz-Lopez, A., Jupp, R., Wu, H. J. J., Kasper, D. L., Benoist, C., & Mathis, D. (2016). Identifying species of symbiont bacteria from the human gut that, alone, can induce intestinal Th17 cells in mice. *Proceedings of the National Academy of Sciences of the United States of America*, *113*(50), E8141–E8150. https://doi.org/10.1073/PNAS.1617460113/SUPPL_FILE/PNAS.201617460SI.PDF

Taneja, V., Taneja, I., Mihali, A. B., & Pawar, R. (2021). Excipient Hypersensitivity Masquerading as Multidrug Allergy. *The American Journal of Medicine*, *134*(8), e447–e448. https://doi.org/https://doi.org/10.1016/j.amjmed.2021.02.015

Tannock, G. W., Miller, J. R., & Savage, D. C. (1984). Host specificity of filamentous, segmented microorganisms adherent to the small bowel epithelium in mice and rats. *Applied and Environmental Microbiology*, *47*(2), 441–442. https://doi.org/10.1128/AEM.47.2.441-442.1984

Tian, Y., Gui, W., Rimal, B., Koo, I., Smith, P. B., Nichols, R. G., Cai, J., Liu, Q., & Patterson, A. D. (2020). Metabolic impact of persistent organic pollutants on gut microbiota. *Gut Microbes*, *12*(1), 1–16. https://doi.org/10.1080/19490976.2020.1848209

Turnbaugh, P. J., Ley, R. E., Hamady, M., Fraser-Liggett, C. M., Knight, R., & Gordon, J. I. (2007). The human microbiome project. *Nature*, *449*(7164), 804–810. https://doi.org/10.1038/nature06244

Umesaki, Y., Okada, Y., Matsumoto, S., Imaoka, A., & Setoyama, H. (1995). Segmented Filamentous Bacteria Are Indigenous Intestinal Bacteria That Activate Intraepithelial Lymphocytes and Induce MHC Class II Molecules and Fucosyl Asialo GM1 Glycolipids on the Small Intestinal Epithelial Cells in the Ex-Germ-Free Mouse. *Microbiology and Immunology*, *39*(8), 555–562. https://doi.org/10.1111/J.1348-0421.1995.TB02242.X

Vaishnava, S., Yamamoto, M., Severson, K. M., Ruhn, K. A., Yu, X., Koren, O., Ley, R., Wakeland, E. K., & Hooper, L. V. (2011). The antibacterial lectin RegIIIγ promotes the spatial segregation of microbiota and host in the intestine. *Science*, *334*(6053), 255–258. https://doi.org/10.1126/SCIENCE.1209791/SUPPL_FILE/VAISHNAVASOM.PDF

van Dongen, S. (2008). Graph Clustering Via a Discrete Uncoupling Process. *Https://Doi.Org/10.1137/040608635*, *30*(1), 121–141. https://doi.org/10.1137/040608635

van Hogezand, R. A., Kennis, H. M., van Schaik, A., Koopman, J. P., van Hees, P. A. M., & van Tongeren, J. H. M. (1992). Bacterial acetylation of 5-aminosalicylic acid in faecal suspensions cultured under aerobic and anaerobic conditions. *European Journal of Clinical Pharmacology 1992 43:2*, *43*(2), 189–192. https://doi.org/10.1007/BF01740669

van Kessel, S. P., Auvinen, P., Scheperjans, F., & El Aidy, S. (2021). Gut bacterial tyrosine decarboxylase associates with clinical variables in a longitudinal cohort study of Parkinsons disease. *Npj Parkinson's Disease 2021 7:1*, *7*(1), 1–8. https://doi.org/10.1038/s41531-021-00260-0

van Kessel, S. P., Frye, A. K., El-Gendy, A. O., Castejon, M., Keshavarzian, A., van Dijk, G., & El Aidy, S. (2019). Gut bacterial tyrosine decarboxylases restrict levels of levodopa in the treatment of Parkinson's disease. *Nature Communications 2019 10:1*, *10*(1), 1–11. https://doi.org/10.1038/s41467-019-08294-y

Vandenberg, L. N., Maffini, M. V., Sonnenschein, C., Rubin, B. S., & Soto, A. M. (2009). Bisphenol-A and the Great Divide: A Review of Controversies in the Field of Endocrine Disruption. *Endocrine Reviews*, *30*(1), 75–95. https://doi.org/10.1210/ER.2008-0021

Velmurugan, G., Ramprasath, T., Swaminathan, K., Mithieux, G., Rajendhran, J., Dhivakar, M., Parthasarathy, A., Babu, D. D. V., Thumburaj, L. J., Freddy, A. J., Dinakaran, V., Puhari, S. S. M., Rekha, B., Christy, Y. J., Anusha, S., Divya, G., Suganya, K., Meganathan, B., Kalyanaraman, N., … Ramasamy, S. (2017). Gut microbial degradation of organophosphate insecticides-induces glucose intolerance via gluconeogenesis. *Genome Biology*, *18*(1). https://doi.org/10.1186/S13059-016-1134-6

Walker, B. J., Abeel, T., Shea, T., Priest, M., Abouelliel, A., Sakthikumar, S., Cuomo, C. A., Zeng, Q., Wortman, J., Young, S. K., & Earl, A. M. (2014). Pilon: An Integrated Tool for Comprehensive Microbial Variant Detection and Genome Assembly Improvement. *PLOS ONE*, *9*(11), e112963. https://doi.org/10.1371/JOURNAL.PONE.0112963

Wallace, B. D., Wang, H., Lane, K. T., Scott, J. E., Orans, J., Koo, J. S., Venkatesh, M., Jobin, C., Yeh, L. A., Mani, S., & Redinbo, M. R. (2010). Alleviating cancer drug toxicity by inhibiting a bacterial enzyme. *Science*, *330*(6005), 831–835. https://doi.org/10.1126/SCIENCE.1191175/SUPPL_FILE/WALLACE.SOM.PDF

Walter, J., & Shanahan, F. (2023). Fecal microbiota-based treatment for recurrent Clostridioides difficile infection. *Cell*, *186*(6), 1087. https://doi.org/10.1016/j.cell.2023.02.034

Wang, B., Tsakiridis, E. E., Zhang, S., Llanos, A., Desjardins, E. M., Yabut, J. M., Green, A. E., Day, E. A., Smith, B. K., Lally, J. S. V., Wu, J., Raphenya, A. R., Srinivasan, K. A., McArthur, A. G., Kajimura, S., Patel, J. S., Wade, M. G., Morrison, K. M., Holloway, A. C., & Steinberg, G. R. (2021). The pesticide chlorpyrifos promotes obesity by inhibiting diet-induced thermogenesis in brown adipose tissue. *Nature Communications 2021 12:1*, *12*(1), 1–12. https://doi.org/10.1038/s41467-021-25384-y

White, A. P., Gibson, D. L., Grassl, G. A., Kay, W. W., Finlay, B. B., Vallance, B. A., & Surette, M. G. (2008). Aggregation via the red, dry, and rough morphotype is not a virulence adaptation in Salmonella enterica serovar Typhimurium. *Infection and Immunity*, *76*(3), 1048–1058. https://doi.org/10.1128/IAI.01383-07

Wick, R. R., Judd, L. M., Gorrie, C. L., & Holt, K. E. (2017). Unicycler: Resolving bacterial genome assemblies from short and long sequencing reads. *PLOS Computational Biology*, *13*(6), e1005595. https://doi.org/10.1371/JOURNAL.PCBI.1005595

Wickham, H., Averick, M., Bryan, J., Chang, W., McGowan, L., François, R., Grolemund, G., Hayes, A., Henry, L., Hester, J., Kuhn, M., Pedersen, T., Miller, E., Bache, S., Müller, K., Ooms, J., Robinson, D., Seidel, D., Spinu, V., … Yutani, H. (2019). Welcome to the tidyverse. *Journal of Open Source Software*, *4*(43), 1686. https://doi.org/10.21105/joss.01686

Woese, C. R., & Fox, G. E. (1977). Phylogenetic structure of the prokaryotic domain: The primary kingdoms. *Proceedings of the National Academy of Sciences of the United States of America*, *74*(11), 5088–5090. https://doi.org/10.1073/PNAS.74.11.5088/SUPPL_FILE/SCIENCEOFMICROBESPODCAST.MP3

Woese, C. R., Kandler, O., & Wheelis, M. L. (1990). Towards a natural system of organisms: proposal for the domains Archaea, Bacteria, and Eucarya. *Proceedings of the National Academy of Sciences of the United States of America*, *87*(12), 4576–4579. https://doi.org/10.1073/PNAS.87.12.4576

Xu, Z., Tian, L., Liu, L., Goodyer, C. G., Hales, B. F., & Bayen, S. (2023). Food Thermal Labels are a Source of Dietary Exposure to Bisphenol S and Other Color Developers. *Environmental Science & Technology*, *57*(12), 4984–4991. https://doi.org/10.1021/acs.est.2c09390

Yates, J., Deeney, M., Rolker, H. B., White, H., Kalamatianou, S., & Kadiyala, S. (2021). A systematic scoping review of environmental, food security and health impacts of food system plastics. *Nature Food*, *2*(2), 80–87. https://doi.org/10.1038/s43016-021-00221-z

Yim, G., McClure, J., Surette, M. G., & Davies, J. E. (2010). Modulation of Salmonella gene expression by subinhibitory concentrations of quinolones. *The Journal Of Antibiotics*, *64*, 73. https://doi.org/10.1038/ja.2010.137

Zhao, L., Zhang, F., Ding, X., Wu, G., Lam, Y. Y., Wang, X., Fu, H., Xue, X., Lu, C., Ma, J., Yu, L., Xu, C., Ren, Z., Xu, Y., Xu, S., Shen, H., Zhu, X., Shi, Y., Shen, Q., … Zhang, C. (2018). Gut bacteria selectively promoted by dietary fibers alleviate type 2 diabetes. *Science*, *359*(6380), 1151–1156. https://doi.org/10.1126/SCIENCE.AAO5774/SUPPL_FILE/AAO5774_ZHAO_SM.PDF

Zheng, D., Liwinski, T., & Elinav, E. (2020). Interaction between microbiota and immunity in health and disease. *Cell Research*, *30*(6), 492–506. https://doi.org/10.1038/s41422-020-0332-7

Zheng, L., Tan, Y., Hu, Y., Shen, J., Qu, Z., Chen, X., Ho, C. L., Leung, E. L.-H., Zhao, W., & Dai, L. (2022). CRISPR/Cas-Based Genome Editing for Human Gut Commensal Bacteroides Species. *ACS Synthetic Biology*, *11*(1), 464–472. https://doi.org/10.1021/acssynbio.1c00543

Zhulin, I. B. (2016). Classic Spotlight: 16S rRNA Redefines Microbiology. *Journal of Bacteriology*, *198*(20), 2764–2765. https://doi.org/10.1128/JB.00616-16

Zimmermann, M., Zimmermann-Kogadeeva, M., Wegmann, R., & Goodman, A. L. (2019). Mapping human microbiome drug metabolism by gut bacteria and their genes. *Nature*. https://doi.org/10.1038/s41586-019-1291-3

Zou, L., Spanogiannopoulos, P., Pieper, L. M., Chien, H. C., Cai, W., Khuri, N., Pottel, J., Vora, B., Ni, Z., Tsakalozou, E., Zhang, W., Shoichet, B. K., Giacomini, K. M., & Turnbaugh, P. J. (2020). Bacterial metabolism rescues the inhibition of intestinal drug absorption by food and drug additives. *Proceedings of the National Academy of Sciences of the United States of America*, *117*(27), 16009–16018. https://doi.org/10.1073/PNAS.1920483117/SUPPL_FILE/PNAS.1920483117.SD02.XLSX

Appendix

Appendix File 1. RNASnap: Isolation of total RNA

Please cite: Stead, M. B., Agrawal, A., Bowden, K. E., Nasir, R., Mohanty, B. K., Meagher, R. B., & Kushner, S. R. (2012). RNA snap ™: a rapid, quantitative and inexpensive, method for isolating total RNA from bacteria. *Nucleic Acids Research*, *40*(20), e156–e156. https://doi.org/10.1093/NAR/GKS680

This protocol has been adapted from the Barrick lab:
https://barricklab.org/twiki/bin/view/Lab/RNAPrep

Preamble: This protocol requires fresh samples; plan time accordingly to allow strains to grow, sub-culture, set up conditions and perform this protocol immediately when the condition has been met to ensure an accurate transcriptional snapshot is captured in your extracted RNA. This protocol takes approximately 1-2 hours depending on the number of samples (maximum 24 at a time). Samples need to reach approximately 0.2OD_{600} to provide enough nucleic acid for downstream applications. In advance have the following:

- RNA extraction solution made up fresh before starting the protocol:
    - For 24 samples, or 12.5ml:
        - 450ul of 0.5M EDTA (final 18mM)
        - 31.25ul of 10% SDS (final 0.025%)
        - 125ul of 2-mercaptoethanol (final 1%)
        - 11.875ml formamide (RNA grade; final 95%)
- Heat block set to 95°C
- Zymo RNA Clean & Concentrator-25 kit (#R1017) with DNase 1 (#E1010) from Zymo for on-column digestion
- Freshly made ethanol 80%

General principles for working with RNA: Minimize nuclease exposure – use filter tips, use RNaseZap, use nuclease-free reagents, use nuclease free tubes from the box (i.e. not autoclaved), work in the PCR hood.

1. **Extraction:**
    a. Move 1ml of samples to 1.7ml Eppendorf tubes using adjustable multi-channel pipette.
    b. Immediately place tubes in centrifuge at 10,000xg x 1 minute.
    c. Discard supernatants.
    d. Rapidly and working as quick as possible, resuspend cell pellet in 500ul of RNA extraction solution.
    e. Incubate sample at 95°C on heatblock for 7min to lyse cells.
    f. Centrifuge at 16,000xg x 5 minutes
        i. While waiting, set up the next batch of tubes for the next step
    g. Transfer 200ul of supernatant to a fresh 1.7ml tube
        i. Remaining 300ul can be stored in -80°C for backup.

2. **Zymo kit:**
    a. Use the repeater as much as possible for all steps. Work on ice and with centrifuge at 4°C.

b. 2x (400ul) RNA Binding buffer to each volume of RNA sample. Mix well.
c. Add 1x (600ul) 95% EtOH to each sample. Mix well.
d. Run through column with collection tube (do not use the vacuum manifold; not appropriately clean for RNA) at 12,000xg x 1 minute, discarding flowthrough.
    i. During the spin, prepare DNase 1 cocktail by mixing, for each sample:
        1. 5ul DNase 1
        2. 75ul Reaction buffer
e. Add 500ul 80% ethanol to the column and centrifuge at 12,000xg for 30 seconds and discard flowthrough.
f. Add 80ul DNase 1 cocktail to the centre of each column matrix.
g. Place rack of samples in the 37°C incubator for 15-30 minutes.
h. Centrifuge 12,000xg for 30 seconds. Discard flowthrough.
i. Add 400ul RNA prep buffer and centrifuge 12,000xg for 1 minute. Discard flowthrough.
j. Add 800ul RNA wash buffer, centrifuge 12,000xg for 30 seconds. Discard flowthrough.
k. Add 400ul RNA wash buffer, centrifuge 12,000xg for 2 minutes. Discard flowthrough.
l. Transfer column to a new RNAse-free tube (i.e. fresh bag from the supplier and not autoclaved).
m. Add 30ul of nuclease-free water to the column matrix. Incubate 1 minute at room temperature.
n. Centrifuge 10,000xg for 1 minute.
o. Place in -80°C freezer immediately for quantification later or proceed with quantification using the Qubit.

Appendix File 2. RNAtag-seq: Multiplexed library preparation for RNA-sequencing

Please cite: Shishkin, A. A., Giannoukos, G., Kucukural, A., Ciulla, D., Busby, M., Surka, C., Chen, J., Bhattacharyya, R. P., Rudy, R. F., Patel, M. M., Novod, N., Hung, D. T., Gnirke, A., Garber, M., Guttman, M., & Livny, J. (2015). Simultaneous generation of many RNA-seq libraries in a single reaction. Nature Methods 2015 12:4, 12(4), 323–325. https://doi.org/10.1038/nmeth.3313

With minor adaptations by Edward Wallace from the Drummond lab: http://drummondlab.org/protocols/protocol/rnatagseq-library-prep

Preamble: This protocol takes multiple days. Read thoroughly and prepare meticulously, before attempting to avoid critical mistakes.

General principles for working with RNA: Minimize nuclease exposure – use filter tips, use RNaseZap, use nuclease-free reagents, use nuclease free tubes from the box (i.e. not autoclaved), work in the PCR hood. This is essential until cDNA is synthesized.

Otherwise:

- Must avoid mixing up barcodes and contaminating DNA after cDNA is synthesized. Continue to work cleanly.
- Don't take the risk of pausing unless indicated as a pause point.
- Have experience using magnetic beads.
- Barcoded adaptors and control oligos are listed elsewhere and user dependent.

Procedure:

1. Control quality and quantity of RNA with Agilent Bioanalyzer
    - Check RNA quality for 1-3 representative samples per organism by running on the Tapestation at the genomics facility.
    - Place 0.5-5 ug of total RNA in a tube.
    - Increase the volume to 30uL with Nuclease free water
    - Add 2uL of SUPERase-IN (20U/uL)
    - Final total volume = 32uL (25ng/uL)
    - Continue to next step or freeze at -80C until ready to process samples

PAUSE POINT

2. Fragment RNA using 2x FastAP buffer
    - Add 8 uL of 10X FastAP buffer to 32 uL RNA from step 1 (up to 1 ug) and mix well.
    - Incubate on *preheated* thermal cycler for 3 min at 94°C.
    - If RNA is partially degraded (RIN<7), fragment 3 min at 92°C, prevents over-fragmenting samples.
    - Place on cold block on ice.

3. Digest DNA and repair RNA: Combination DNase/FastAP treatment

- Make a DNase/FastAP master mix, 40uL per sample:

Reagent (for 2X FastAP master)	**Amount**	**Final**
nuclease-free water	10 uL	
RNase Inhibitor, Murine (40U/uL)	2 uL	20U
TURBO DNase (2U/uL)	8 uL	16U
FastAP (1U/uL)	20 uL	20U
Total	40 uL	2X

  - Mix well
- Aliquot 40 uL into each tube/well with the 40uL of fragmented RNA from step 1.
- Mix well
- Incubate on preheated thermal cycler for 30 min at 37°C

4. Cleanup (2x SPRI) to remove enzymes and reaction buffer
   - Add 2x reaction volume of Agencourt RNAClean XP beads (160 uL) and capture RNA on beads:
     - Incubate at room temperature for 15min to bind RNA
     - Place on magnet for 5min, until solution is clear
     - Pipette out and discard clear solution
     - Add 200uL fresh 80% EtOH without removing from magnet, incubate for 30sec, Pipette off supernatant.
     - Repeat 80% EtOH wash. Let air dry for 2min
   - Elute off beads with 24 uL nuclease free water (can reduce to 20 uL increase concentration downstream)
   - Take 5 uL of each sample and proceed to 1st ligation
   - QC:
     - Save 1.2 uL from remaining RNA before addition of SUPERase-IN
     - Run 3-4 random samplings on Tapestation to check the fragmentation profile of each batch
   - Add 1uL SUPERase-IN (20U/uL) to the remaining material and store at -80°C as backup

PAUSE POINT

5. Ligate 3' barcoded Adaptor: First Ligation (ssRNA/ssDNA)
   - Add 1 uL of barcoded RNATag adaptor (100 pmole = 1 uL of 100 µM) to 5 uL of dephosphorylated RNA
   - Heat at 70°C for 2 min, place in cold block on ice
   - Set up First Ligation master mix below NOTE:
     - All reagents except enzymes (-20°C) should be stored at -80°C in single use aliquots and brought to room temp just before use
     - Make up mix *at room temp* so the reagents don't start precipitating when combined (if DMSO is added directly into cold buffer it will precipitate)
     - Pipette very slowly with wide-opening/cut tips for accurate aspiration of PEG (very viscous)

- When setting up mix for multiple reactions include 25% extra to account for pipetting error due to the viscosity

Reagent (for Ligation master)	**1 rxn**	**40 rxns**
10× T4 RNA Ligase Buffer	2 uL	80 uL
DMSO (100%)	1.8 uL	72 uL
ATP (100 mM)	0.2 uL	8 uL
PEG 8000 (50%)	8 uL	320 uL
RNase inhibitor, Murine (40U/uL)	0.3 uL	12 uL
Total	12.3 uL	492 uL

- Mix really well by extensive vortexing tube since the solution is very viscous, then spin down briefly in microfuge

- Add 12.3 uL of ligation master mix to each tube/well containing 6 uL denatured RNA + adaptor.
- Add 1.8 uL of T4 RNA Ligase 1 (30,000U/mL) to each tube/well. 20.1 uL reaction volume total.
- Mix well *many* times; mix by flicking since the solution is very viscous
- Incubate at 22°C (room temp) for 1 hour 30 minutes.
- Use barcoded TagDNA+ as a sanity check that barcoding worked appropriately

6. Pool barcoded RNA: RLT buffer + Zymo column
   NOTE: At this point, multiple samples with distinct RNAtag adaptors will be pooled on the same spin column. Do not exceed 5ug RNA per pool, the maximum binding capacity of columns. Attempt to normalize the amounts (using your QC in step 4, or even 1) based on the amount of non-ribosomal RNA in each pool.
   - Add 60 uL of RLT buffer to each sample to inhibit ligase, and mix well (80 uL total)
   - Pool samples in a 15ml falcon tube, centrifuge at 4000xg for 30 seconda and run 750 uL at a time through the Zymo Clean & ConcentratorTM-5 column - follow manufacturer's *200nt* cut off protocol :
     - Add 2x reaction vol (160 uL=2x 80 uL) of 1:1 binding buffer: EtOH (100%) / reaction
     - Carefully add reactions to be pooled to a single Zymo column. NOTE: When pooling >700 uL onto Zymo column use a vacuum manifold then proceed to centrifugation steps according to the manual
     - Wash and spin 0.5 min 12,000 g, then discard flow-through, once with 400 uL RNA Prep buffer, once with 800 uL RNA Wash buffer, once with 400uL Wash buffer for 2 minutes, spin another 1min with no buffer.

- Elute 2 times with 16 uL nuclease free water for a total volume of 32 uL
  NOTE: 2 elutions help improve recovery/yield of RNA
- Save 2 uL for QC-Run on Tapestation if needed

PAUSE POINT

7. Deplete ribosomal RNA with RNase H protocol.

8. Synthesize First Strand cDNA
   - Take 12 uL rRNA depleted RNA (use all the material)
   - Add 2 uL (50 pmoles) of AR2 primer
   - Mix well
   - Heat the mixture to 70°C for 2 min and immediately place on cold block on ice
   - Make RT master mix
     - Add in order on ice

Reagent (for RT master)	**1 rxn**	**2.5 rxns**
10× AffinityScript RT Buffer	2 uL	5 uL
DTT (0.1M)	2 uL	5 uL
25mM dNTP Mix (25mM each)	0.8 uL	2 uL
RNase inhibitor, murine (40U/uL)	0.4 uL	1 uL
Total	5.2 uL	13 uL

     - Mix well
   - Add 5.2 uL of RT mix to the 14 uL rRNA depleted RNA + AR2 RTprimer on ice
   - Add 0.8 uL of AffinityScript RT Enzyme
   - Mix well and spin for 5 sec
   - Place in *preheated* (55 °C) incubator or thermocycler. Incubate at 55 °C for 55 minutes.

9. Degrade RNA after reverse transcription
   NOTE: make fresh working stock solutions of NaOH and Acetic Acid
   - Add 10% reaction vol. of 1M NaOH (2 uL) to each reaction
   - Incubate at 70 °C for 12 minutes
   - Neutralize with 4 uL of 0.5M Acetic Acid; mix well
   - Total volume = 26 uL

10. Cleanup reverse transcription (2x SPRI) to remove enzyme, primers, and reaction buffer
    - Add 14 uL of sterile water to each reaction for a final volume of 40 uL
    - Transfer to new tubes (NaOH may start degrading tubes)
    - Add 2x reaction volume SPRI beads (80uL) to the sample in new tubes, and mix up/down 10x
    - Incubate at room temperature for 15min
    - Place on magnet for 5 min or until solution is clear
    - Pipette out and discard clear solution

- Wash: Add 200 uL fresh 80% EtOH without removing from magnet and incubate for 30 sec. Pipette off and discard the EtOH.
- Repeat 80% EtOH wash, and let air dry for 3min, remove from magnet.
- Add 5 uL RNase/DNase free water to beads – *KEEP BEADS AND TUBES, do not transfer, do not pause*

11. Ligate 3' Universal Adaptor: Second Ligation (ssDNA/ssDNA) with beads
    - Add 2 uL (80 pmoles) of 3Tr3 adaptor to cDNA
    - Heat at 75°C for 3 min; Place on cold block on ice
    - Make ligation reaction master mix (can be prepared ahead of time, at RT):
    - 2nd Ligation Master Mix:
        - Mix in order

Reagent (for Ligation 2 master)	**1 rxn**	**2.5 rxns**
10× T4 RNA Ligase Buffer	2 uL	5 uL
DMSO (100%)	0.8 uL	2 uL
ATP (100 mM)	0.2 uL	0.5 uL
PEG 8000 (50%)	8.5 uL	21.3 uL
T4 RNA Ligase 1 (30,000U/mL)	1.5 uL	3.8 uL
Total	13.0 uL	32.6 uL

        - Mix really well by extensive vortexing tube since the solution is very viscous
        - Spin down briefly in microfuge
    - Swirl the 7uL cDNA/beads/water with pipet tip, THEN add 13 uL ligation 2 master mix.
    - Mix well by pipetting up and down 20x or cap tubes and flick several times; solution is viscous
    - Quick spin (low speed centrifuge, to get everything to bottom of tube)
    - Incubate overnight at 22 °C

12. Cleanup (2x SPRI) to remove adaptors
    - Add 2x reaction volume SPRI beads (80uL) to the sample in new tubes, and mix up/down 10x
    - Incubate at room temperature for 15min
    - Place on magnet for 5 min or until solution is clear
    - Pipette out and discard clear solution
    - Wash: Add 200 uL fresh 80% EtOH without removing from magnet and incubate for 30 sec. Pipette off discard the EtOH.
    - Repeat 80% EtOH wash, and let air dry for 3min
    - Elute DNA by adding 30 uL RNase/DNase free water, transfer to new tube.

13. 2nd Cleanup (1.5x SPRI) to remove the remaining adaptors

- Add 1.5x reaction volume SPRI beads (45 uL) to the sample in new tubes, and mix up/down 10x
- Incubate at room temperature for 15min
- Place on magnet for 5 min or until solution is clear
- Pipette out and discard clear solution
- Wash: Add 200 uL fresh 80% EtOH without removing from magnet and incubate for 30 sec. Pipette off and discard the EtOH.
- Repeat 80% EtOH wash, and let air dry for 3min
- Elute DNA by adding 25 uL RNase/DNase free water, transfer to new tube.

PAUSE POINT

14. TEST PCR Amplification to determine final cycle number
    NOTE: P5 primer: P5_RNATag, 5'-AAT GAT ACG GCG ACC ACC GAG ATC TAC ACT CTT TCC CTA CAC GAC GCT CTT CCG ATC T-3', 52% GC, 58bp; standard DNA oligo. Make 100uM stock and 12.5uM working stock.

    - Set up a test PCR using 5 uL of ss cDNA sample and 9-12 cycles of PCR (based on experience with pool of 16 reactions, each starting with ~400ng total RNA)
    - Include a negative control (water) for each primer set
    - Make PCR Master Mix (4 rxns=2 libraries, +ve ctrl, -ve ctrl):
        - Add in order:

Reagent (for PCR master mix)	**1 rxn**	**4 rxns**
Water, PCR-clean	14.3 uL	57.2 uL
10X Pfu Ultra II Buffer	2.5 uL	10 uL
dNTP mix (10mM each)	0.7 uL	2.8 uL
P5 primer (P5_RNATag, 12.5 µM)	1 uL	4 uL
Total	18.5 uL	74 uL

        - Mix well
        - Aliquot 18.5 uL / sample into PCR tubes
    - Add 1 uL of appropriate P7 index primer to each well
    - Add 5 uL of ss cDNA from step 11, or water (for negative control)
    - Add 0.5 uL of Pfu Ultra II Polymerase.
    - Mix well and aliquot 8 ul into each of 3 tubes
    - Place each in a thermal cycler with cycling conditions:
        - start: 98°C, 3min
        - cycle: 9, 12, 15 cycles (for test PCR) 98°C, 30sec; 55°C, 30sec; 70°C, 30sec
        - end: 70°C, 2min; 4°C, hold

15. Cleanup (1.5x SPRI) to remove reaction buffer and PCR primers:
    - increase reaction to 40uL with sterile water
    - Add 1.5x reaction volume SPRI beads (60 uL) to the sample in new tubes, and mix up/down 10x

- Incubate at room temperature for 15min
- Place on magnet for 5 min or until solution is clear
- Pipette out and discard clear solution
- Wash: Add 200 uL fresh 80% EtOH without removing from magnet and incubate for 30 sec. Pipette off and discard the EtOH.
- Repeat 80% EtOH wash, and let air dry for 3min
- Elute off beads with 10 uL 1x low TE (10 mM Tris, 0.1M EDTA)

16. QC test PCR amplification on Tapestation
    - Based on test results change the cycle number, if necessary, and set up more reactions to provide enough material to send for sequencing
    - UChicago functional genomics core asks for ~15 uL of 10 nM library; aim for at least 25 uL = 0.25 pmol = 60 ng of 400nt dsDNA (~250 kDa).
    - To pass QC, library should have smooth profile 200-500nt long; visible single bands, or a "shoulder" of larger products, indicate PCR artefacts.
    -

PAUSE POINT

17. PCR for Sequencing library
    - Choose the optimal PCR cycle # based on Bioanalyzer QC of test (step 15).
    - Include a negative control (water) for each primer set
    - Make PCR Master Mix (3 rxns=2 libraries, half size +ve ctrl, half size -ve ctrl):
        - Add in order:

Reagent (for PCR master mix)	**1 rxn**	**3 rxns**
Water, PCR-clean	28.6 uL	85.8 uL
10X Pfu Ultra II Buffer	5 uL	15 uL
dNTP mix (10mM each)	1.4 uL	4.2 uL
P5 primer (P5_RNATag, 12.5 µM)	2 uL	6 uL
Total	37 uL	111 uL

        - Mix well
        - Aliquot 37 uL / sample into PCR tubes
    - Add 2 uL of appropriate P7 index primer to each well
    - Add 10 uL of ss cDNA from step 11, or water (for negative control)
    - Add 1 uL of Pfu Ultra II Polymerase.
    - Mix well and aliquot 10 ul into each of 5 wells of a 96-well plate (amplification is apparently more robust in smaller volumes), cap.
    - Place each in a thermal cycler with the cycling conditions:
        - start: 98°C, 3min
        - cycle: # determined from test PCR 98°C, 30sec; 55°C, 30sec; 70°C, 30sec
        - end: 70°C, 2min; 4°C, hold

18. Cleanup (1.5x SPRI) to remove reaction buffer and PCR primers:

- Pool PCR reaction (50 uL)
- Add 1.5x reaction volume SPRI beads (75 uL) to the sample in new tubes, and mix up/down 10x
- Incubate at room temperature for 15min
- Place on magnet for 5 min or until solution is clear
- Pipette out and discard clear solution
- Wash: Add 200 uL fresh 80% EtOH without removing from magnet and incubate for 30 sec. Pipette off and discard the EtOH.
- Repeat 80% EtOH wash, and let air dry for 3min
- Elute off beads with 50 uL water and transfer to new tubes.

19. Final Cleanup (0.8x SPRI) to remove remaining PCR primers:
    - Add 0.8x reaction volume SPRI beads (40 uL) to the sample in new tubes, and mix up/down 10x
    - Incubate at room temperature for 15min
    - Place on magnet for 5 min or until solution is clear
    - Pipette out and discard clear solution
    - Wash: Add 200 uL fresh 80% EtOH without removing from magnet and incubate for 30 sec. Pipette off and discard the EtOH.
    - Repeat 80% EtOH wash, and let air dry for 3min
    - Elute off beads with 25 uL 1x low TE (10 mM Tris, 0.1M EDTA)

20. Proceed to sequence

Appendix File 3. RNase H based rRNA depletion with oPool ssDNA oligos for RNAtag-seq samples.

Please cite: Yiming Huang, Ravi U Sheth, Andrew Kaufman, Harris H Wang, Scalable and cost-effective ribonuclease-based rRNA depletion for transcriptomics, *Nucleic Acids Research*, Volume 48, Issue 4, 28 February 2020, Page e20, https://doi.org/10.1093/nar/gkz1169

Preamble: This protocol takes approximately 2-3 hours to perform. Book 2 thermocyclers. oPools probes used for all strains are available as an online supplement at https://github.com/thessyed/dissertation.

General principles for working with RNA: Minimize nuclease exposure – use filter tips, use RNaseZap, use nuclease-free reagents, use nuclease free tubes from the box (i.e. not autoclaved), work in the PCR hood.

3. **RNA-ssDNA probe annealing:** 1:5 RNA:ssDNA probe mix standard but can go to 1:10
    a. Per sample setup:

Quantity	Reagent
500ng	Sample RNA
2500ng	50pmol oPool (ssDNA probe mix)
0.6ul	5M NaCl
1.5ul	1M Tris-HCl (pH7.5)
Top up reaction to 15ul	Nuclease-free water

    b. Place in thermocycler: **ENSURE THERMOCYCLER IS CAPABLE OF STEP 2 (THERMOCYCLER 2 ONLY IN SURETTE LAB – Program called "RNase H rRNA Depletion – Step 1")**

Lid temperature 105°C

Temp	Time
95°C	2 minutes
-0.1°C/sec to 45°C	~9 minutes
45°C	5 minutes

Proceed immediately to next step.

4. **Prepare RNase H master mix:**
    a. Preheat a separate thermocycler to 45°C (lid temperature 60°C) and hold temp.
    b. Prepare RNase H master mix in a PCR strip as needed based on number of reactions set up. Make 1X extra to account for pipetting error**.** Any extra can be added to a reaction as increased RNase H may improve/optimize reaction. **Per reaction (multiply as needed):**

Quantity	Reagent
3ul	Hybridase Thermostable RNase H (Lucigen)
0.5ul	1M Tris-HCl
0.2ul	5M NaCl
0.4ul	1M MgCl2
0.9ul	Nuclease-free water

a. Mix master mix by pipetting up and down 10+ times
b. Briefly spin down.
c. Place in thermocycler preheated to 45°C and preheat mix to 45°C for immediate use.

5. **Final reaction:**
    a. Upon completion of step 1B, remove RNA-ssDNA reaction from thermocycler and preheated master mix from step 2.
    b. Leave thermocycler 2 holding at 45°C.
    c. Add 5ul of preheated master mix to 15ul RNA-ssDNA reaction.
    d. Mix by pipetting up and down 10+ times.
    e. Briefly spin down and immediately proceed to next step.
    f. Place samples in thermocycler 2 (45°C) for 30 minutes.
    g. After incubation spin samples down briefly.
    h. Place on ice and immediately proceed to next step.

6. **RNA clean-up:**
    a. Clean-up round 1: Use RNAClean XP beads at 2X ratio of beads to reaction volume. Clean up as per usual with the following modifications: 80% ethanol (made fresh) rather than 70%. Elute into 26ul nuclease-free water.
    b. Clean-up round 2: Use RNAClean XP beads at 2X ratio of beads to reaction volume. Clean up as per usual with the following modifications: 80% ethanol (made fresh) rather than 70%. Elute into 15ul nuclease-free water.
    c. Continue with RNAtag-seq protocol or add 1ul SUPERase-In RNase Inhibitor to each sample and store at -80°C.

For our strain, to achieve a final concentration of 1000ng/ul:

Strain	# of Probes	Amount (Probes x 50pmol)	Lowest MW	Resuspension Volume
Ba	91	4.55nmol	15101	68.7ul
Bx	87	4.35nmol	15018	65.3ul
Ec	88	4.40nmol	15092	66.4ul
Ak	86	4.30nmol	15105	65.0ul
Eu	87	4.35nmol	15069	65.6ul
Mt	89	4.45nmol	15054	67.0ul
Ao	87	4.35nmol	15113	65.7ul

Round everything down to the lowest whole number number (i.e. 68.7ul to 68ul).

Appendix File 6. *Salmonella* random promoter library identification PCR

Day 0

- Grow random promoter library plate(s) for PCR in 384-well liquid culture plate.

Day 1

- Set up master mix as per below. Mix master mix well. Place master mix in reservoir and, using a 12-channel pipette, pipette 10.3ul into each well of a 384-well PCR plate.

PCR Reaction:	X1 (ul)	X400 (ul)
Invitrogen 10X Taq Buffer	1.25	500
BSA	0.5	200
DMSO	0.5	200
50mM $MgCl_2$	0.375	150
10mM dNTPs	0.25	100
1uM Primer – SS1	1	400
dH_20	6.4	2560
Taq polymerase (5U/ul)	0.0625	25
Template (pinned O/N culture)	~0.2	
0.5uM Barcoded Primer	2	
Total:	12.5	

- Using the new 384-well manual pin replicator (located on the top shelf, right most corner of Saad's bench), add template to the PCR plate, ensuring that orientation of the plates are the same (i.e. A1 from the O/N growth goes into A1 of the PCR plate).
- Add barcoded primers to the PCR plate such that barcoded primer # corresponds with column number on the PCR plate.
- Briefly (~5-10 seconds) spin down in the plate spinner. Place in thermocycler.

Thermocycler protocol:

Step	Temperature (Celsius)	Time (MM:SS)
1	94	5:00
2	94	0:30
3	53.5	0:30
4	72	3:00
5	Repeat steps 2-4 X35	
6	72	5:00

******Salmonella* **species possess a thermostable nuclease which degrades PCR products. This protocol uses whole cell culture and therefore transfers this nuclease to the PCR reaction. The following steps must be done immediately following completion of PCR.***

Run a subset of samples, ideally a row of 24 samples, to confirm successful amplification.

Pool samples rowwise. Add EDTA to each pooled sample and freeze at -20C.

Appendix File 4, Appendix File 5, and **Appendix File 7** are available online at https://github.com/thessyed/dissertation